ตัวยับยั้งแอลฟากลูโคซิเดสจากพืชที่รับประทานได้

นายธนากรณ์ ดำสุด

α-GLUCOSIDASE INHIBITORS FROM EDIBLE PLANTS

Mr. Thanakorn Damsud

A Dissertation Submitted in Partial Fulfillment of the Requirements

for the Degree of Doctor of Philosophy Program in Biotechnology

Faculty of Science

Chulalongkorn University

Academic Year 2013

Thesis Title	α-GLUCOSIDASE INHIBITORS FROM EDIBLE PLANTS
By	Mr. Thanakorn Damsud
Field of Study	Biotechnology
Thesis Advisor	Assistant Professor Preecha Phuwapraisirisan, Ph.D.
Thesis Co-Advisor	Associate Professor Sirichai Adisakwattana, Ph.D.

Accepted by the Faculty of Science, Chulalongkorn University in Partial Fulfillment of the Requirements for the Doctoral Degree

⋯⋯⋯⋯⋯⋯⋯⋯⋯⋯⋯⋯⋯Dean of the Faculty of Science

(Professor Supot Hannongbua, Dr.rer.nat.)

THESIS COMMITTEE

⋯⋯⋯⋯⋯⋯⋯⋯⋯⋯⋯⋯⋯Chairman

(Associate Professor Vudhichai Parasuk, Ph.D.)

⋯⋯⋯⋯⋯⋯⋯⋯⋯⋯⋯⋯⋯Thesis Advisor

(Assistant Professor Preecha Phuwapraisirisan, Ph.D.)

⋯⋯⋯⋯⋯⋯⋯⋯⋯⋯⋯⋯⋯Thesis Co-Advisor

(Associate Professor Sirichai Adisakwattana, Ph.D.)

⋯⋯⋯⋯⋯⋯⋯⋯⋯⋯⋯⋯⋯Examiner

(Associate Professor Nattaya Ngamrojanavanich, Ph.D.)

⋯⋯⋯⋯⋯⋯⋯⋯⋯⋯⋯⋯⋯Examiner

(Professor Mary Ann Lila, Ph.D.)

⋯⋯⋯⋯⋯⋯⋯⋯⋯⋯⋯⋯⋯Examiner

(Assistant Professor Kanoktip Packdibamrung, Ph.D.)

⋯⋯⋯⋯⋯⋯⋯⋯⋯⋯⋯⋯⋯External Examiner

(Assistant Professor Wimolpun Rungprom, Ph.D.)

ธนากรณ์ ดำสุด : ตัวยับยั้งแอลฟากลูโคซิเดสจากพืชที่รับประทานได้. (α-GLUCOSIDASE INHIBITORS FROM EDIBLE PLANTS) อ.ที่ปรึกษาวิทยานิพนธ์หลัก: ผศ. ดร. ปรีชา ภูวไพรศิริศาล, อ.ที่ปรึกษาวิทยานิพนธ์ร่วม: รศ. ดร. สิริชัย อดิศักดิ์วัฒนา, 121 หน้า.

ในการศึกษาสารยับยั้ง α-glucosidase จะนำไปสู่การพัฒนาการรักษาโรคเบาหวานชนิดที่ 2 ได้ เราจึงศึกษาสารยับยั้ง α-glucosidase จากพืชที่รับประทานได้ ในงานวิจัยนี้ได้เลือกศึกษาใบช้าพลู งาขาว และส่วนเหนือพื้นดินของหญ้าหนวดแมว โดยการทดสอบฤทธิ์ทางด้านชีวภาพจึงนำไปสู่การแยกสารบริสุทธิ์ที่มีฤทธิ์ยับยั้ง α-glucosidase การแยกสารสกัดไดคลอโรมีเทนและส่วนสกัดเมทานอลจากใบช้าพลู ได้สารใหม่ประเภท ฟีนิวโปรพานอลเอมายด์ 3 ชนิด คือ chaplypupyrrolidones A (1), B (2) และ deacetylsarmentamide B (7) รวมทั้งสารที่มีการรายงานแล้ว 6 ชนิด คือ N-(3-(4′methoxyphenyl)propanoyl)pyrrole (3), N-(3-phenylpropa-noyl)pyrrole (4), asaricin (5), cinnamic acid (6), kaemferol-3-O-rhamnoside (8) และ dihydrokaempferol-3-O-glucoside (9) จากสารทั้งหมดที่แยกได้ สาร 2 มีฤทธิ์ในการยับยั้ง α-glucosidase จากยีสต์ ที่ IC50 430±1.2 μM การศึกษาทางด้านจลศาสตร์ของ 2 พบว่าเป็นการยับยั้งแบบ noncompetitive การแยกส่วนสกัดเมทานอลจากงาขาว สามารถแยกสารประเภทลิกแนน ที่แตกต่างกัน 3 ชนิด คือ sesamin (10), sesamolin (11) และ sesaminol monoglucoside (12). จากสารทั้งหมดที่แยกได้ สาร 10 มีฤทธิ์ในการยับยั้ง α-glucosidase จากยีสต์ ที่ IC50 450±1.9 μM การศึกษาทางด้านจลศาสตร์ของสาร 10 พบว่าเป็นการยับยั้งแบบ competitive การแยกสารสกัดไดคลอโรมีเทนจากส่วนเหนือพื้นดินของหญ้าหนวดแมว โดยใช้วิธีการแยกแบบ α-glucosidase-guided พบสารประเภทฟลาโวนอยด์ 4 ชนิด คือ sinensetin (13), salvigenin (14), tetramethylscutellarein (15) และ 3,7,4'-tri-O-methylkaempferol (16) ร่วมกับสารจำพวกไดเทอร์ปีนอีก 1 ชนิด คือ orthosiphol A (17) สารฟลาโวนอยด์ 15 และ 16 มีฤทธิ์ในการยับยั้ง α-glucosidase จากยีสต์ ที่ IC50 6.34 และ 0.75 mM ตามลำดับ ในทางตรงกันข้าม สาร orthosiphol A (17) ได้ถูกเลือกมาศึกษายับยั้งมอลเทสที่ IC50 6.54 mM การศึกษาจลศาสตร์ของสาร 17 พบว่าเป็นแบบ noncompetitive

นอกจากการศึกษาพืชที่รับประทานได้แล้ว เรายังได้ศึกษาสารยับยั้งแอลฟากลูโคซิเดส การต้านอนุมูลอิสระ และ การเหนี่ยวนำการอักเสบ จาก berry-defatted soybean flour (DSF) complexes ชนิดต่างๆ blueberry-DSF complex (BB-DSF) และ blackcurrant-DSF complex (BLC-DSF) พบว่า มี แอนโทไซยานิน (ANC) และ โปรแอนโทไซยานิน (PAC) ในปริมาณสูงที่สุด Polyphenol-enriched DSF ทั้งหมดมีฤทธิ์ในการยับยั้งเอนไซม์ α-glucosidase จากหนู ในมอลเทส และ ซูเครส BB-DSF มีฤทธิ์ในการยับยั้งเอนไซม์ α-glucosidase จากหนูที่ IC50 2.46 mg/mL ในมอลเทส และ 0.90 mg/mL ในซูเครส ตามลำดับ การศึกษากลไกการยับยั้งเอนไซม์มอลเทส พบว่าเป็นแบบ mixed-type ในขณะที่เอนไซม์ซูเครสเป็นแบบ noncompetitive Polyphenol-enrich DSF ทั้งหมดพบว่ามีปริมาณสารพอลีฟีนอลที่สูง ส่งผลให้มีฤทธิ์ในการต้านอนุมูลอิสระ และการเหนี่ยวนำการอักเสบโดย LPS ใน เซลล์ RAW 264.7 จากข้อมูลที่ได้แสดงให้เห็นว่า polyphenol-enriched DSF สามารถที่จะใช้เป็นอาหารที่มีปริมาณให้โปรตีน และให้ปริมาณน้ำตาลที่ต่ำ สำหรับใช้เป็นผลิตภัณฑ์เสริมอาหาร ที่ใช้เทคโนโลยีแบบใหม่ในการผลิต

สาขาวิชา เทคโนโลยีชีวภาพ	ลายมือชื่อนิสิต _____
ปีการศึกษา 2556	ลายมือชื่อ อ.ที่ปรึกษาวิทยานิพนธ์หลัก _____
	ลายมือชื่อ อ.ที่ปรึกษาวิทยานิพนธ์ร่วม _____

5273816423 : MAJOR BIOTECHNOLOGY

KEYWORDS: ALPHA-GLUCOSIDASE INHIBITOR / PIPER SARMENTOSUM ROXB. / SESAMUM INDICUM L. / ORTHOSIPHON ARISTATUS (BLUME) MIQ / POLYPHENOL-ENRICHED DSF / DIABETES MELLITUS

THANAKORN DAMSUD: α-GLUCOSIDASE INHIBITORS FROM EDIBLE PLANTS. ADVISOR: ASST. PROF. PREECHA PHUWAPRAISIRISAN, Ph.D., CO-ADVISOR: ASSOC. PROF. SIRICHAI ADISAKWATTANA, Ph.D., 121 pp.

The present study investigated α-glucosidase inhibitors with the aim of developing therapeutics for the treatment of type 2 diabetes mellitus. We examined the inhibitory effect of edible plants against α-glucosidase. The leaves of Piper sarmentosum Roxb, seed pulp of Sesamum indicum L. and aerial part of Orthosiphon aristatus (Blume) Miq were selected for this investigation. Bioassay-guided fractionation led to the isolation of active compounds. The dichloromethane and methaol extracts from leaves of P. sarmentosum afford three new phenylpropanoyl amides, named chaplypupyrrolidones A (1) and B (2) and deacetylsarmentamide B (7),along with six known named N-(3-(4′methoxyphenyl)propanoyl)pyrrole (3), N-(3-phenylpropa-noyl)pyrrole (4), asaricin (5) and cinnamic acid (6), kaemferol-3-O-rhamnoside (8) and dihydrokaempferol-3-O-glucoside (9). Of isolated compounds, 2 showed most potent inhibition against yeast α-glucosidase with IC50 value of 430±1.2 μM. Kinetic evaluation of 2 suggested that it acts as a noncompetitive inhibitor. The methanol crude extract from seed pulp of Sesamum indicum L. afforded various three lignans named sesamin (10), sesamolin (11) and sesaminol monoglucoside (12). Of the compounds isolated, sesamin (10), the major component revealed inhibitory activity against yeast α-glucosidase with IC50 value of 450±1.9 μM. The kinetic study indicated that 10 showed competitive manner. The dichloromethane extract of aerial part of Orthosiphon aristatus (Blume) Miq was investigated using an α-glucosidase-guided isolation. Four flavonoids named sinensetin (13), salvigenin (14), tetramethylscutellarein (15) and 3,7,4'-tri-O-methylkaempferol (16) together with a diterpenoid named orthosiphol A (17) were isolated. Flavonoids 15 and 16 inhibited yeast α-glucosidase with IC50 values of 6.34 and 0.75 mM, respectively, whereas orthosiphol A (17) selectively inhibited maltase with an IC50 value of 6.54 mM. A kinetic investigation of 5 indicated that it retarded maltase function in a noncompetitive manner.

In addition to edible plants, we also investigated α-glucosidase inhibition, antioxidant and LPS-elicited induction of various berry-defatted soybean flour (DSF) conmplexes. Blueberry-DSF complex (BB-DSF) and blackcurrant-DSF complex (BLC-DSF) were rich in anthocyanins (ANC), and proanthocyanidins (PAC). All polyphenol-enriched DSF exhibited significant against rat α-glucosidase (maltase and sucrase). BB-DSF was the most potent rat α-glucosidase inhibitor with IC50 values of 2.46 for maltase and 0.90 mg/mL for sucrase respectively. The mechanism underling inhibition against maltase was proved to be mixed-type manner while sucrase inhibited by noncompetitive manner. All polyphenol-enrich DSF demonstrated higher level of phenolic components, antioxidant capacity (DPPH) and exhibited LPS-elicited induction in RAW 264.7 cells. The data suggested that polyphenol-enriched DSF can provide a high-protein, low-sugar ingredient for novel food and dietary supplements.

Field of Study: Biotechnology

Academic Year: 2013

Student's Signature _____

Advisor's Signature _____

Co-Advisor's Signature _____

ACKNOWLEDGEMENTS

CONTENTS

LIST OF FIGURE

LIST OF TABLE

LIST OF SCHEME

LIST OF ABBEVIATIONS

ANC	Anthocyanins
BB	Blueberry
BB-DSF	Blueberry defatted soybean four
BLC	Blackcurrant
BLC-DSF	Blackcurrant defatted soybean four
brs	Broad singlet (NMR)
brd	Broad doublet (NMR)
BSA	Bovine serum albumin
DSF	Defatted soy four
CB	Cranberry
CB-DSF	Cranberry defatted soybean four
^{13}C NMR	Carbon-13 nuclear magnetic resonance
DM	Diabetes mellitus
DMSO	Dimethyl sulfoxide
$CDCl_3$	Deuterated chlorofrom
CD_3OD	Deuterated methanol
COSY	Correlated spectroscopy
Calcd	Calculated
d	Doublet (NMR)
dd	Doublet of doublet (NMR)

dw	Dry weight
2D NMR	Two dimensional nuclear magnetic resonance
^{1}H NMR	Proton nuclear magnetic resonance
HSQC	Heteronuclear single quantum correlation
HMBC	Heteronuclear multiple bond correlation experiment
Hz	Hertz
HRESIMS	High resolution electrospray ionization mass spectrum
IDDM	Insulin dependent diabetes mellitus
IC$_{50}$	Concentration that required for 50% inhibition in vitro
J	Coupling constant
g	Gram
kDa	Kilo Dalton
Km	Michaaelis constant
l	Liter
min	Minute
μl	Microliter
μM	Micormolar
ml	Milliliter
mg	Milligram
MG	Muscadine grape
MG-DSF	Muscadine grape defatted soybean four

mM	Milimolar
M	Molar
m/z	Mass per charge
Na_2CO_3	Sodium carbonate
NIDDM	Non-insulin-dependent diabetes mellitus
NMR	Nuclear magnetic resonance
pNPG	p-nitrophenyl α-D-glucopyranoside
PAC	Proanthocyanidins
PG	Pomegranate
PG-DSF	Pomegranate defatted soybean four
UV	Ultraviotet
U	Unit
VCC	Vacuum column chromatography
TE	Trolox equivalent
TP	Total phenolics
δ	Chemical shift
δ_C	Chemical shift of carbon
δ_H	Chemical shift of proton
λ_{max}	Maximum wavelength
ε	Molar extinction coefficient
$[\alpha]_D$	Specific optical rotation

CHAPTER I

INTRODUCTION

Diabetes mellitus is a commonly metabolic disorder of heterogeneous endocrine characterized by elevated blood glucose levels caused by defect in insulin action, insulin secretion or both. The patients of diabetes are increasing 4-5 % every year (Wagman & Nuss, 2001). According to the World Health Organization (WHO, 2006), there were 171 million patients in 2000 and will grow 366 millions in 2030 (Figure 1.1). Diabetes is associated to risk of microvascular damage (retinopathy, nephropathy and neuropathy) that can lead to complications and loss of quality of life. American Diabetes Association (ADA) estimated cost of disease $US132 billion for 2002, increasing $US192 billion in 2020.
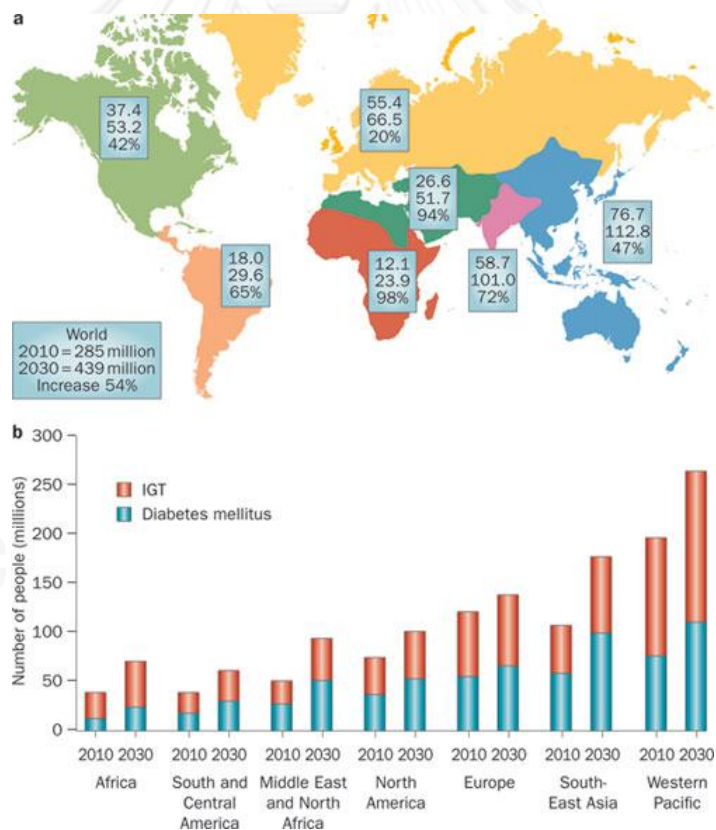
Figure 1.1 Global projections for the diabetes epidemic: 2010–2030 (L. Chen, Magliano, & Zimmet, 2012)

Insulin is a hormone produced by beta cell of pancreas, which is required to utilize glucose from digested food. Therefore, glucose is transported into cell once insulin binds to insulin receptor, which straddles cell membrane of many cells. (Figure 1.2)
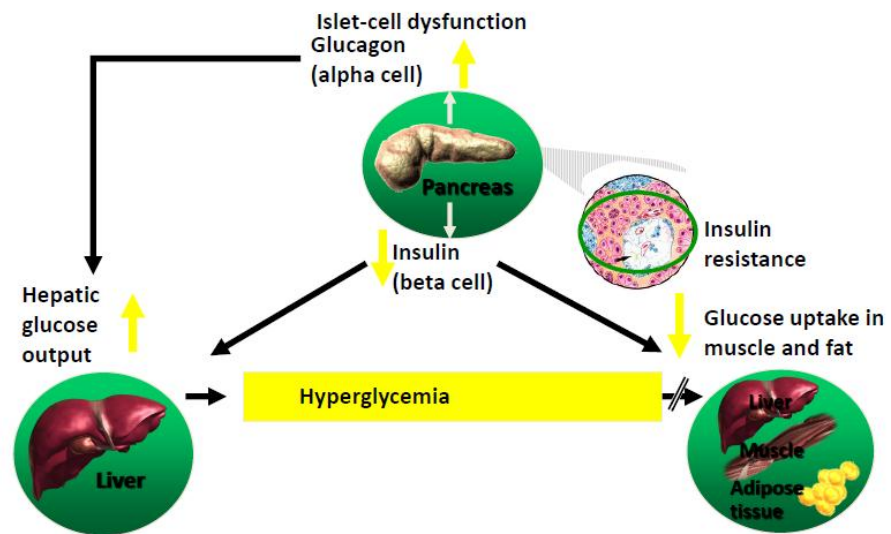
Figure 1.2 Mechanism of diabetes mellitus

1.1 Type of diabetes

Diabetes mellitus can be divided into two types based on presumed etiology. Type 1 is called insulin-dependent diabetes mellitus (IDDM) while type 2 is designed as non-insulin-dependent diabetes mellitus (NIDDM) (Figure 1.3).
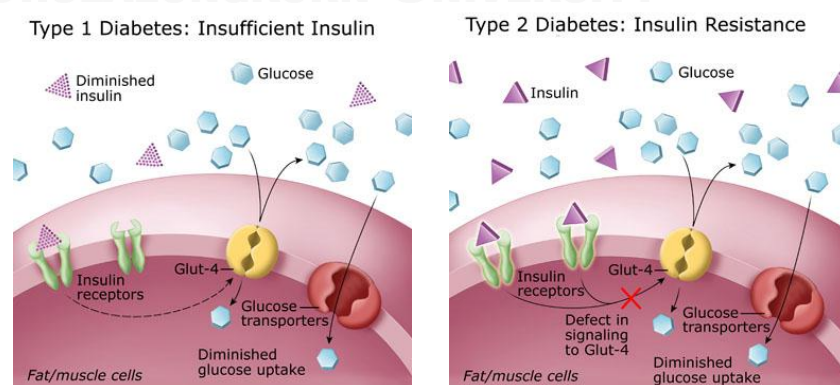
Figure 1.3 Defective insulin secretions for type I and II diabetes

1.1.2 Type 1 (insulin-dependent diabetes mellitus (IDDM)):

The body's inability to produce insulin from pancreatic β-cell islets leads to a deficiency of insulin. IDDM usually appear before the age of 40 (during childhood) or early adolescence. Therefore, the patients required daily insulin injection. Type 1 diabetes has been postulated that environmental factors such as certain viral infections and possibly chemical or nutritional agents may worsen these genetic factors (Acharjee, Ghosh, Al-Dhubiab, & Nair, 2013).

1.1.3 Type 2 (non-insulin-dependent diabetes mellitus (NIDDM):

The body can still produce insulin, but not enough, or the insulin that is produced does not work properly (known as insulin resistance) as shown in Figure 1.3. The pancreas secretes insulin to reduce glucose output by the liver, maintain glucose uptake by skeletal muscle, and suppress fatty acid release from fat issue. Consequently, the insulin less secretion will reduce insulin signaling in its target tissue, leading to increased circulating fatty acid. In turn, the raised concentrations of glucose and fatty acids in the bloodstream will feed back to worsen both insulin secretion and insulin resistance.

Type 2 diabetes is characterized by three abnormalities: relative insulin deficiency, insulin resistance involving myocytes and adipocytes, and hepatic insulin resistance as resulting in increased gluconeogenesis and impaired glycogen synthesis). The biochemical abnormalities of type 2 diabetes may include hyperinsulinemia and high levels of serumtriglycerides (TG).

The people at risk of developing type 2 diabetes are associated with obesity, age, lack of physical activity, genetic and condition associated of insulin resistance.

1.2 Oral anti-diabetic drugs

The pathogenesis of diabetes mellitus and its management by the oral medications of hypoglycemic agents have stimulated great interest in recent years. Control of hyperglycemia can be potentially achieved by different mechanisms:

(1) Increase in insulin secretion

(2) Decrease in nutrient ingestion

(3) Removing free glucose from the bloodstream and capturing it in glycogen

(4) Decrease in hepatic glucose production.

Various groups of oral medications agents are available for clinical use such as sulfonylureas (increase insulin secretion), biguanides (increase in glucose uptake) (Figure 1.5), and digestive enzyme inhibitors (delay digestion and absorption of carbohydrate) (A. J. Krentz & Sinclair, 2012)

To date, one potential therapeutic approach for treating diabetes is to decrease the post-prandial hyperglycemia. This approach can be achieved by retarding absorption of glucose through the inhibition of the carbohydrate-hydrolysing enzyme, including α-glucosidase (sucrase, maltase and isomaltase) and amylase in the digestive system of the small intestine (Figure 1.4). The enzyme inhibitor can prolong overall carbohydrate digestion time, thus reducing in the rate of glucose absorption and consequently blunting the post-prandial plasma glucose level (Chiasson & Rabasa-Lhoret, 2004). In addition, the enzyme inhibitors decrease the posprandial increment in insulin levels, therefore reducing triglyceride levels and anti-HIV activity (Bridges, Brennan, Taylor, McPherson, & Tyms, 1994). Nevertheless, their administration is limited by the wide range gastrointestinal side effect such as abdominal discomfort, diarrhea, and flatulence (A. Krentz & Bailey, 2005).
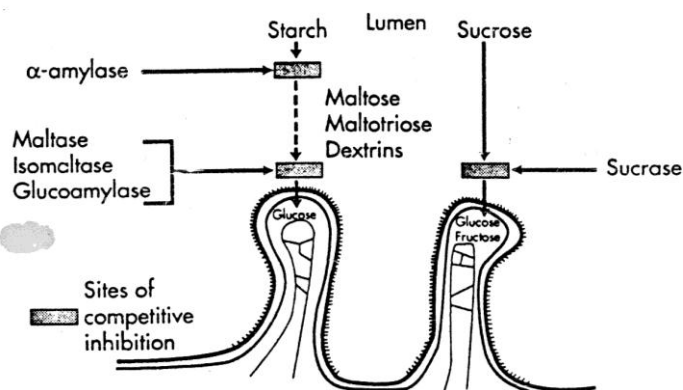
Figure 1.4 In normal digestion, pancreatic α-amylase hydrolyzes complex starches into oligosaccharides, which are further hydrolyzed by α-glucosidase located in the intestinal brush border to glucose and other monosaccharides, which are then absorbed.

Digestive enzyme inhibitors used currently for treatment type 2 diabetes include acarbose (Precose[®] or Glucobay[®]), miglitol (Glyset[®]) and voglibose (Basen[®]) (Figure 1.5) (Borges de Melo, da Silveira Gomes, & Carvalho, 2006).
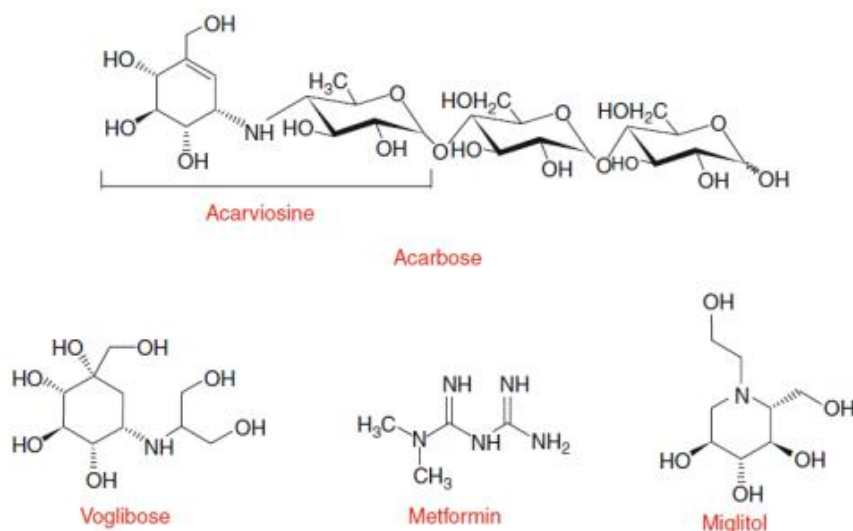
Figure 1.5 Structures of various digestive enzyme inhibitor

Acarbose (Precose® or Glucobay®) (Figure 1.5), produced from *Actinoplanes* sp, is the most widely used among digestive enzyme inhibitors because of its potent inhibition against sucrase, maltase and α-amylase. Acarbose inhibits α-glucosidase located in brush border in the small intestine and pancreatic α-amylase located in the lumen of the intestine competitively (Figure 1.6). Importantly, the patient used medication doses of acarbose do not cause malabsorption but long-term administration causes many side effects such as bloating, flatulence, diarrhea and soft stools.
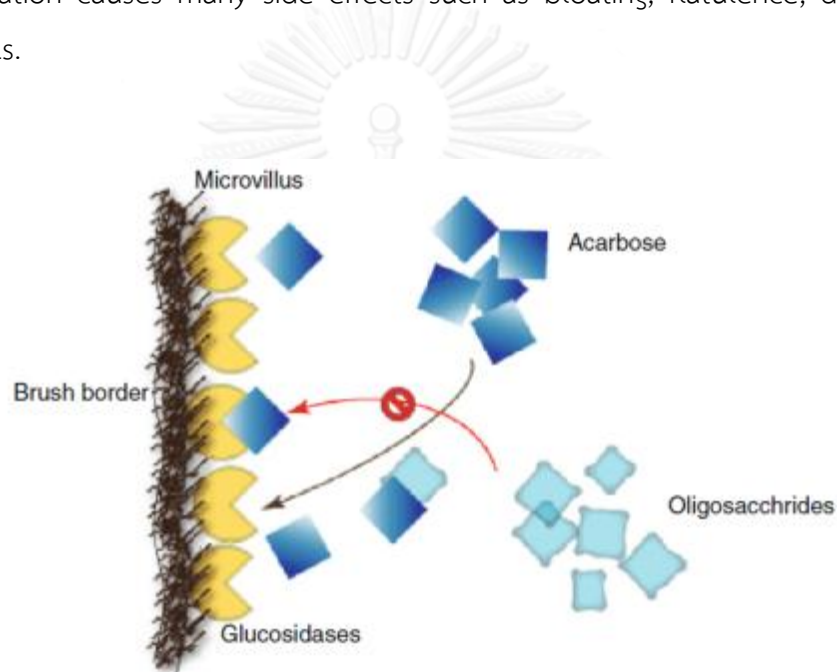
Figure 1.6 Mechanism of action of acarbose competitively inhibis the enzymatichydrolysis of oligosaccharide by α-glucosidase in the small intestine

1.3 Antidiabetic drugs from medicinal plants

Recently, more than 400 different plants and plant extracts have been used for diabetes therapy. Medical plants drugs are demonstrated alternative, safe effect and relatively low cost. Indian and Chinese medicines have long used plant and plant extract as treat diabetic (H. Chen, Feng, Guo, Sun, & Jiang, 2001). Consequently, determination of natural active components from medicinal plants become more important and result in discovery of new drug leads for diabetes treatment.

Singab reviewed α- and β-glucosidase inhibitor from natural source and synthesis pathway. 1-deoxynojirimycin (DNJ), (Figure 1.7) that isolated form *Morus alba* (Borges de Melo et al., 2006). The *N*-alkyl derivatives were effective and this led to development of *N*-hydroxythyl deoxynojirimycin (Miglitol or Glyset [®]) (Borges de Melo et al., 2006).
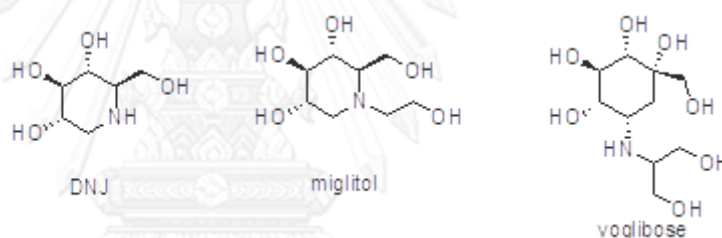
Figure 1.7 Structure of antidiabetic drug and derivatives

Voglibose (Basen [®]) is a derivative of 1-deoxynojirimycin (DNJ), which revealed high inhibitory activity against maltase and sucrase. It has been distributed in Japan since 1994 and their effectiveness is more potent than acarbose. In addition, voglibose led to less side effects of flatulency and abdominal disorders
Salacinol, a new type of α-glucosidase inhibitor, was isolated from an aqueous extract of the roots and stems of *Salacia reticulate* that are traditionally used in Sri Lanka and India. Salacinol revealed a strong activity for α-glucosidase inhibition such as maltase, sucrase and isomaltase;in which, the inhibition against isomaltase was higher than that of acrbose. In 1998, Yoskikawa and coworker (Yoshikawa, Murakami, Yashiro, & Matsuda, 1998) was synthesized derivative of 1, 2, 3-trihydroxy-propyl-salacinol (kotalanol) (Figure 1.8), which revealed more potent inhibitory activity against sucrase than salacinol and acarbose. The discovery of

kotalanol subsequently led to the development of antidiabetic drug named as Diaosol[®].
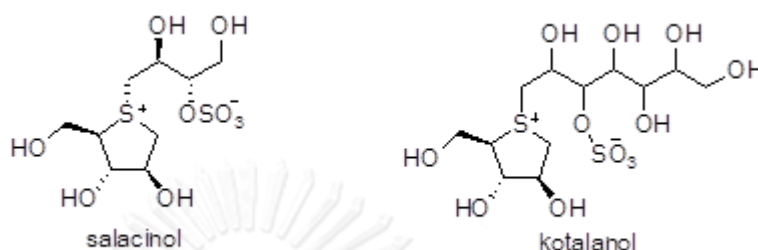
Figure 1.8 Structure of salacinol and kotalanol

1.4 α-Glucosidase inhibitor from edible plants

Some of the plants used by the population as anti-diabetic remedies are edible plants. These have added interest because they join two basic factors: food and medication. A menu including these types of plants could be developed for diabetic patients in order to improve their health and control their disease.

Sweet potato (*Ipomoea batatas*) is shown to be beneficial to diabetes. For instance, purple sweet potato is high in anthocyanins which have antidiabetic activity. Matsui and coworker (Matsui et al., 2001) found that anthocyanin extract from sweet potato had potent maltase inhibitory activity (IC_{50} value 0.36 mg/mL).

The tea drink is suggested to be beneficial to blood glucose control because the tea contains catechins, major component that might inhibit α-glucosidase. In addition, epicatechin gallate, epigallocatechin and gallocatechin gallate were shown to be yeast α-glucosidase inhibitor with IC_{50} values of 7.9, 7.6, and 3.2 μM, respectively (Yilmazer-Musa, Griffith, Michels, Schneider, & Frei, 2012). Their strong inhibition may be from the galloyl group esterified to the 3-position of the C-ring. Yao and coworkers (Yao, Cheng, Wang, Wang, & Ren, 2011) isolated viexin and isovitexin as α-glucosidase inhibitors from Azuki beans (*Vigna angularis*). Viexin and isovitexin inhibited rat intestinal α-glucosidase with IC_{50} values of 0.93 and 11 mM, respectively. The presence of glycosyl moieties in viexin possibly enhanced the inhibition. Sengupta and coworkers (Sengupta, Mukherjee, Goswami, & Basu, 2009) isolated saponarin from the leaves of *Tinospora cordifolia*. The saponarin showed inhibitory

activity against α-glucosidase of different origins. The IC_{50} values were 5.5 µM (fungi α-glucosidase), 48 µM (yeast), 48 µM (rat intestinal maltase), and 35 µM (rat intestinal sucrase). However, it inhibit α-glucosidase though mixed-type manner. Quercetin and Isorhamnetin isolated from aerial parts from *Brikellia cavanillesii* showed the activity against yeast α-glucosidase with IC_{50} value of 530 and 160 µM, respectively (Escandón-Rivera et al., 2012). The kinetic study showed that isorhamnetin is a mixed-type (K_i 1.91 mM).

Table 1.1 α-glucosidase inhibitors from edible plants

Plants	Inhibitor	Enzyme origin	IC$_{50}$	Mechanism	Ref
Ipomoea batatas **(Sweet potato)**	Anthocyanin	Rat intestinal	0.36 mg/ml	-	(Matsui et al., 2001)
Vigna angularis	Vitexin	Rat intestine	926 µM	-	(Yao et al., 2011)
	Isovitexin	Rat intestine	11 mM	-	

Table 1.2 α-glucosidase inhibitors from edible plants (cont'd)

Plants	Inhibitor	Enzyme origin	IC_{50}	Mechanism	Ref
Camellia sinensis **(Green tea)**					
	Epicatechin gallate	Barker's yeast	7.9 μM	-	(Yilmazer-Musa et al., 2012)
	Epigallocatechin		7.6 μM		
	Gallocatechin gallate		3.2 μM		
Tinospora cordifolia					
	Saponarin	Fungal maltase (*Aspergillus niger*) M-125	55 μM	Mixed	(Sengupta et al., 2009)
		Invertase (Barker's yeast)	48 μM	Mixed	
		Maltase/Sucrase (Rat intestine)	48/35 μM	Mixed	

Table 1.3 α-glucosidase inhibitors from edible plants (cont'd)

Plants	Inhibitor	Enzyme origin	IC_{50}	Mechanism	Ref
Brikellia cavanillesii					
	Quercetin	Barker's yeast	530 µM	-	(Matsui et al., 2001)
	Isorhamnetin	Barker's yeast	160 µM	Mixed	

CHAPTER II

α-GLUCOSIDASE INHIBITORS FROM *Piper sarmentosum* Roxb. Leave

2.1 Introduction

2.1.1 Botanical aspect and distribution

Piper sarmentosum Roxb., (Piperaceae, Thai name: Chaplu) (Figure 2.1). According to were reported that piperaceae consists of 4 genera and 2,000 species. This plant distributes in tropical zone, leave are simple, alternate, and cor-date, 5-10 cm wide, and 7-15 cm long. The flower has bar shape that call ovary and improves to a berry. In 1996, Saralamp (Saralamp P, 1996) reported that the leaves of piper are used as food and traditional medicine in Thailand.

2.1.2 Phytochemical and pharmacological investigation

In previous investigations *of P. sarmentosum*, it consists many phytochemicals such as amide alkaloids, phenylpropanoids (ascaricin, α-ascarone), lignans xanthophylls, tannins, total phenolic compounds, β-sitosterol, calcium, iron, vitamin B1, 2, C, E, β- carotene (T. Rukachaisirikul et al., 2004).

Figure 2.1 *Piper sarmentosum*

Kittisak and Nijsiri (Likhitwitayawuid, Ruangrungsi, Lange, & Decicco, 1987) studied the chemical constituents of petroleum ether dry leaves extract of *P. sarmentosum*. Six of them were identified as 1-(3,4-methylenedioxyphenyl)-1*E*-tetradecene, *N*-(3-phenylpropanoyl)pyrrole, β-sitosterol, pellitorine, sarmentine and sarmentosine. β-Sitosterol shows anti-tumor and anti-tuberculosis activity. In 1988, it reported constituents in non-polar part as α-asarone, asaronaldehyde.

Stohr and colleagues (Stöhr, Xiao, & Bauer, 2001) extracted *P. sarmentosum* aerial parts with hexane. The research found *N*-isobutly-2*E*, 4*E*-octadienamide, pellitorine,*N*-isobutyl-2*E*,4*E*-dodecadienamide,*N*-isobutyl-2*E*,4*E*-tetradecadienamide,*N*-isobutyl-2*E*,4hexadecadienamide, *N*-isobutyl-2*E*,4*E*-octadecadienamide, and *N*-2'-methylbutyl-2*E*,4*E*-decadienamide.

Aunpak and colleagues (Ridtitid, 2007) investigated chemical compounds of essential oil distilled from the leaves of *P. sarmentosum*, which contained that longifolene (24.30%), β-caryophyllene (10.10%), allo-aromadendrene (13.51%) and 9-epi-(*E*)-caryophyllene (18.24%).

Chanwitheesuk and colleagues (Chanwitheesuk, Teerawutgulrag, & Rakariyatham, 2005) determined the antioxidant of leaves. The methanol extract contained Vitamin E, Vitamin C, Carotenes, tannins, xanthophylls and other phenolic compounds.
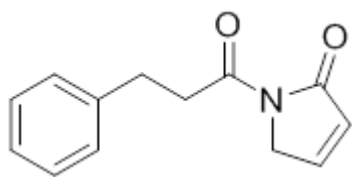
N-(3-phenylpropanoyl)pyrrole
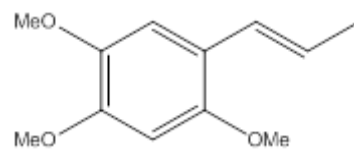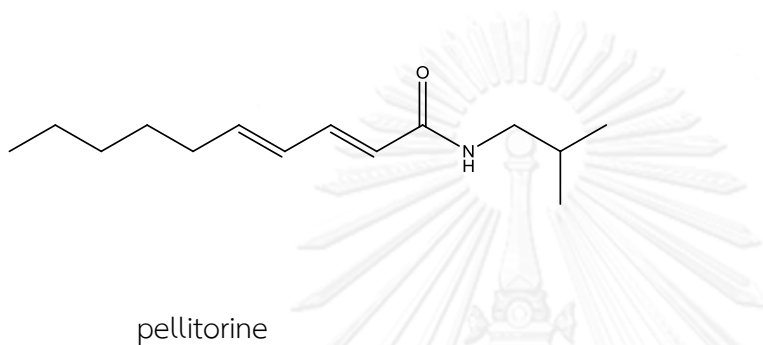
α-asarone

pellitorine
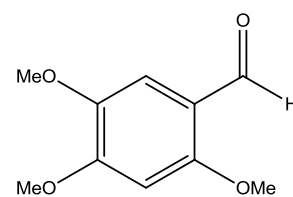
asaronaldehyde
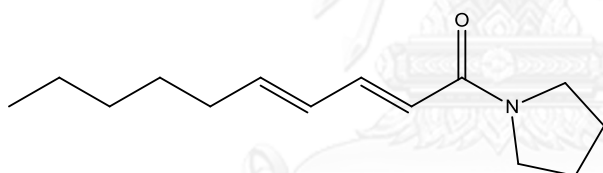
sarmentine
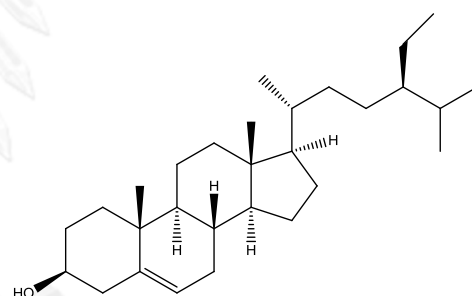
β-sitosterol
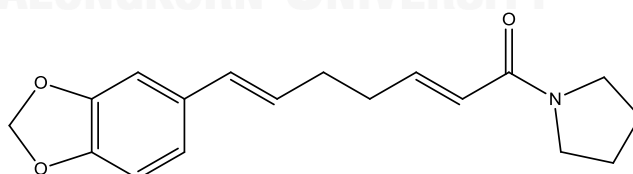
sarmentosine

Figure 2.2 Chemical compounds **found in** *Piper sarmentosum*

According to many reports of ethnopharmacologicaln use of *P. sarmentosum*, it can enhance appetite, relieve flatulent and asthma, relieved, refresh throat, carminative, expectorant, prevent platelet aggregation, reduce blood glucose level (Peungvicha et al., 1998) posses, anti-bacterial effect, reduce fever in influenza and help digestion (Thitima Rukachaisirikul et al., 2004). *P. sarmentosum* is of interest due to its inhibitory activity against α-glucosidase in our preliminary screening, In addition to previous report of its anti-diabetic activity (Thitima Rukachaisirikul et al., 2004). Consequently, the purpose of this are aimed at isolate, separate and identifying active components using α-glucosidase inhibition.

2.2 Results and discussion

2.2.1 Isolation

The dried leaves of *P. sarmentosum* were extracted with hexane and MeOH. The MeOH extract was partitioned by CH_2Cl_2. The CH_2Cl_2 layer was evaporated to dry and separated through vacuum column chromatography eluted with gradient system to obtain seven major fractions. Fraction 3 was purified by Sephadex LH-20 with 1:9 (v/v) MeOH: CH_2Cl_2 to remove chlorophylls and siliga gel column chromatography to afford chaplupyrrolidone A (**1**), chaplupyrrolidone B (**2**), *N*-(3-(4′Methoxyphenyl)propanoyl)pyrrole (**3**), *N*-(3-phenylpropa- noyl)pyrrole (**4**) and asaricin (**5**). Fraction 5 was purified by Sephadex LH-20 with 1:9 (v/v) MeOH: CH_2Cl_2 to remove chlorophylls and siliga gel column chromatography to afford cinnamic acid (**6**). Fraction 7 was purified by Sephadex LH-20 with 1:9 (v/v) MeOH: CH_2Cl_2 to remove chlorophylls and siliga gel column chromatography to afford deacetylsarmentamide B (**7**). The MeOH extract was predicated and isolated by vacuum column chromatography to obtain 3 fractions. Fraction 3 was purified by Sephadex LH-20 (MeOH: CH_2Cl_2 to remove chlorophylls and siliga gel column chromatography to afford kaemforol-3-*O*-rhamnoside (**8**) and dihydrokaempferol-3-*O*- glucoside (**9**).

Dried leave of *P. sarmentosum* (812 mg)

1) Extract with Hexane and MeOH

MeOH extract

2) Sespension in water

3) Partition with CH$_2$Cl$_2$

MeOH-H$_2$O crude extract

CH$_2$Cl$_2$ crude extract

11) VLC, CH$_2$Cl$_2$:MeOH   F1   F2   F3   F4   F5   F6   F7

F1   F2   F3

7) Sephadex LH-20
   MeOH:CH2Cl2
8) Crystallization
   with MeOH

9) Sephadex LH-20
   MeOH:CH$_2$Cl$_2$
10) Siliga gel
    MeOH:CH$_2$Cl$_2$

12) Sephadex LH-20, MeOH
13) Silica gel, MeOH:CH$_2$Cl$_2$

kamforal-3-*O*-rhamnoside
(**8**, 42.7 mg)

dihydrokamferol-3-*O*-glucoside
(**9**, 18.02 mg)

cinnamic acid (**6**, 380 mg)

deacetylsamentamide B
(**7**, 40 mg)

F3

5) Sephadex LH-20
   MeOH:CH$_2$Cl$_2$
6) Silica gel
   EtOAc:hexane

asaricin (**5**, 18 mg)

chaplupyrrolidone A (**1**); R = H (24 mg)   *N*-(3-(4'-Methoxyphenyl)propanoyl)pyrrole (**3**); R = OCH$_3$ (12 mg)
chaplupyrrolidone B (**2**); R = CH$_3$ (20 mg) *N*-(3-phenylpropanoyl)pyrrole (**4**); R = H (9 mg)

Scheme 2.1 Isolation procedure of isolated compounds from *P.samentosum* leaves.

2.2.2 Structure elucidation of chaplupyrrolidone A (1)

Chaplupyrrolidone A (**1**) was obtained as yellow powder. The molecular formula $C_{13}H_{13}NO_3$ was determined by HRESIMS of pseudomolecular ion (M+H)$^+$ at m/z 232.0975 (calcd 232.0974), in conjunction with NMR data analysis. The ^{13}C NMR spectrum showed ten carbon signals that were ascribable to two methylene (δ_C 29.9 and 38.0), eight methine (δ_C 81.9, 126.3 (2x), 128.5 (3x) 128.6 and 147.4) and three quaternary carbons (δ_C 140.5, 167.7 and 173.6), based on the HSQC data analysis. In addition, **1** revealed ^{1}H NMR signals in three distinct regions: phenyl protons [δ_H 7.13–7.24 (m, 5H)], olefinic protons [δ_H 6.12 and 7.07 (each 1H)] and downfield methylene protons [δ_H 3.20 and 2.93 (each 2H)]. The COSY spectrum also showed three separate spin systems (Fig 2.3) that were comprised of monosubstituted benzene, two contiguous methylenes as well as olefinic methines linked with oxygenated proton at δ_H 6.07. Each established residue was assembled using the HMBC data analysis. The left end of the two contiguous methylenes was connected with a benzene ring, as evident by the cross peaks of H-3'/C-9' and H-2'/C-4', while the right terminal was linked to C-1' (δ_C 173.6), as indicated by the HMBC correlations of H-2' and H-3' to C-1', thereby establishing the phenylpropanoyl motif. The remaining portion ($C_4H_4NO_2$) contained an α,β-unsaturated amide, as deduced by the presence of the quaternary carbon at δ_C 167.7 and the olefinic signals [δ_H 6.12 (d, J = 6.0 Hz) and δ_C 128.5, and δ_H 7.07 (dd, J = 4.4, 6.0 Hz) and δ_C 147.4]. This portion was similar to the Δ^3-2-pyrrolidone moiety of sarmentamide A (Tuntiwachwuttikul, Phansa, Pootaeng-On, & Taylor, 2006), except for the presence of unusual downfield shifts of the methine signal (δ_H 6.07 and δ_C 81.9). The aforementioned data indicated that the methylene group in the Δ^3-2-pyrrolidone moiety of sarmentamide A was replaced by an oxygenated methine in **1**, thereby establishing the 5-hydroxy-Δ^3-2-pyrrolidone portion. The diagnostic HMBC cross peak of H-5/C-1' indicated the connectivity of phenylpropanoyl and 5-hydroxy-Δ^3-2-pyrrolidone moieties through a nitrogen atom, thus constructing the overall structure of **1**.
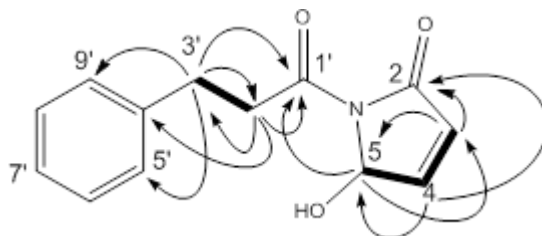
Figure 2.3 Selected HMBC (arrow curves) and COSY (bold lines) correlations

of chaplupyrrolidone A (**1**)

2.2.3 Structure elucidation of chaplupyrrolidone B (2)

Chaplupyrrolidone B (**2**) was obtained as yellow powder. The molecular formula was deduced from the HRESIMS analysis of pseudomolecular ion $(M+H)^+$ at m/z 246.1121 (calcd 246.1130), which accounted for the $C_{14}H_{15}NO_3$ formulae. It displayed ^{1}H and ^{13}C NMR resonances nearly identical to those of **1**, except for subtle difference in signals of the H-5 (δ_H 5.93) and C-5 (δ_C 88.9). Careful examination of the NMR spectra together with additional 14 amu and one methoxy signal (δ_H 3.32 and δ_C 55.4) in **2** pointed out the presence of the methoxy group, which was positioned at C-5 by the discernable HMBC cross peaks of 5-OCH$_3$ (δ_H 3.32) to C-5 and H-5 to 5-OCH$_3$ (δ_H 55.4). Although **2** has one chiral center at C-5, the absolute configuration could not be readily addressed by applying Moscher's method. However, the closely related NMR spectra of **1**and **2** along with the negative specific rotation of **2** allowed us to propose the *S* configuration for **2** that the configuration of corresponding chairal center of **1** and **2** are identical.

2.2.3 Structure elucidation of deacetylsarmentamide B (7)

Deacetylsarmentamide B (**7**) was obtained as yellow solid. The molecular formula $C_{13}H_{15}NO_3$ was established by the HRESIMS analysis of the pseudomolecular ion (M+Na)$^+$ at m/z 256.0944 (calcd 256.0950). **7** showed ^{1}H and ^{13}C NMR spectra that only resembled those of **1** and **2** in the aromatic region. Although signals of olefinic protons (H-2' and H-3') were also observed in **7**, a large coupling constant of 15.6 Hz indicated their *trans*-orientation. The HMBC cross peaks of H-2'/C-4', H-3'/C-1', H-3'/C-2' and H-3'/C-9'suggested that *trans*-olefinic protons were located between the benzene ring and the quaternary carbonyl (δ_C 167.7), which was relatively upfield compared to those observed in **1** and **2**, which together established the *trans*-cinnamoyl moiety. The remaining residue of $C_4H_8NO_2$ was assigned to be a dioxygenated pyrrole based on the COSY and HMBC data analysis (Figure 2.3). The COSY spectrum showed contiguous correlations of H-2 (δ_H 3.68 and 3.71), H-3 (δ_H 4.20), H-4 (δ_H 4.13) and H-5 (δ_H 3.60 and 3.95), suggesting a spin system of –N–CH$_2$–CH(O)–CH(O)–CH$_2$–N–. The ^{1}H and ^{13}C NMR chemical shifts of this residue were related to those of the deoxygenated pyrrole group in sarmentamide B, except for the striking upfield shifts of C-3 and C-4. This information indicated that the two acetoxy groups in sarmentamide B were both replaced by hydroxy groups in **7**. The dioxygenated pyrrole moiety was connected to the cinnamoyl residue through an amide bond, supported by the HMBC correlations of H-2/C-1' and H-5/C-1'. Once the overall structure of **7** was established, the relative configuration of C-3 and C-4 were addressed by NOESY and coupling constant analysis. The observed NOESY correlations of H-2β/H-5 β and H-2 β /H-3 (Figure 2.4) indicated that they occupied the same phase, whilst the small coupling constant (4.1 Hz) of H-3 and H-4 suggested their *trans*-orientation of the vicinal protons in the dihydroxy pyrrolidine ring (Clerc, 1989).
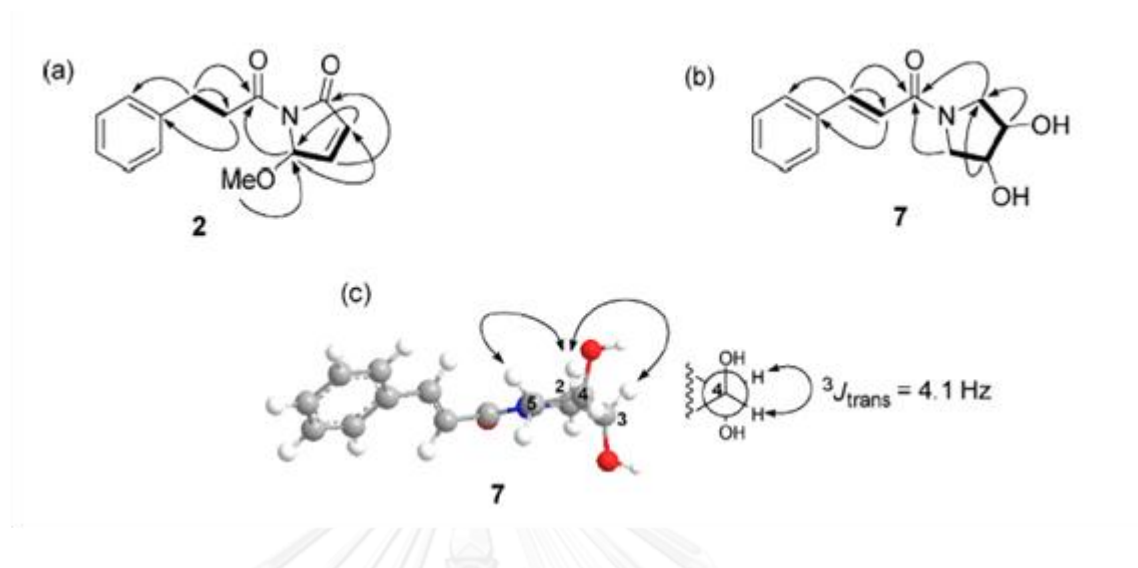
Figure 2.4 (a and b) Selected HMBC (arrow curves) and COSY (bold lines) correlations of **2** and **7**, respectively; (c) diagnostic NOESY correlations and Newman projection showing dihedral angle of H-3 and H-4 on deoxygenated pyrrole of **7**.

Table 2.1 ^{1}H (400 MHz) and ^{13}C (100 MHz) NMR data of chaplupyrrolidones A (**1**), B (**2**) recorded in CDCl$_3$ and deacetylsarmentamide B (**7**) recorded in CD$_3$OD.

Position	1		2		7	
	δ_C	δ_H, mult, J in Hz	δ_C	δ_H, mult, J in Hz	δ_C	δ_H, mult, J in Hz
2	167.7		168.5		53.7	α 3.71, dd, 4.1, 11.2 β 3.68, d, 11.2
3	128.5	6.12, d, 6.0	128.5	6.08, d, 5.9	75.1	4.20, brd, 4.1
4	147.4	7.07, dd, 4.4, 6.0	146.7	7.00, dd, 4.8, 5.9	77.9	4.13, brd, 4.1
5	81.9	6.07, brd, 4.4	88.9	5.93, brd, 4.8	55.3	α 3.60, d, 13.2 β 3.95, dd, 4.4, 13.2
5-OH		4.34, brs^a				
5-OCH$_3$			55.4	3.32, s		
1'	173.6		173.1		167.7	
2'	38.0	3.20, m	38.5	3.20, m	119.4	6.94, d, 15.6
3'	29.9	2.93, t, 7.6	30.2	2.94, t, 7.6	143.6	7.63, d, 15.6
4'	140.5		140.7		136.4	
5', 9'	128.5	7.24, m	128.7	7.22, m	129.1	7.64, m
6', 8'	126.3	7.13, m	126.6	7.12, m	129.9	7.40, m
7'	128.6	7.13, m	128.8	7.12, m	131.0	7.40, m

^{a} The signal underwent deuterium exchange completely soon before acquiring 2D NMR experiment

2.2.4 α-Glucosidase inhibitory activity of compounds 1-9

α-Glucosidase inhibitor used baker's yeast and rat intestinal for activity of isolated compounds 1-9 and comparison with type II diabetes drugs (acarbose).

Table 2.2 α-glucosidase inhibitory effect of isolated compounds **1-9**

Compounds	α-glucosidase inhibitory IC_{50} (µM)		
	Baker's yeast	Rat intestinal	
		Maltase	Sucrase
1	7,842.0±6.0	NI	NI
2	430.0±1.2	NI	NI
3	NI	NI	NI
4	NI	NI	NI
5	NI	NI	NI
6	NI	NI	NI
7	NI	NI	NI
8	NI	NI	NI
9	NI	NI	NI
acarbose	403.9±0.4	1.52±0.14	2.38±0.02

[a]NI, no inhibition, inhibitory effect less than 30% at 10 mg/mL.

Compounds **1** and **2** inhibited α-glucosidase from yeast with IC_{50} values of 7820 and 430 mM, respectively, while **3–7** showed no detectable inhibition (Table 2.2). Interestingly, compound **2** was 18-fold more potent than that of **1** and was comparable to the antidiabetic drug acarbose (IC_{50} value of 404 mM). To gain insight into the mechanism underlying the inhibitory effect of **2**, a kinetic study was also conducted. The Lineweaver–Burk plots (Figure 2.5) revealed a linear relationship at each tested concentration of **2**, all of which intersected the x-axis at a single negative value. The analysis demonstrated that V_{max} decreased with increasing concentrations of **2** while K_m remained constant (Table 2.3), supporting that **2** inhibits α-glucosidase in a noncompetitive manner (K_i of 1.04 mM) by equally forming enzyme-inhibitor and substrate–enzyme-inhibitor complexes.

Table 2.3 Inhibition mechanism

Type of inhibition	K_m	V_{max}	Intersection
Competitive	increase	unchanged	Y axis, Y>0
Non-competitive	unchanged	decrease	X axis, X<0
Uncompetitive	decrease	decrease	no intersection
Mixed	increase	decrease	second quadrant
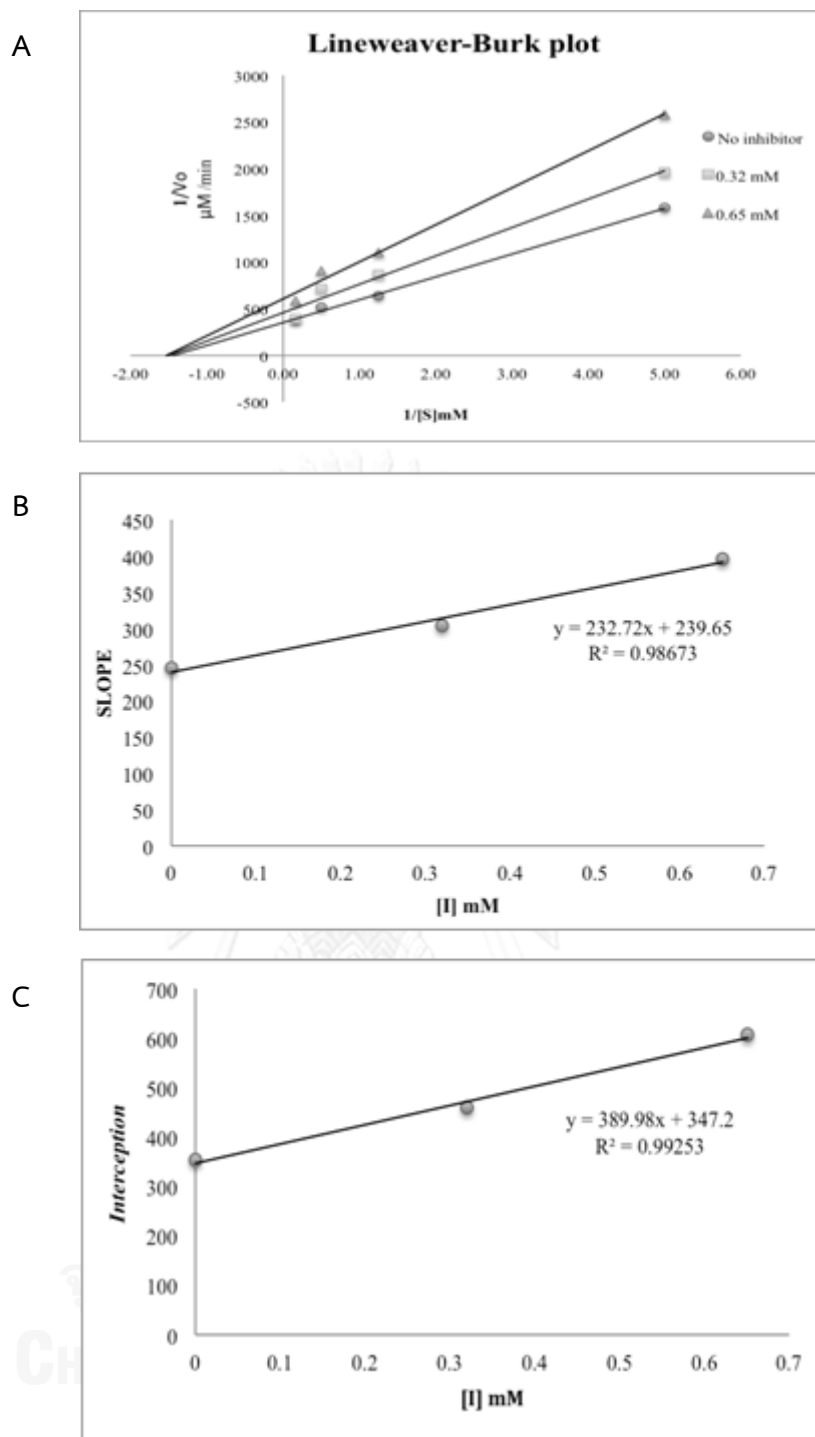
Figure 2.5 (A) Lineweaver-Burk plot of chaplupyrrolidone B (**2**), $1/V$ aginst $1/[S]$. (B) Secondary replot of slope *vs.* [*I*] from a primary Linewaaver-Burk plot for the determination of K_i. (C) Secondary replot of intercept *vs.* [I] from a primary Lineweaver-Burk plot for determination of $K_{i'}$.

2.3 Experiment section

2.3.1 General experimental procedures

UV spectra were measured with a UV-7504 spectrophotometer. Optical rotations were determined using a Perkin-Elmer 341 polarimeter using a cell with a 2-mL capacity and a 10 cm path length. High-resolution mass spectra were recorded on a Bruker micrOTOF mass spectrometer, equipped with an electrospray ionization (ESI) ion source. The ^{1}H and ^{13}C NMR spectra were acquired by Varian Mercury+ 400 and Bruker AVANCE 400 spectrometers. Chemical shifts were reported in d (ppm) relative to deuterated solvent residues (7.25 and 77.0 ppm for $CDCl_3$ and 3.30 and 49.0 ppm for CD3OD). TLC was performed on precoated Merck silica gel 60 F_{254} plates (0.25 mm thick layer), and spots were visualized under UV or dipped in 3% (v/v) anisaldehyde, 9.7% (v/v) H_2SO4, 87.3% (v/v) MeOH followed by heating. α-Glucosidase (EC 3.2.1.20) from *Saccharomyces cerevisiae* and 4-nitrophenyl- α - D-glucopyranoside (PNPG) were obtained from Sigma–Aldrich (St. Louis, MO, USA). Acarbose was obtained from Bayer Vitol Leverkusen, Germany. Spectrophotometric measurements for the α-glucosidase inhibition and kinetic study were taken on a Sunrise microplate reader.

2.3.2 Plant material

The leaves of *P. samentosum* were collected from Samutprakan, in February 2011. Plant authentication was performed Mrs. Parinyanutch Klinrat, Department of Botany, Faculty of Science, Chulalongkorn University. A voucher specimen (BCU013525) has been deposited at the Department of Botany, Faculty of Science, Chulalongkorn University (Bangkok, Thailand).

2.3.3 Extraction and isolation

The active CH_2Cl_2 extract obtained from the dried leaves (812.09 g). These were sequentially extracted at room temperature with hexane (3x4 L) and MeOH (3x 5 L), respectively. The MeOH extract was suspended in water and partitioned with CH_2Cl_2 (3x1 L) to afford the active CH_2Cl_2 extract, which was chromatographed by Vacuum column chromatography and eluted with a six step gradient mobile phase of 0:1, 1:9, 3:7, 1:1, 4:1 and 1:1 (v/v) ratio EtOAc:hexane, to afford seven major fractions. Fraction 3 was preliminarily chromatographed on Sephadex LH-20 with a 1:9 (v/v) MeOH:CH_2Cl_2 mobile phase to remove the residual chlorophylls, which eluted in the early fractions. The fractions that eluted after the chlorophylls were combined, concentrated and subsequently purified by silica gel centrifugal chromatography using mixtures of EtOAc:hexane as the eluting mobile phase. Two major bands eluted in the 3:7 (v/v) EtOAc:hexane fractions and were collected separately to yield **1** (24 mg) and **2** (20 mg). *N*-(3-(4´-Methoxyphenyl)propanoyl)pyrrole (**3**, 12 mg), *N*-(3-phenylpropa- noyl)pyrrole (**4**, 9 mg) and asaricin (**5**, 18 mg) were subsequently obtained in the fractions eluted with 4:6 (v/v) EtOAc:hexane. Fraction 5 was chromatographed on Sephadex LH-20 (1:9 MeOH–CH2Cl2) followed by crystallization (MeOH) to afford cinnamic acid (**6**, 380 mg). Fraction 7 was chromatographed on Sephadex LH-20 (1:9 MeOH–CH_2Cl_2) to remove the chlorophylls, and the combined fractions eluted after the chlorophylls were further purified by silica gel centrifugal chromatography and eluted with a 2:8 (v/v) MeOH:CH_2Cl_2 mobile phase to give deacetylsarmentamide B (**7**, 40 mg). The MeOH-H_2O extract (96.41 g) was purification and isolated by Vacuum column chromatography of (0:1, 1:9, 2:8, 3:7 and5:5 ratio CH_2Cl_2: MeOH to obtain 3 fractions. Fraction 3 was preliminarily chromatography on Sephadex LH-20 with MeOH after purified by silica gel using mixtures of MeOH:CH2Cl2 to give keamforal-3-*O*-rhamnoside (**8**, 42.7 mg) and dihydrokaempferol -3-*O*-glucoside (**9**, 18.02 mg).

Chaplupyrrolidone A (1) Yellow powder; $[\alpha]_D^{20}$ -2.4° (c 0.335, CH_2Cl_2); UV (CH_2Cl_2) λ_{max} (log ϵ) 266 (6.46) nm; HRESIMS m/z $[M+H]^+$ 232.0975 (calcd for $C_{13}H_{14}NO_3$, 232.0974); ^{1}H NMR (CDCl$_3$, 400 MHz) and ^{13}C NMR (CDCl$_3$, 100 MHz) spectral data are given in Table 2.1

Chaplupyrrolidone B (2) Yellow powder; $[\alpha]_D^{20}$ -3.5° (c 0.425, CH_2Cl_2); UV (CH_2Cl_2) λ_{max} (log ϵ) 266 (7.31) nm; HRESIMS m/z $[M+H]^+$ 246.1121 (calcd for $C_{14}H_{16}NO_3$, 246.1130); ^{1}H NMR (CDCl$_3$, 400 MHz) and ^{13}C NMR (CDCl$_3$, 100 MHz) spectral data are given in Table 2.1

***N*-(3-(4'- Methoxyphenyl)propanoyl)pyrrole (3)** Yellow solid; ^{1}H NMR (CDCl$_3$, 400 MHz) δ_H 7.28 (d, J = 14.5 Hz, 2H), 7.17 (d, J = 8.38 Hz, 2H), 6.85 (J = 8.50 Hz, 2H), 6.28 (d, J = 2.07 Hz, 2.07), 3.79 (s, 3H), 3.10 (dd, J = 12.29 Hz, 2H), 3.05 (dd, J = 6.27 Hz, 2H) and ^{13}C NMR (CDCl$_3$, 100 MHz) δ_C 169.7, 158.2, 129.7, 129.1, 120.56, 114.0, 113.1, 52.4, 34.3, 27.2

***N*-(3-phenylpropa-noyl)pyrrole (4)** Yellow solid; ^{1}H NMR (CDCl$_3$, 400 MHz) δ_H 7.27 (m, 7H), 7.27 (overlapped, 1H), 6.28 (t, J = 2.4 Hz, 1H), 3.13 (t, J = 6.4 Hz, 1H), 3.12 (t, J = 6.4 Hz, 1H) and ^{13}C NMR (CDCl$_3$, 100 MHz) δ_C 169.61, 140.2, 128.7, 128.4, 126.5, 119.2, 113.0, 36.3, 30.4

Asaricin (5) Colorless oil; ^{1}H NMR (CDCl$_3$, 400 MHz) δ_H 6.40 (s, 1H), 6.37 (s, 1H), 5.95 (s, 2H), 5.89-5.98 (m, 1H), 5.09-5.13 (m, 2H), 3.91 (s, 3H), 3.31 (d, J = 6.0 Hz, 2H) and ^{13}C NMR (CDCl$_3$, 100 MHz) δ_C 148.8, 143.5, 137.4, 134.6, 133.5, 115.9, 107.6, 102.7, 101.2, 56.5, 40.2

Cinnamic acid (6) Yellow solid; ^{1}H NMR (CDCl$_3$, 400 MHz) δ_H 7.65-7.54 (m, 2H), 7.5-7.36 (m, 3H), 6.48 (d, J = 15.9 Hz, 1H) and ^{13}C NMR (CDCl$_3$, 100 MHz) δ_C 167.7, 144.0, 134.3, 130.3, 128.9, 128.5, 119.4

Deacetylsarmentamide B (7) Yellow solid; $[\alpha]_D^{20}$ +5.1° (c 0.180, CH$_3$OH); UV (CH$_3$OH) λ_{max} (log ϵ) 277 (1.71) nm; HRESIMS m/z $[M+Na]^+$ 256.0944 (calcd for $C_{13}H_{15}NO_3Na$, 256.0950); ^{1}H NMR (CD$_3$OD, 400 MHz) and ^{13}C NMR (CD$_3$OD, 100 MHz) spectral data are given in Table 2.1

Kaemferol-3-*O*-glucoside (8) Yellow powder; ^{1}H NMR (CD$_3$OD, 400 MHz) δ_H 7.69 (d, *J* = 8.5 Hz, H-2'', H6',), 6.98 (d. *J* = 8.5 Hz, H-3',), 6.93 (d, *J* = 5.8, H-5'), 6.42 (d, *J* = 1.6 Hz, H-8), 6.21 (d, *J* = 1.6 Hz, H-6), 5.49 (s, H-11"), 5.46 (t, *J* = 2.38 Hz, H-2"), 3.74 (d, *J* = 8.07 Hz, H-3"), 3.27 (t, *J* = 9.55 Hz, H-4"), 3.18 (t, *J* = 6.21 Hz, H-5"), 0.91(d, *J* = 6.09 Hz, H-6") and ^{13}C NMR (CD$_3$OD, 100 MHz) δ_C 176.9, 164.9, 161.7, 160.7, 157.8, 157.0, 133.1, 131.2, 120.9, 116.0, 99.5, 98.9, 94.4, 72.5, 72.1, 69.0, 18.2

Dihydrokaemferol-3-*O*-glucoside (9) Yellow solid; ^{1}H NMR (CD$_3$OD, 400 MHz) δ_H 7.24 (2H, d, *J* = 8.5 Hz, H-2', H-6'), 7.10 (2H, s, H-6''',H-3'''), 6.73 (2H, d, *J* = 8.5 Hz, H-3' ,H-5'), 5.93 (1H, d, *J* = 2 Hz, H-6), 5.87 (1H, d, *J* = 2 Hz, H-8), 5.24 (1H, d, *J* = 11 Hz, H-2), 4.81 (1H, *J* = 11 Hz, H-3), 4.36 (1H, d, *J* = 6 Hz, H-6"a and H-6"b), and 3.04-3.45 (4H, m, sugar portion). ^{13}C NMR (CD$_3$OD, 100 MHz) δ_C 64.5, 71.3, 74.5, 75.7, 76.70, 77.5, 83.5, 96.4, 102.1, 102.6, 110.4, 110.2, 121.5, 139.9, 146.6, 116.2, 128.5, 130.4, 130.7, 159.2, 164.0, 164.9, 168.3, 169.0, 195.8

2.3.4 α-Glucosidase inhibitory activity

α-Glucosidase inhibitory activity from baker's yeast

The α-glucosidase (EC 3.2.1.20) was produced from Baker's yeast. Briefly, 10 µL of the test sample was mixed with α-glucosidase (0.1 U/mL, 40 mL) in 1 mM phosphate buffer (pH 6.9) and incubated at 37 °C for 10 min. Then 40 mL of 0.1 mM *p*-nitrophenyl-α -D-glycopyrano- side (PNPG) was added and the mixture was then incubated for 30 min prior to being quenched with the addition of 100 mL 0.1 M Na$_2$CO$_3$. The enzymatic activity was monitored by following the concentration of released *p*-nitrophenol, evaluated via monitoring the absorbance at 415 nm. The percent inhibition was determined according to the equation: $[(A_0-A_1)/A_0] \times 100$, where A_1 and A_0 are the absorbance with and without the sample, respectively The IC$_{50}$ value was determined from a plot of percentage inhibition on the y-axis against the sample concentration on the x-axis. Acarbose was used as the positive control.

Kinetic study

The enzyme kinetic analysis was performed according to the above reaction except that the quantity of α-glucosidase from barker's yeast was maintained at 0.3 U/mL while the concentration of each tested inhibitor was varied at 0, 0.32 and 0.65 mM. The type of inhibition was determined from Lineweaver–Burk plots, where the K_i values were determined from the secondary plots of slope vs. [I] and the interception vs. [I] of the Lineweaver–Burk plot.

α-Glucosidase inhibitory activity from rat intestine

α-Glucosidase is crude enzyme that produced from rat intestine consist maltase and sucrase. The enzyme received from rat intestinal acetone powder (Sigma, St. Louis); then, the powder (1 g) was homogenized with 0.9% NaCl (30 ml) and centrifugation (12,000 g) for 30 min. Briefly, 10 μL of the test sample and substrate solution (maltose: 10mM, 20μl; sucrose: 100mM, 20 μl, respectively) in 0.1 M phosphate buffer (pH 6.9); therefore, incubate reaction 37°C for maltose (20 min) and sucrose (60 min). The mixtures were discontinued in boiling water for 10 min to stop reaction were determined by the glucose assay kit and measured at 500 nm. The percentage inhibition was calculated by $[(A_0-A_1)/A_0] \times 100$, where A_1 and A_0 are the absorbance with and without the sample, respectively. The IC_{50} value was determined from a plot of percentage inhibition on the y-axis against the sample concentration on the x-axis. The positive control used acarbose.

Supporting information
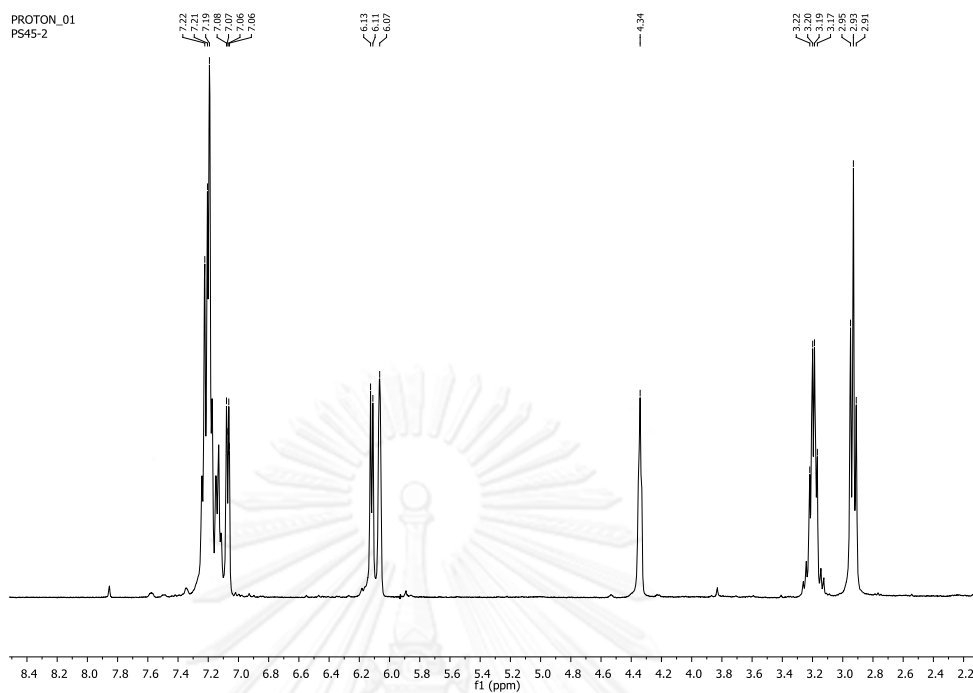
Figure 2.6 ^{1}H-NMR spectrum (400 MHz, in CDCl$_3$) of chaplupyrrolidones A (**1**)
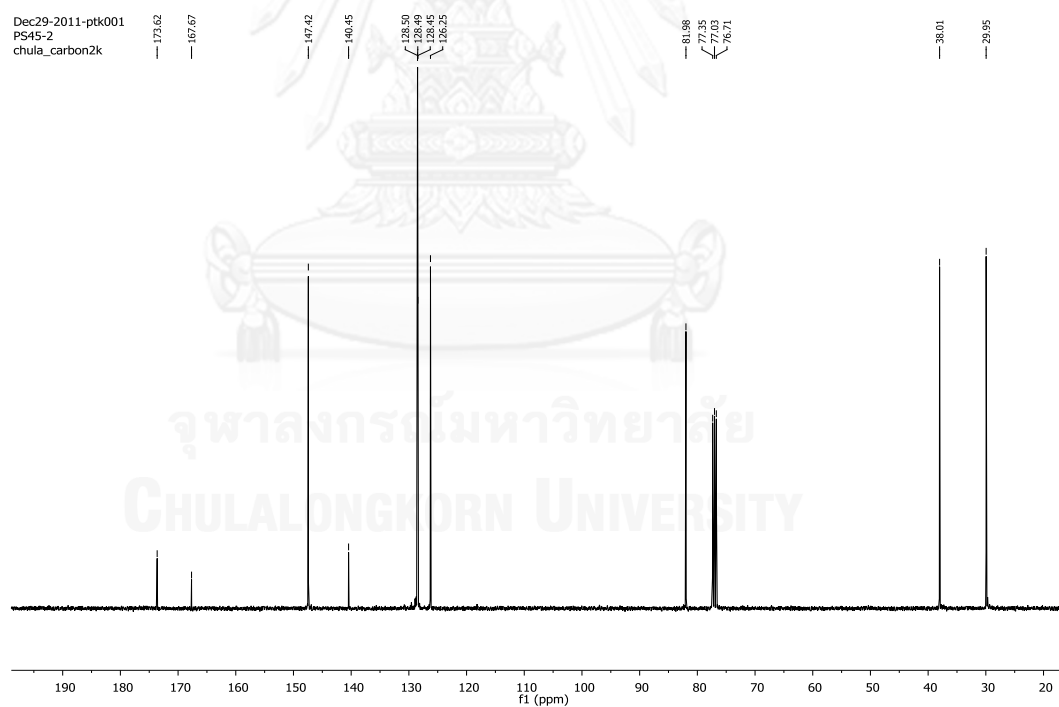
Figure 2.7 ^{13}C-NMR spectrum (100 MHz, in CDCl$_3$) of chaplupyrrolidones A (**1**)
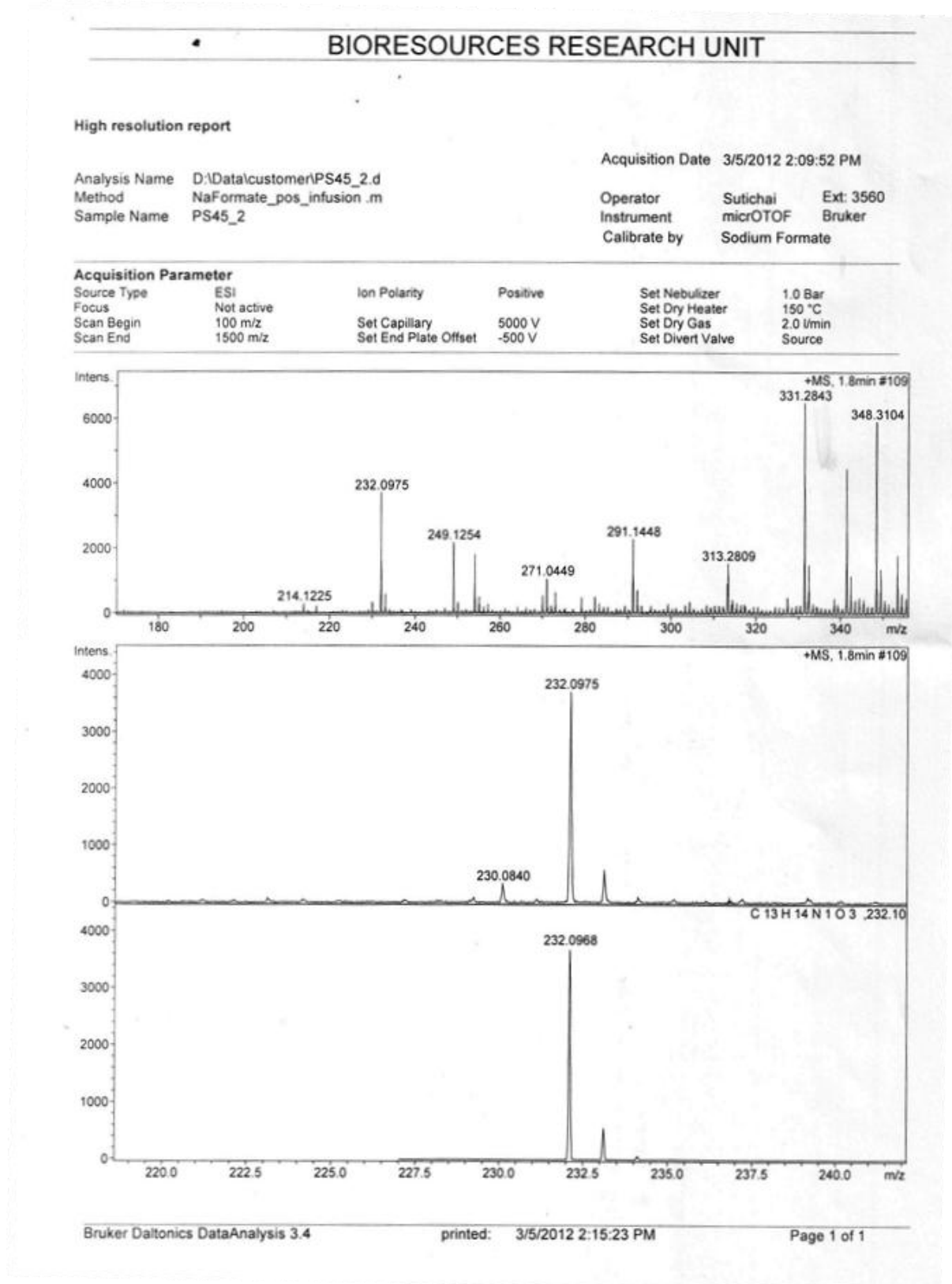
Figure 2.8 HR-EIMS spectrum of chaplupyrrolidones A (**1**)
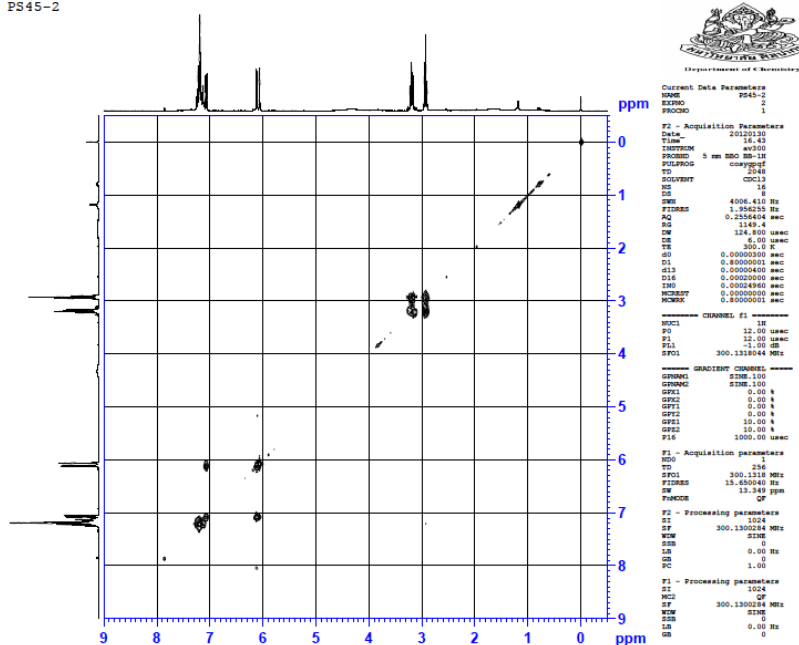
Figure 2.9 ^{1}H-^{1}H COSY spectrum (300 MHz, in CDCl$_3$) of chaplupyrrolidones A (**1**)
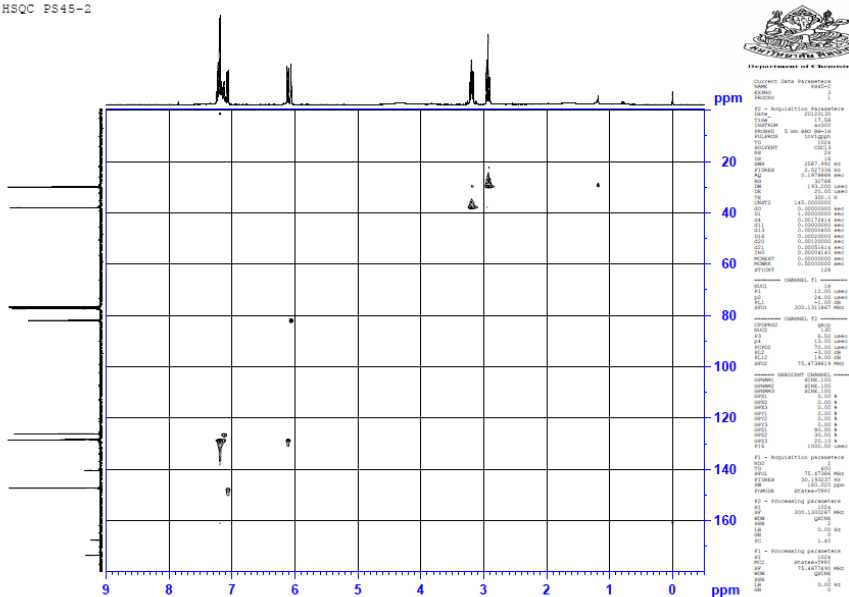
Figure 2.10 HSQC spectrum (300 MHz, in CDCl$_3$) of Chaplupyrrolidones A (**1**)
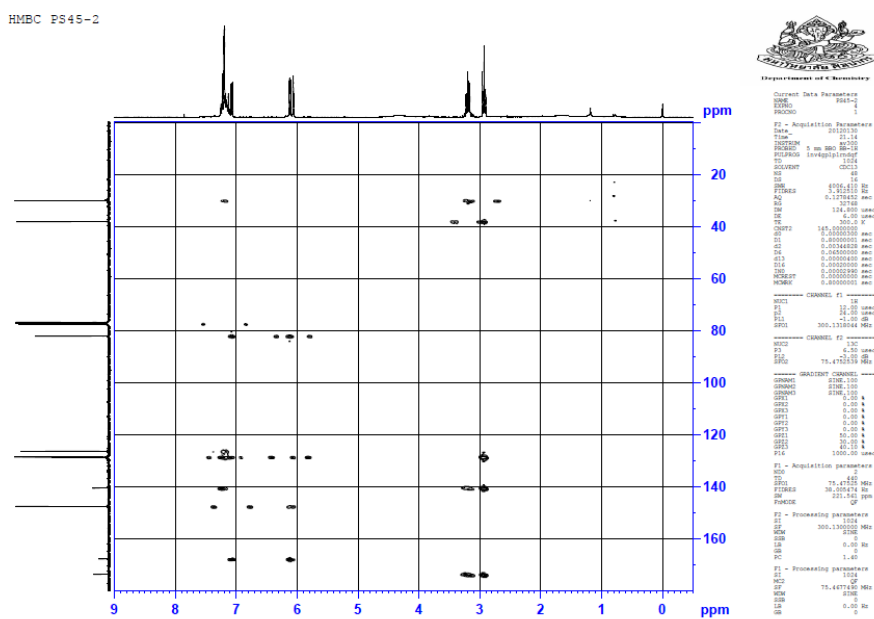
Figure 2.11 HMBC spectrum (300 MHz, in CDCl₃) of chaplupyrrolidones A (**1**)
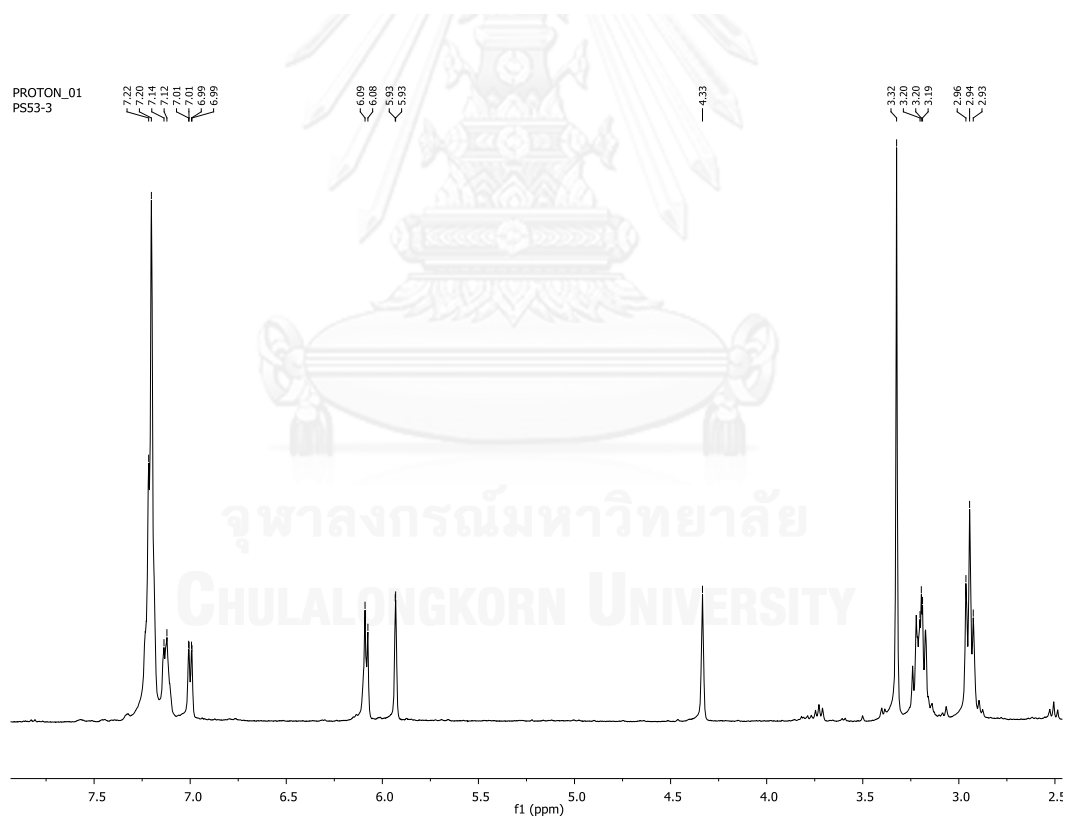
Figure 2.12 ¹H-NMR spectrum (400 MHz, in CDCl₃) of chaplupyrrolidones B (**2**)
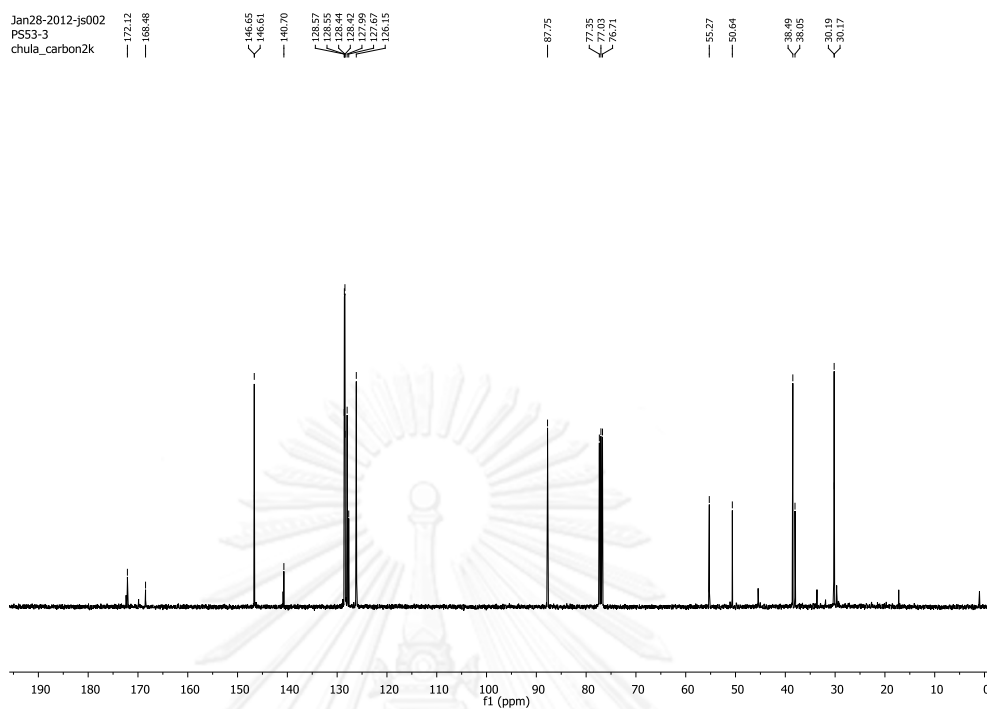
Figure 2.13 ^{13}C-NMR spectrum (100 MHz, in CDCl₃) of chaplupyrrolidones B (**2**)

Figure 2.14 ^{1}H-^{1}H COSY spectrum (300 MHz, in CDCl₃) of chaplupyrrolidones B (**2**)

Figure 2.15 HR-EIMS spectrum of chaplupyrrolidones B (**2**)

Figure 2.16 HSQC spectrum (300 MHz, in CDCl₃) of chaplupyrrolidones B (**2**)

Figure 2.17 HMBC spectrum (300 MHz, in CDCl₃) of chaplupyrrolidones B (**2**)

PROTON_01
PS43-1
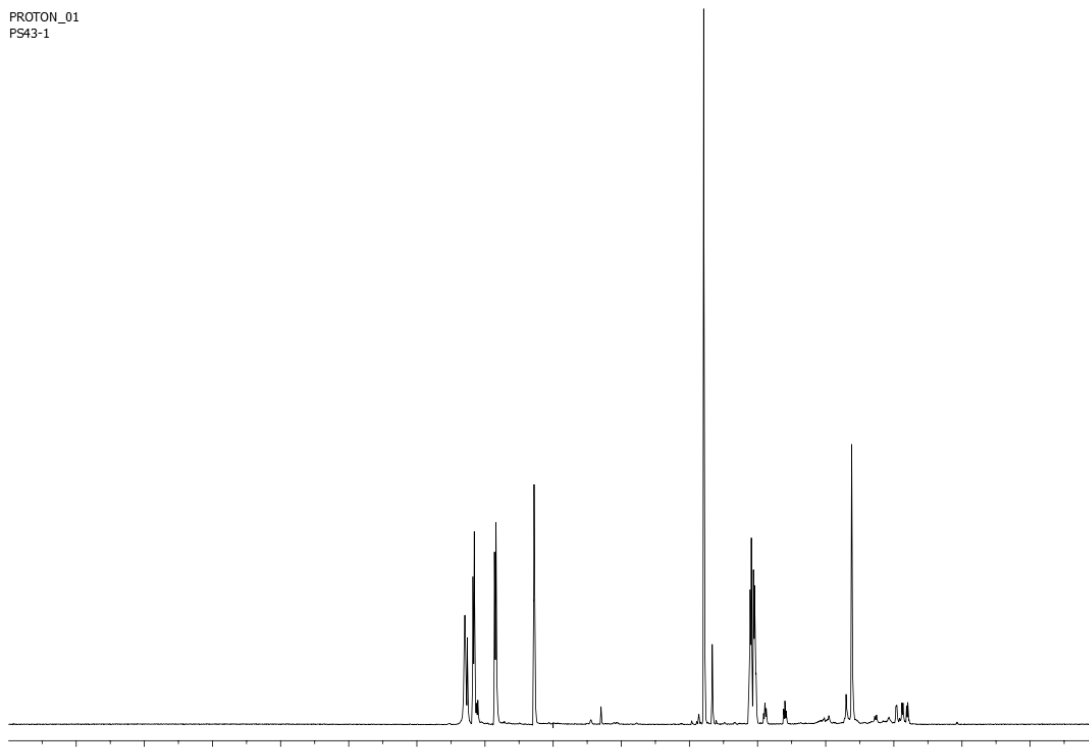
Figure 2.18 ^{1}H-NMR spectrum (400 MHz, in CDCl$_3$) of *N*-(3-(4'methoxyphenyl)propanoyl)pyrrole **(3)**

Jan07-2012-ww001
PS43-1
chula_carbon3k

230 220 210 200 190 180 170 160 150 140 130 120 110 100 90 80 70 60 50 40 30 20 10 0 -10 -20 -30
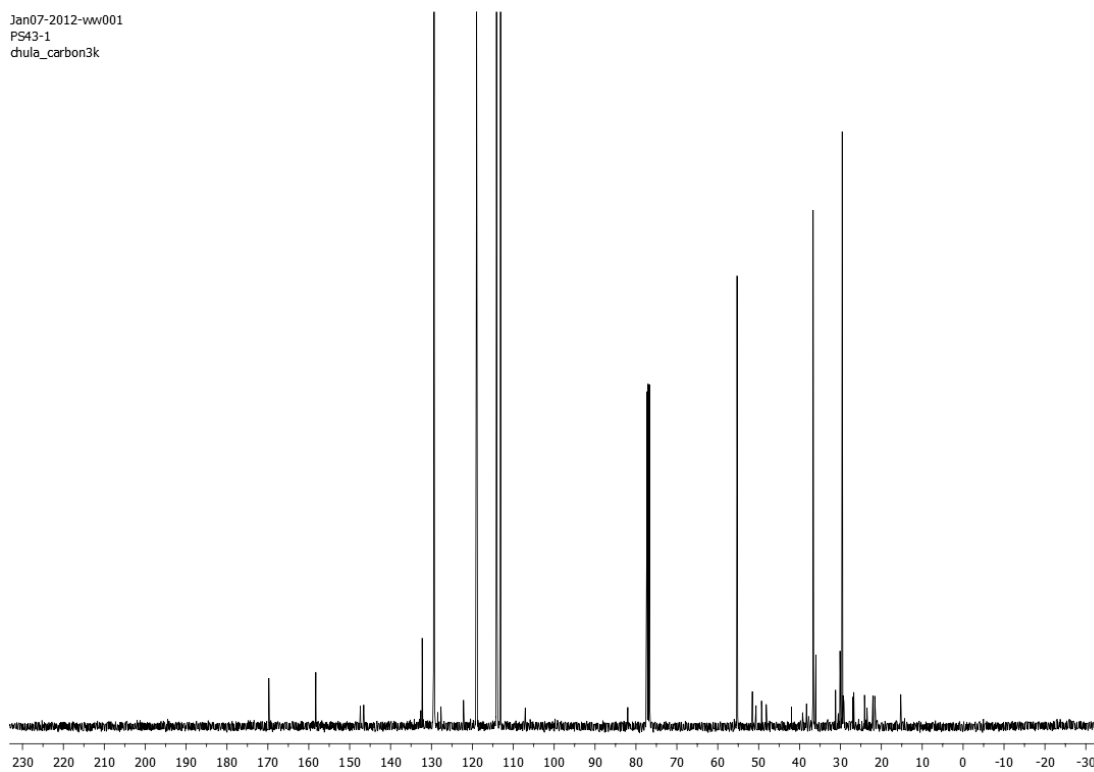
Figure 2.19 ^{13}C-NMR spectrum (100 MHz, in CDCl$_3$) of *N*-(3-(4'methoxyphenyl)propanoyl)pyrrole **(3)**
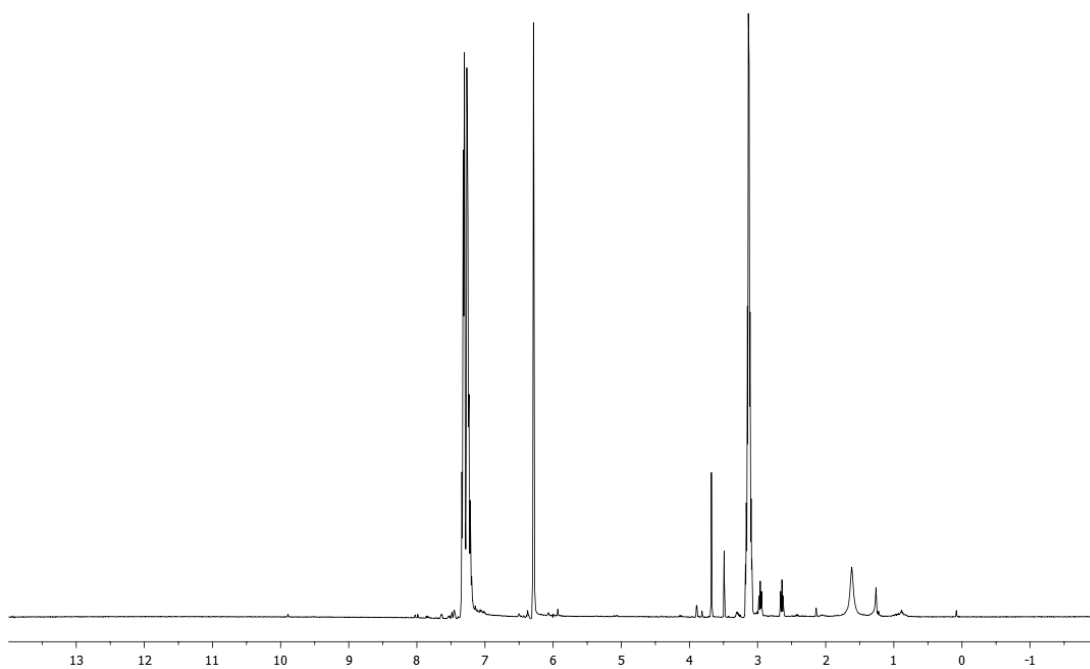
Figure 2.20 ^{1}H-NMR spectrum (400 MHz, in CDCl$_3$) of *N*-(3-phenylpropa-noyl)pyrrole (**4**)
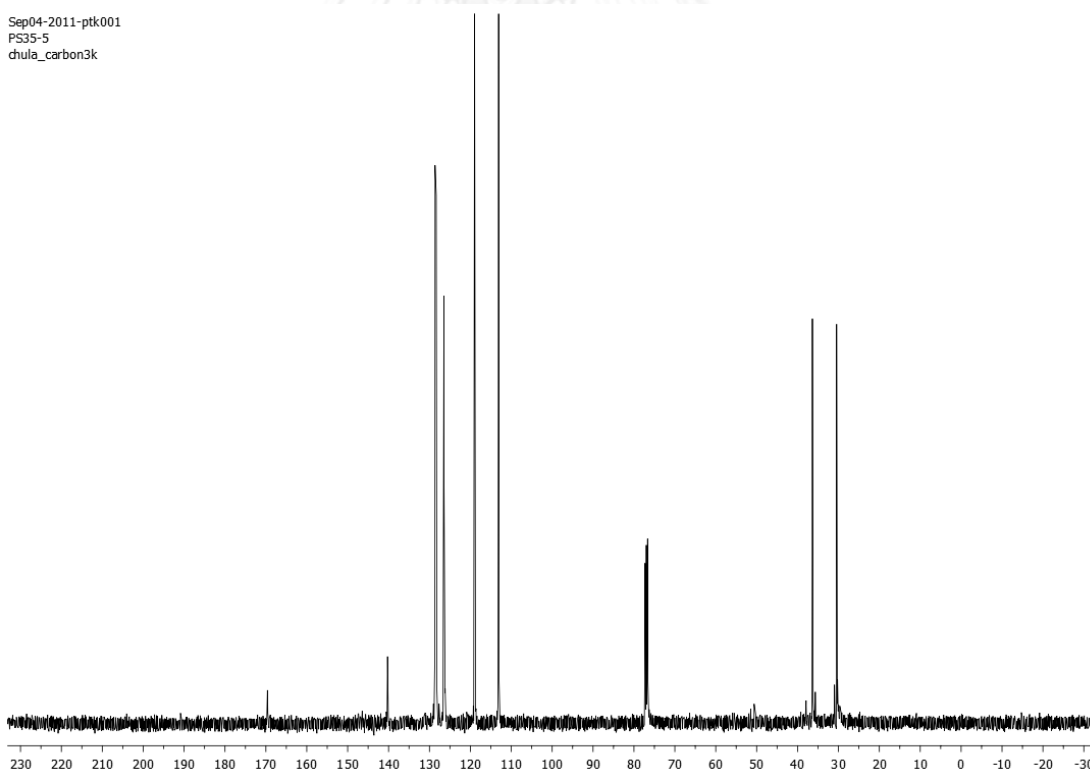
Figure 2.21 ^{13}C-NMR spectrum (100 MHz, in CDCl$_3$) of *N*-(3-phenylpropa-noyl)pyrrole(**4**)
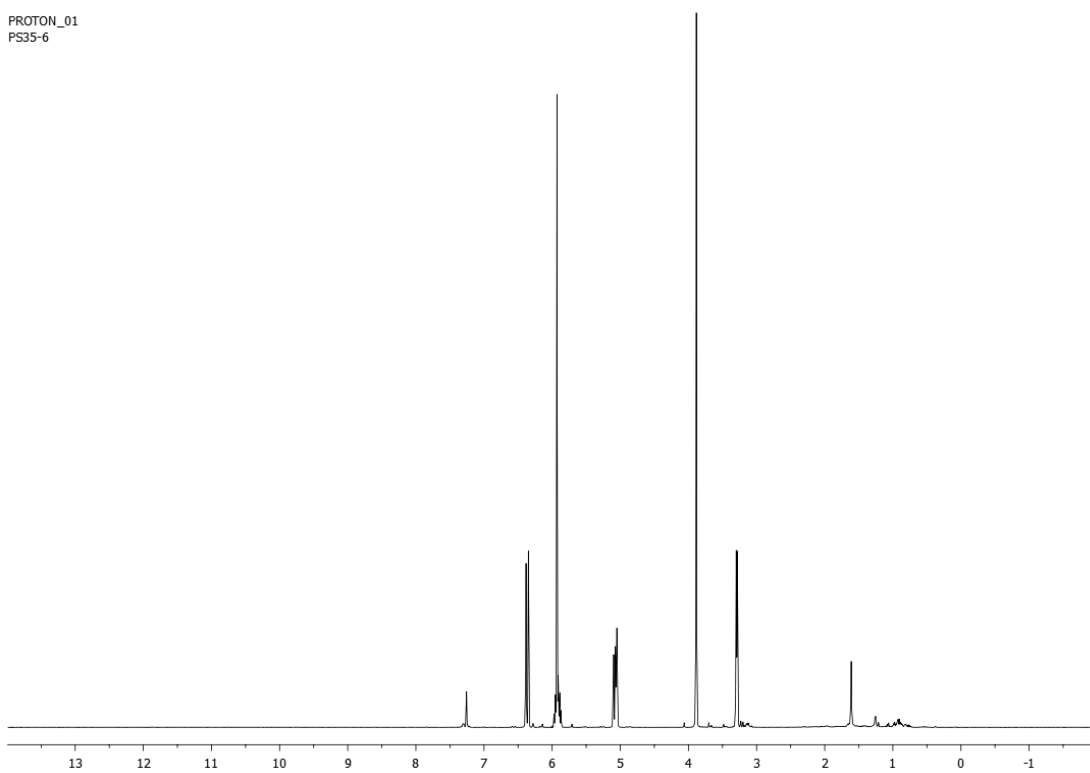
PROTON_01
PS35-6

Figure 2.22 ^{1}H-NMR spectrum (400 MHz, in CDCl$_3$) of asaricin (**5**)

Aug29-2011-ptk001
PS35-6
chula_carbon3k
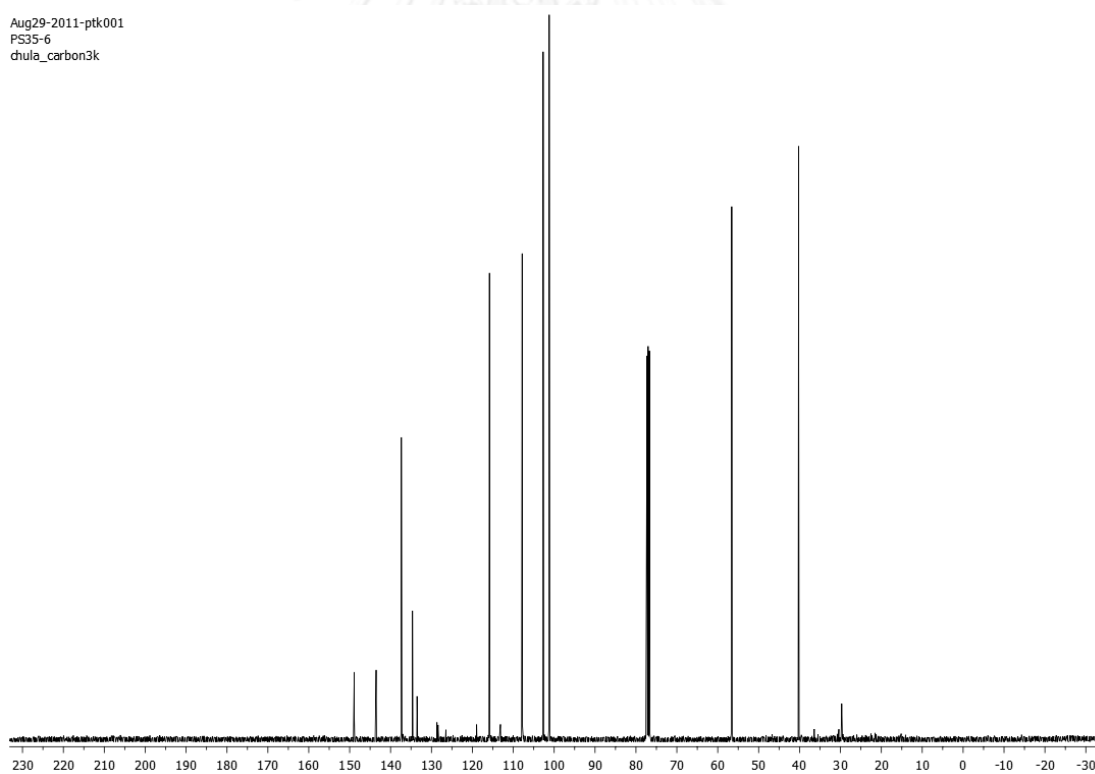
Figure 2.23 ^{13}C-NMR spectrum (100 MHz, in CDCl$_3$) of asaricin (**5**)

PROTON_01
PS 27-6
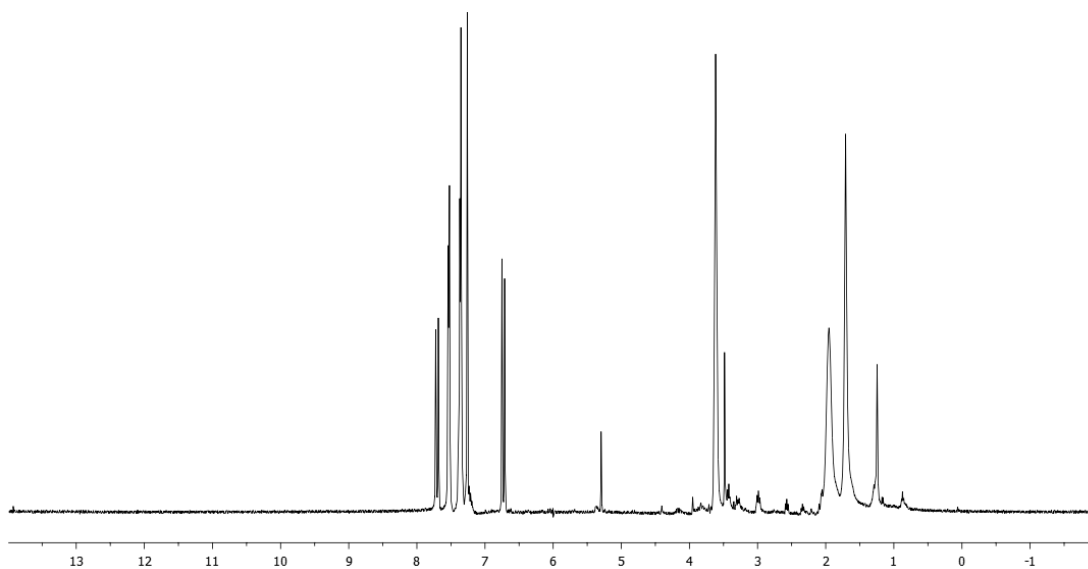
Figure 2.24 ^{1}H-NMR spectrum (400 MHz, in CDCl₃) of cinnamic acid (**6**)

Aug03-2011-ww001
PS27-6
chula_carbon3k
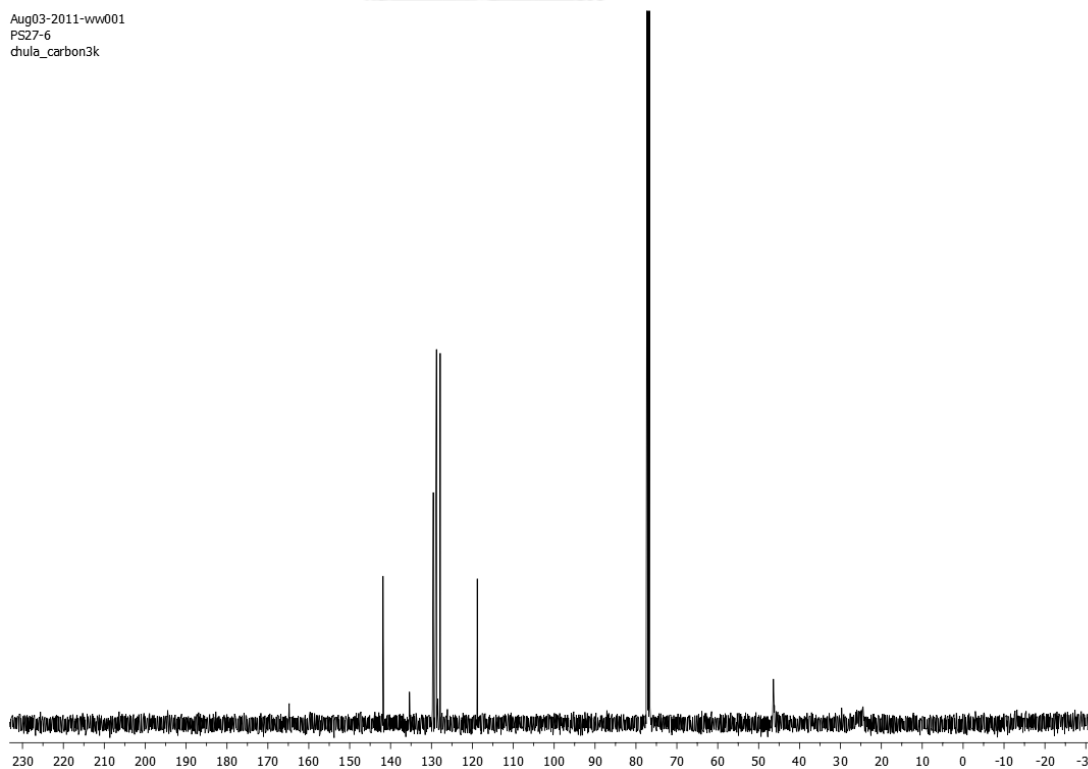
Figure 2.25 ^{13}C-NMR spectrum (100 MHz, in CDCl₃) of cinnamic acid (**6**)
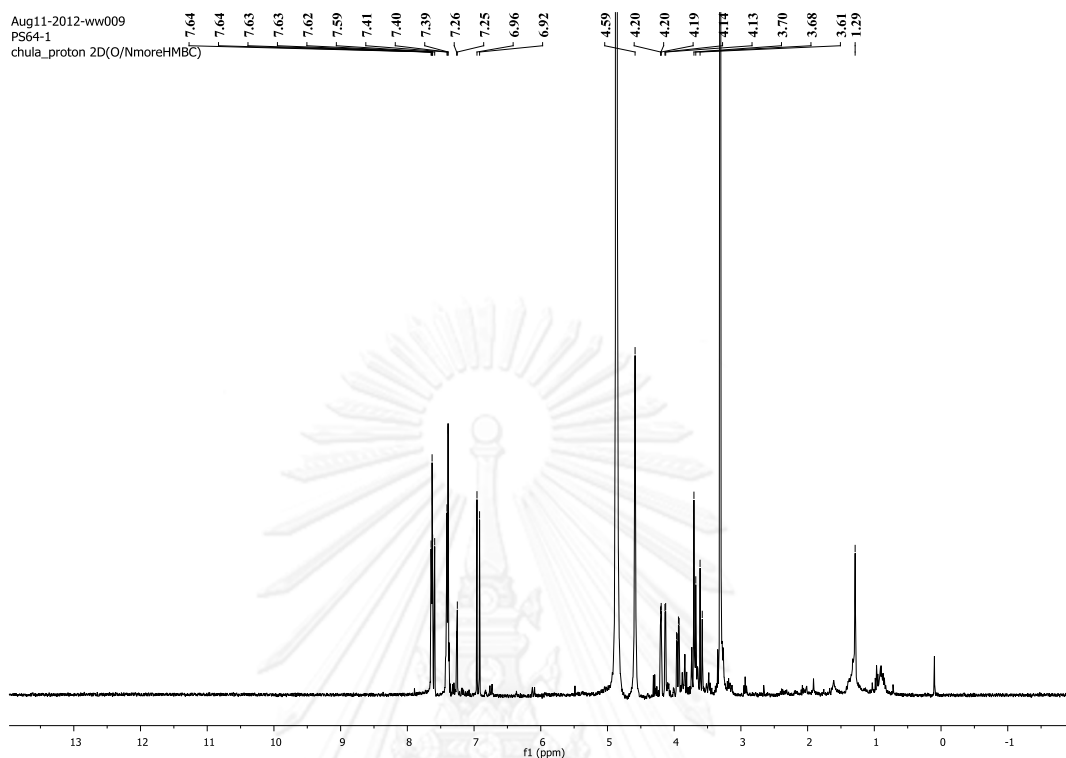
Figure 2.26 ^{1}H-NMR spectrum (400 MHz, in Methanol D$_4$) of deacetlysarmentamide B (**7**)
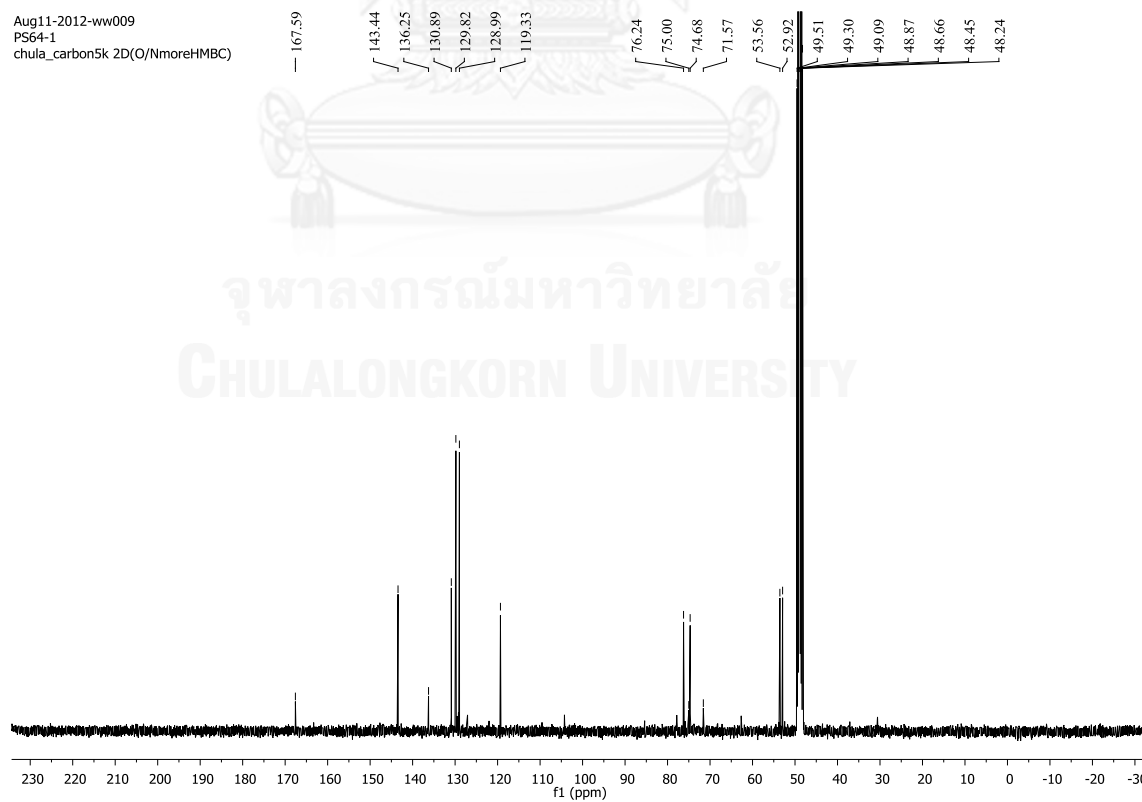
Figure 2.27 ^{13}C-NMR spectrum (100 MHz, in Methanol D$_4$) of deacetlysarmentamide B (**7**)
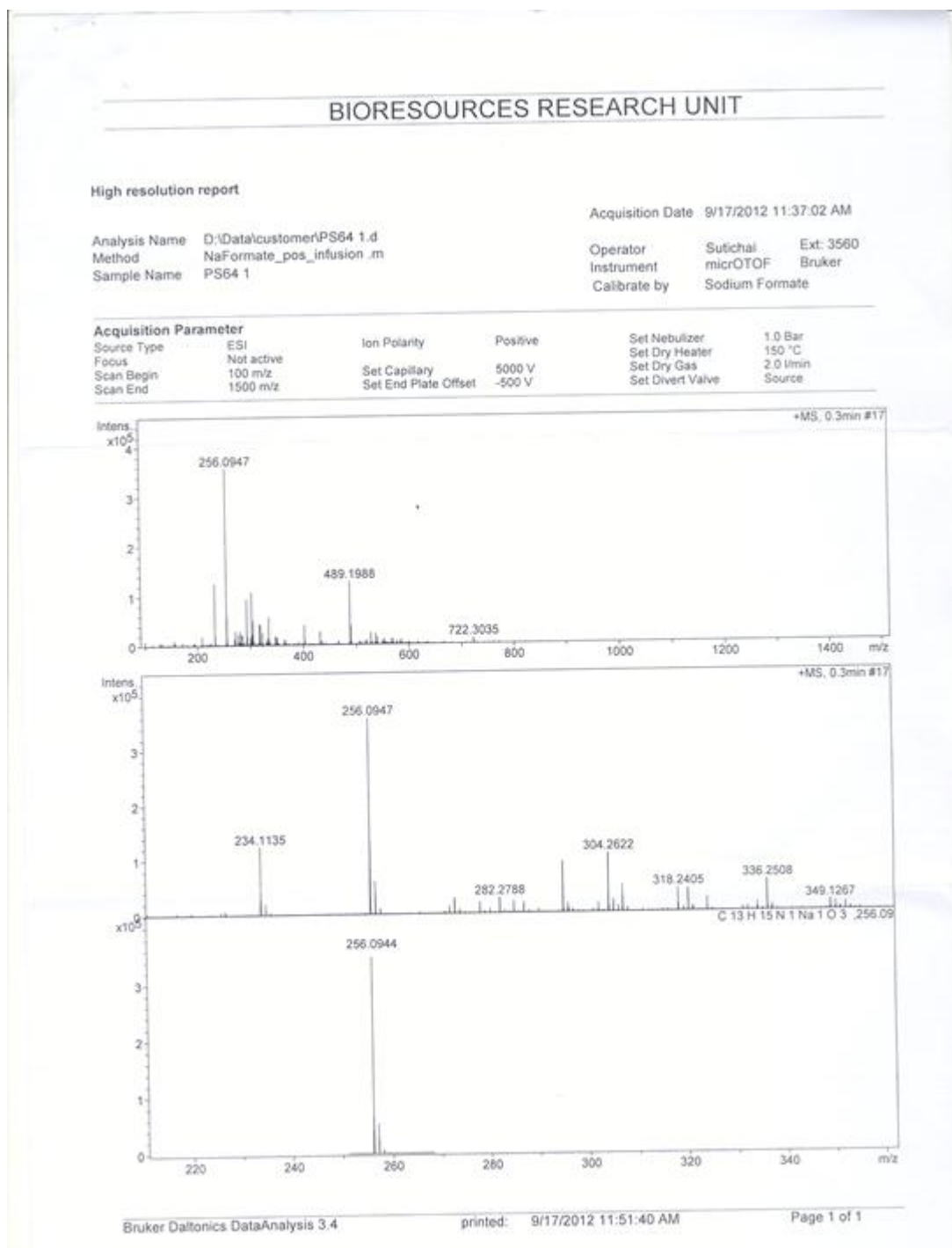
Figure 2.28 HR-EIMS spectrum of deacetlysarmentamide B (**7**)
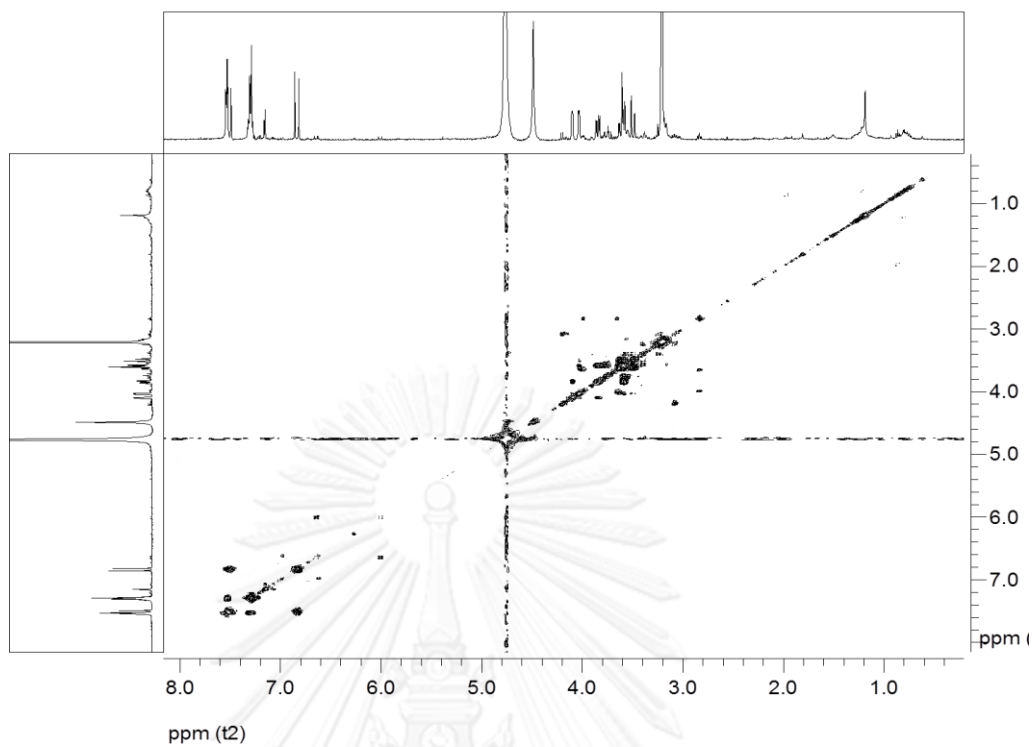
Figure 2.29 ^{1}H-^{1}H COSY spectrum (300 MHz, in Methanol D$_4$) of deacetlysarmentamide B (**7**)
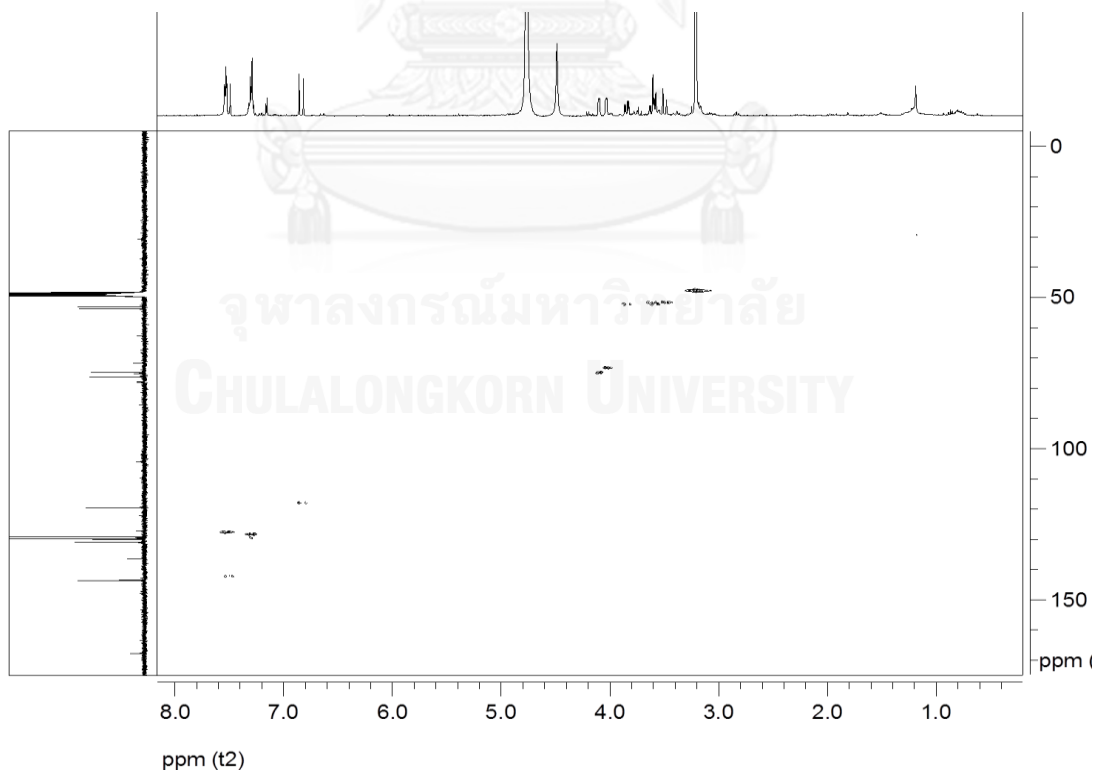
Figure 2.30 HSQC spectrum (300 MHz, in Methanol D$_4$) of deacetlysarmentamide B (**7**)
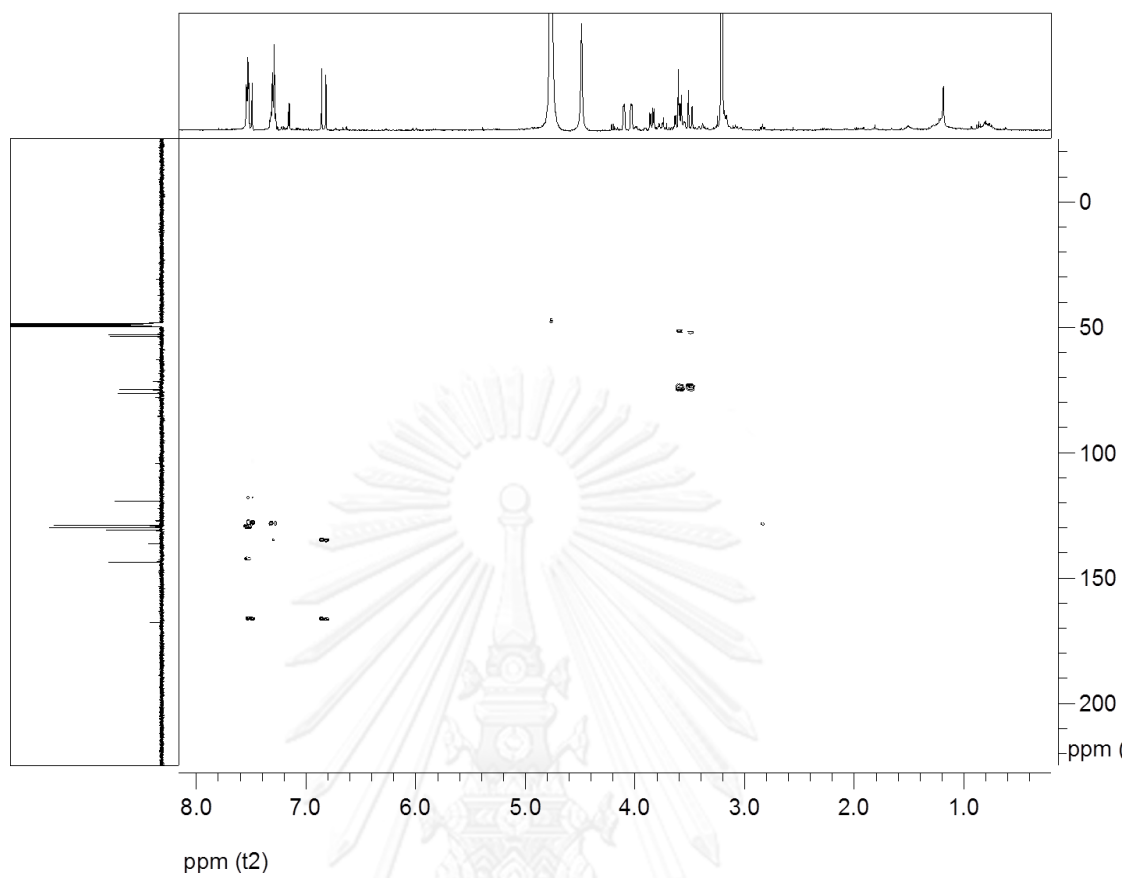
Figure 2.31 HMBC spectrum (300 MHz, in Methanol D$_4$) of deacetlysarmentamide B (**7**)
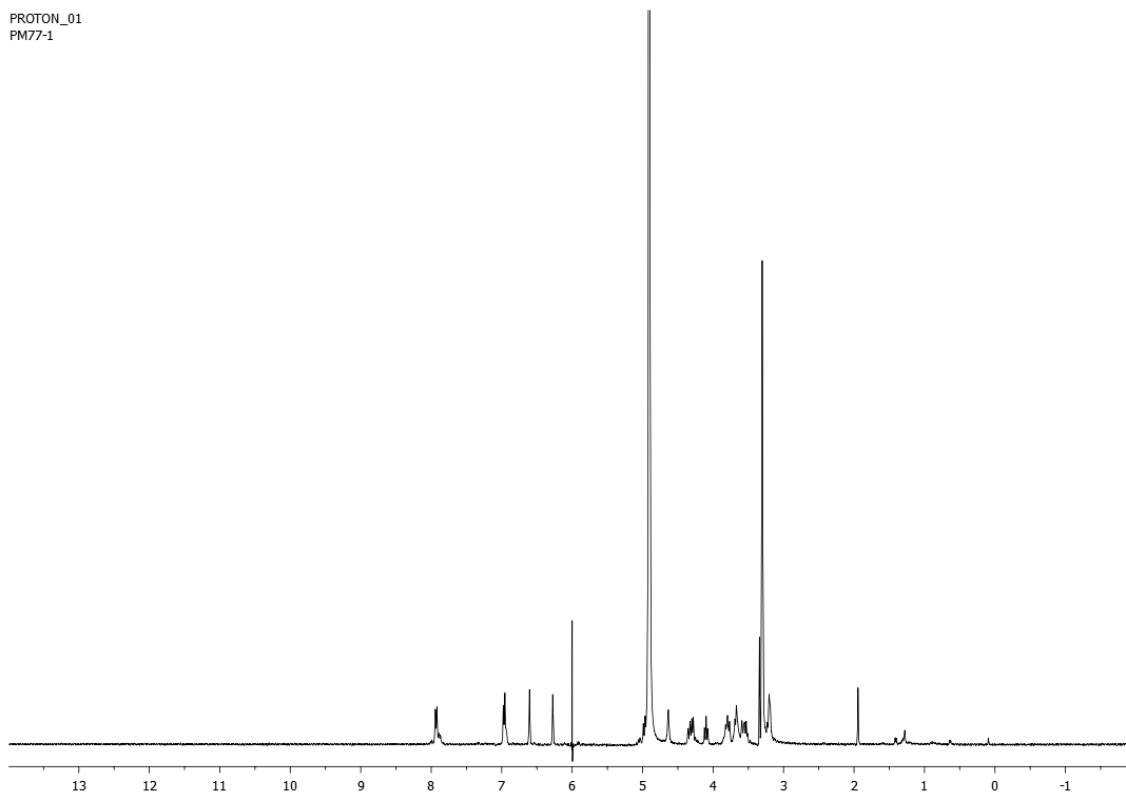
Figure 2.32 ^{1}H-NMR spectrum (400 MHz, in Methanol D$_4$) of keamforal-3-*O*-rhamnoside (**8**)

PROTON_01
PM73-17
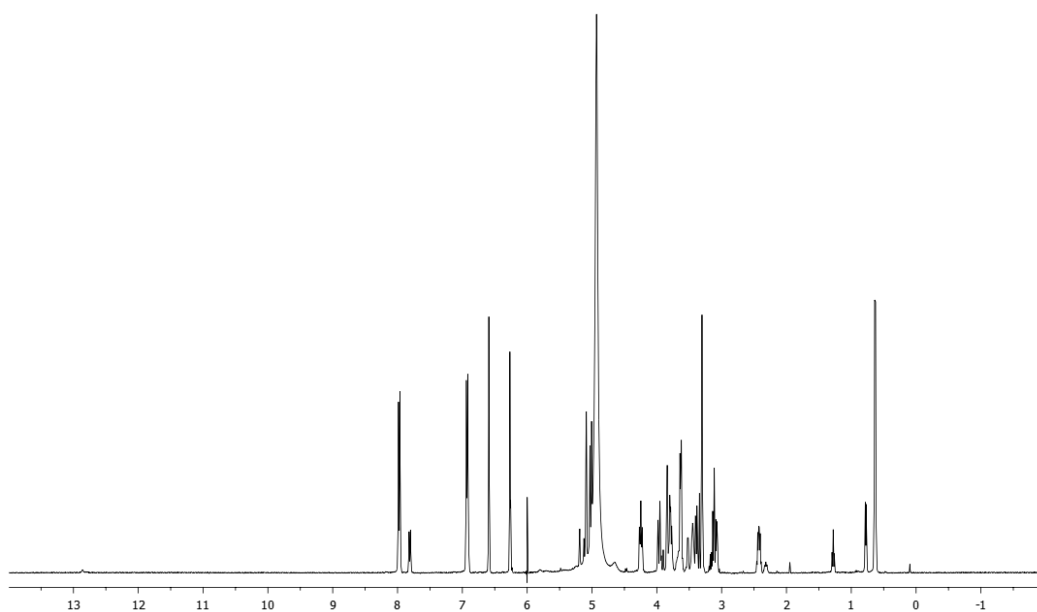
Figure 2.33 ^{1}H-NMR spectrum (400 MHz, in Methanol D$_4$) of dihydrokaempferol-3-O-glucoside (**9**)

CHAPTER III

α-GLUCOSIDASE INHIBITORS FROM WHITE *Sesamum indicum* L. SEED PULP

3.1 Introduction

3.1.1 Botanical aspect and distribution

Sesamum indicum L. belongs to family Pedaliaceae. The common name sesame stemmed from Arabic word "simsim" and commonly known as Til (Hindi), hu ma (Chinese), se'same (French), goma (Japanese), gergelim (Portuguese) and ajonjoli' (Spanish) (Figure 3.1). Sesame has several varieties, classified by seed color ranging from cream-white to charcoal-black. This plant has distributed from Africa, India and tropical regions. The plant is erect, simple or branched annual, 60-180 cm. in height. The leaves are opposite below and alternate above. The flowers are zygomorphic, solitary, white bell-shaped, born on the upper part of the stem. Flower color may vary as white, pink or mauve-pink with darker markings. The petals of the flower is tubular, approximately 3 cm long, with an applicate margin slightly bivariate. The fruit is a capsule, erect and oblong. The capsule contains numerous small ovate seeds. Sesame grows best in hot weather and moderate rainfall (Nath, Chakraborty, & Chakraborty, 2001).

Figure 3. 1 *Sesamum indicum* L.

3.1.2 Phytochemical and pharmacological investigation

For a long time, sesame has been considered as one of the traditional healthy foods because it contains linoleic-acid-rich oil and major lignans consisting of sesamin, sesaminol, sesaminol and sesamolinol (Figure 3.2) (A. Moazzami & Kamal-Eldin, 2006). Lignans have been reported for biological effects such as antioxidant (Fukuda, Nagata, Osawa, & Namiki, 1986), hypocholesterolemic (Nakabayashi et al., 1995) and antihypertensive activities (Nakano et al., 2006).
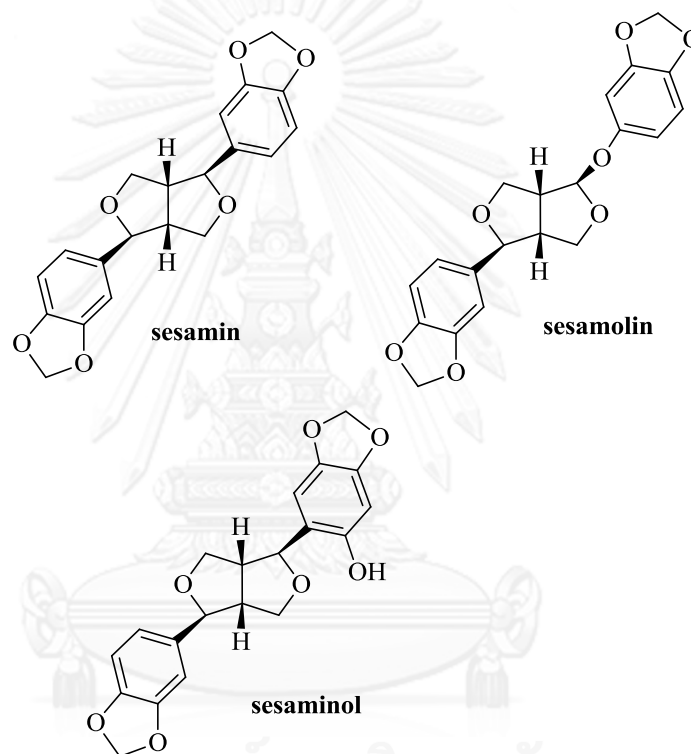
Figure 3.2 Major lignans in *Sesamum indicum* seeds

Moreover, the defatted sesame flour (DSF) obtained after removal of oil contained protein (Kang, Kawai, Naito, & Osawa, 1999) and lignan glycosides, mainly sesaminol di- and tri-glucosides (Figure 3.3) (A. A. Moazzami, Haese, & Kamal-Eldin, 2007).

Sesaminol monoglucoside   R = Glc
Sesaminol diglucoside   R = Glc-Glc
Sesaminol triglucoside   R = Glc-Glc-Glc

Pinoresinol monoglucoside   R = Glc
Pinoresinol diglucoside   R = Glc-Glc
Pinoresinol triglucoside   R = Glc-Glc-Glc
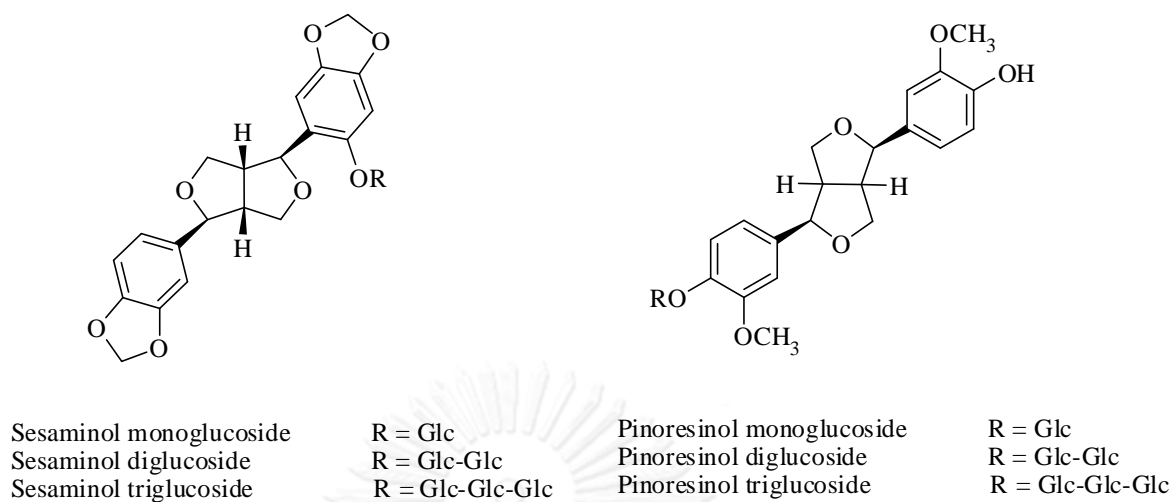
Figure 3.3 Lignan glucosides in defatted sesame seeds

Hypoglycemic effect of hot water extract of defatted sesame seeds was first discovered by Takeuchi and coworker (Kakuda et al., 1996). Significant reduction (33%) in plasma glucose was detected within 2 h in genetically diabetic kk-Ay mice, fed with maltose solution containing 4% hot water extract. Similar results were also observed in ethanol extract of sesame seeds. Additional investigation in T2DM women proved potent hypoglycemic effect of defatted sesame seeds together with benefit linked to regulation of weight gain (Bigoniya, Nishad, & Singh, 2012). However, the compounds responsible for hypoglycemic effect have not have been identified.

3.2 Results and discussion

3.2.1 Isolation

The white sesame seed (3 kg) were ground and defatted with hexane to obtain sesame flour, which was extracted with 70% MeOH-H_2O for 24 h and partition with hexane to obtain a crude extract. The MeOH extract was subjected to VCC (Silica gel) to give 5 main fractions. Fraction 1 was purified by Shephadex LH-20 (MeOH) and silica gel CC (EtOAc-Hexane) to afford sesaminol monoglucoside (**12**). Fraction2 was purified by Shephadex LH-20 (MeOH) and silica gel CC (EtOAc-Hexane) to afford sesamin (**10**) and sesamolin (**11**).

White Sesame Seed (3,000 g)

1) Growned by motor
2) Extract with Hexane

Hexane layer   Defatted Pulp

3) Dried under open air
4) Extract with 70%MeOH-H$_2$O
5) Filtered with cotton
6) Partition with Hexane

70%MeOH

MeOH extract   Water extract

F1   F2   F3   F4   F5

7) Sephadex LH-20 MeOH

8) Sephadex LH-20 (MeOH)   10) Sephadex LH-20 (MeOH)
9) Siliga gel (EtOAc-hexane)   11) Siliga gel (EtOAc-hexane)

sesaminol monoglucoside(**12**,181 mg)   sesamin (**10**,480 mg)   sesamolin (**11**,90mg)

Scheme 3.1 Isolation procedure of isolated compounds from white *Sesamum indicum* L.

3.2.2 Structure elucidation of Sesamin (10)

Sesamin was obtained as a canary yellow solid. The structure was deduced by the results from ^{1}H, ^{13}C NMR spectroscopic methods. The ^{1}H NMR spectral reveled doublet methane proton signal at δ_H 3.05 (J = 1.2 Hz). The methylene proton group, showed that doublet of doublet axial proton signal at δ_H 3.87 (J = 6 Hz) and doublet of doublet equatorial proton signal at δ_H 4.23 (J = 2 Hz). The doublet benzylic proton at δ_H 4.71 (J = 3.6 Hz) could be ascribed to H-2 and H-6. The singlet proton at δ_H 5.95 integrated as 4 protons were assigned to two methylenedioxy group, whereas two ABX system at δ_H 6.79 (dd, J = 2 Hz, H-5', H-6' and H-5" and H-6") and δ_H 7.26 (s) were assigned as H-2' and H-2". The ^{13}C NMR spectral was confirmed. In addition, the structure of sesamin as the same previously studies (Khaleel, 2007)
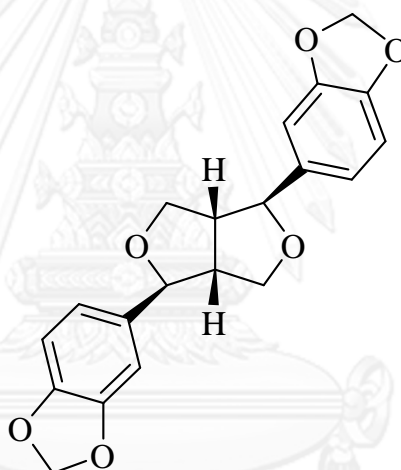
Figure 3.4 Sesamin (**10**)

3.2.3 Structure elucidation of Sesamolin (11)

Sesamolin was obtained as a canary yellow amorphous. The structure was deduced by the results from ^{1}H, ^{13}C NMR spectroscopic methods. The ^{1}H NMR spectral showed two quatet methine protons at δ_H 2.94 and 3.31 (J = 7.6 Hz)). Two pair of methylene proton signals at δ_H 3.64 (q, J = 1.6 Hz) and 4.42 (m, J = 8.9 Hz) were assigned as H-8, whereas δ_H 3.96 (d, J = 9.2 Hz) and 4.41 (q, J = 3.2 Hz) were assigned as H-4. Two benzylic proton signals at δ_H 4.41 (m, J = 8.4 Hz) and 5.50 (s) could be ascribed to H-6 and H-2, respectively. In addition, two singlet proton signals at δ_H 5.92 and 5.96 were assigned to the methylenedioxy protons. while, two ABX system at δ_H 6.62-6.81 assigned to H-6", H-2", H-5" and H-5', H-6', H-2', respectively. The ^{13}C NMR spectral was confirmed. Therefore, the structure of sesamolin as the same previously studies (Khaleel, 2007).
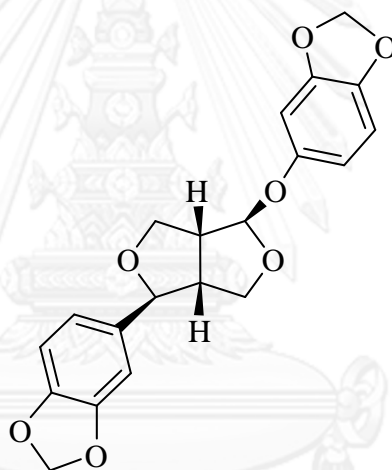
Figure 3.5 Sesamolin (**11**)

3.2.4 Structure elucidation of Sesaminol monoglucoside (12)

Sesaminol monoglucoside was obtained as white needle crystal. The sturture showed positive ESIMS a [M+Na]$^+$ peak m/z 555.146 with molecular formular of $C_{26}H_{28}O_{12}$. The ^{1}H NMR (400 MHz) showed the methylene dioxy group (δ_H 5.92 and 5.22) and a furanofuran moiety (δ_H 2.70, 3.89, 4.10, 3.88, 4.09, 4.65 and 5.22). The anomeric region of sesaminol monoglucoside showed 1,3,4-trisubstituted ring (δ_H 6.81, 6.82 and 6.85) and a *para*-substituted ring (δ_H 6.72). The chemical shift indicating that sesaminol monoglucoside had D-glucose meoiety, HMBC showed coupling between H-2 (δ_H 5.22) and C-8 (δ_C 71.4) and between H-6 (δ_H 4.65) and C-4 (δ_C 72.4). HMBC confirmed coupling between H-1 (δ_H 2.5) and C-1' (δ_C 125.5) and between H-2 and C-5' (δ_C 149.0), between H-5 and C-1" (δ_C 136.5), and between H-6 and C-6" (δ_C 120.7), and between H-6" and C-4" (δ_C 148.0). Therefore, the structure of sesaminol monoglucoside as the same previously studies (A. A. Moazzami, Andersson, & Kamal-Eldin, 2006)
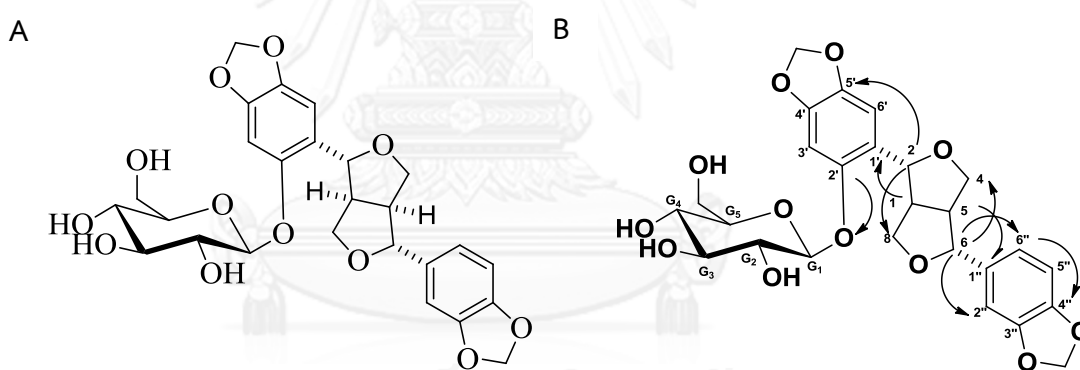
Figure 3.6 A. Sesaminol monogluoside (**12**)

B. Selected HMBC correlations of sesaminol monoglucoside (**12**)

3.2.5 α-Glucosidase inhibitory activity of compounds 10-12

The inhibitions of **10-12** were investigated by using the enzyme from baker's yeast and rat intestine.

Table 3. 1 α-Glucosidase inhibitory effect of isolated compounds (**10-12**)

Compounds	α-glucosidase inhibitory IC$_{50}$ (µM)		
	Baker's yeast	Rat intestinal	
		Maltase	Sucrase
10	450±1.9	NI	NI
11	200±1.2	NI	NI
12	^{a}NI	NI	NI
acarbose	403.9±0.4	1.52±0.14	2.38±0.02

^{a}NI, no inhibition, inhibitory effect less than 30% at 10 mg/mL.

All compounds, except for sesaminol monoglucoside (**12**), inhibited yeast α-glucosidase with IC$_{50}$ in range of 200-450 µM (Table 3.1). Significantly, the present of glucose in the structure of **3** reduced inhibitory activity, compared with **10** and **11**.

Since sesamin (**10**) is a major component and it showed comparable inhibition with acarbose, the understanding of mechanism underlying the inhibition would be useful for further applications.

First, Linweaver-Burk plots (Figure 3.8A) of sesamin against yeast glucosidase were constructed. Sesamin showed a series of straight lines; all of which intersected at Y axis (Table 2.3).

The analysis demonstrated that V_{max} is unchanged with elevated K_m in the presence of increasing concentrations of 1. This behavior indicated that 1 inhibited yeast α-glucosidase by competitive manner, the same as acarbose.

To determine the affinity of 1 toward the enzyme, the secondary plot of slope versus inhibitor concentration was constructed (Figure 3.8 B). The slightly higher K_i value (1.73 mM) of **10** indicated that enzyme preferentially binds to substrate than **10.** The proposed inhibitory mechanism of sesamin against yeast α-glucosidase is shown in Figure 3.7.
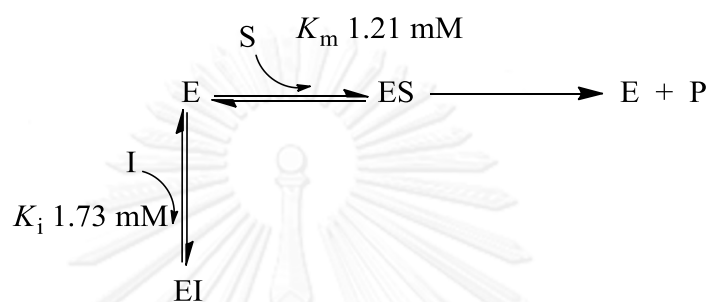
Figure 3.7 Proposed inhibitory mechanism of sesamin against yeast α-glucosidase

Figure 3.8 Lineweaver-Burk plot of sesamin (**10**), 1/*V* aginst 1/[S]. (B) Secondary replot of slope *vs*. [*I*] from a primary Linewaaver-Burk plot for the determination of K_i.

3.3 Experiment section

3.3.1 General experimental procedures

The general experimental procedures were evaluated by the same procedure previously described in Chapter 2.

3.3.2 Plant material

The samples of white sesame seeds (*Sesamum indicum* L.) were supplied by Thai food industry (1964) CO., LTD

3.3.3 Extraction and isolation

The white sesame seed (3 kg) were ground and defatted with hexane to obtain sesame flour, which was extracted with 70% MeOH-H_2O for 24 h and partition with hexane to obtain a crude extract. After removal of solvent in vacuo, the MeOH extract (70.32 g) was subjected to quick CC (Silica gel) eluting with EtOAc, 10% MeOH-EtOAc, 20% MeOH-EtOAc, 50% MeOH-EtOAc (in order of increasing polarity) to give 5 main fractions Fraction1 showed the strongest bioassay guide of α-glucosidase and purified by Shephadex LH-20 (MeOH) and Silica gel CC (70%EtOAc-Hexane, 80% EtOAc-Hexane) as eluent to give sesaminol monoglucoside (**12**,181 mg). Fraction 4 was purified using Sephadex LH-20 (MeOH), Silica gel CC (50%EtOAc-Hexane) to give sesamin (**10**,480 mg) and sesamolin (**11**, 90 mg).

Sesamin (10) Canary Yellow solid; ^{1}H NMR (CDCl$_3$, 400 MHz) δ_H7.26 (1H, s, H-2' and H-2"), 6.79 (4H, q, J = 2 Hz, H-5', H-6' and H-5", H-6"), 5.95 (4H, s, H-OMe), 4.71 (2H, d, J = 3.6 Hz, H-2 and H-6), 4.23 (2H, dd, J = 2 Hz, H-4 and H-8), 3.87 (2H, dd, J = 6 Hz, H-4 and H-8), 3.05 (2H, d, J = 1.2 Hz, H-1 and H-5). ^{13}C NMR (400 MHz, CDCl$_3$) δ_C 147.9 (C-3' and C-3"), 147.1 (C-4' and C-4"), 135.0 (C-1' and C-1"), 119.4 (C-6' and C-6"), 108.6 (C-5' and C-5"), 106.5 (C-2' and C-2"), 101.1 (C-7' and C-7"), 85.8 (C-2 and C-6), 71.7 (C-4 and C-8), 54.3 (C-1 and C-5)

Sesamolin (11) Canary Yellow solid; ^{1}H NMR (CDCl$_3$, 400 MHz) δ_H 7.26 (2H, s, H-2'), 6.81 (4H, m, H-5' and H-6'), 6.72 (1H, s, H-5''), 6.70 (1H, s, H-2''), 6.62 (2H, d, J = 2 Hz, H-6''), 5.96 (4H, s, -7''), 5.92 (4H, s, H-7), 5.50 (2H, s, H-2), 4.42 (4H, m, H-6 and H-8), 4.12 (2H, q, J = 3.2 Hz, H-4), 3.96 (2H, d, J = 9.2 Hz, H-4), 3.64 (2H, q, J = 1.6 Hz, H-8), 3.31 (2H, q, J = 7.6 Hz, H-1), 2.94 (2H, m, H-5). ^{13}C NMR ^{13}C NMR (400 MHz, CDCl$_3$) δ_C 151.8 (C-1''), 148.1 (C-3''), 148.0 (C-3'), 147.1 (C-4'), 142.7 (C-4''), 134.4 (C-1'), 119.7 (C-6'), 109.0 (C-5''), 108.2 (C-5'), 106.9 (C-6''), 106.5 (C-2'), 101.2 (C-2), 101.1 (C-2''), 100.1 (C-7' and C-7''), 87.0 (C-6), 71.3 (C-4), 69.8 (C-8), 53.2 (C-5), 52.7 (C-1)

Sesaminol monoglucoside (12) White needle crystal; ^{1}H NMR (CD$_3$OD, 400 MHz) δ_H 6.87 (1H, s, H-3′), 6.85 (1H, d, J = 1.5Hz, H-2′′), 6.82 (1H, dd, J = 1.5,7.6 Hz,H-6′′), 6.81(1H, d, J = 7.8 Hz, H-5′′), 6.72 (1H, s, H-6′), 5.92(H), 5.22 (1H, d, J = 4.4 H-2), 4.65 (1H, d, J = 5.6 Hz, H-6), 4.10 (2H, dd, J = 4.8, 8.8 Hz, H-4a), 4.09 (2H, dd, J = 6.8, 8.8 Hz, H-4b), 3.89 (2H, dd ,J=4.8, 8.8 Hz), 3.88 (2H, dd ,6.8, 8.8 Hz), 2.70 (1H, m, H-5), 2.5 (1H, m, H-1), 3.89-4.26 (sugar moiety) ^{13}C NMR (CD$_3$OD, 400 MHz) δ_C 150.7 (C-2'), 149.0 (C-5'), 148.0 (C-4''), 147.8 (C-3''), 136.5 (C-1''), 125.5 (C-1'), 120.7 (C-6''), 109.0 (C-5''), 107.6 (C-2''), 106.1 (C-6'), 103.6 (G1), 102.6 (-O-CH$_2$-O-'), 102.4 ((-O-CH$_2$-O-''), 99.8 (C-3'), 87.0 (C-6), 82.9 (C-2), 78.3 (G5), 78.2 (G3), 75.1 (G2), 74.1 (C-4), 72.4 (G4), 71.4 (C-8), 62.6 (G6), 55.7 (C-1), 55.3 (C-5)

3.3.4 α-Glucosidase inhibitory activity

The activity effect of isolated compounds were evaluated using the same procedure described in Chapter 2

Kinetic study of sesamin (10)

The enzyme kinetic analysis was performed according to the above reaction except that the quantity of α-glucosidase from barker's yeast was maintained at 0.3 U/mL while the concentration of each tested inhibitor was varied at 0, 0.018 and 0.028 mM. The type of inhibition was determined from Lineweaver–Burk plots, where the K_i values were determined from the secondary plots of slope vs. [I] and the interception vs. [I] of the Lineweaver–Burk plot.

Supporting information
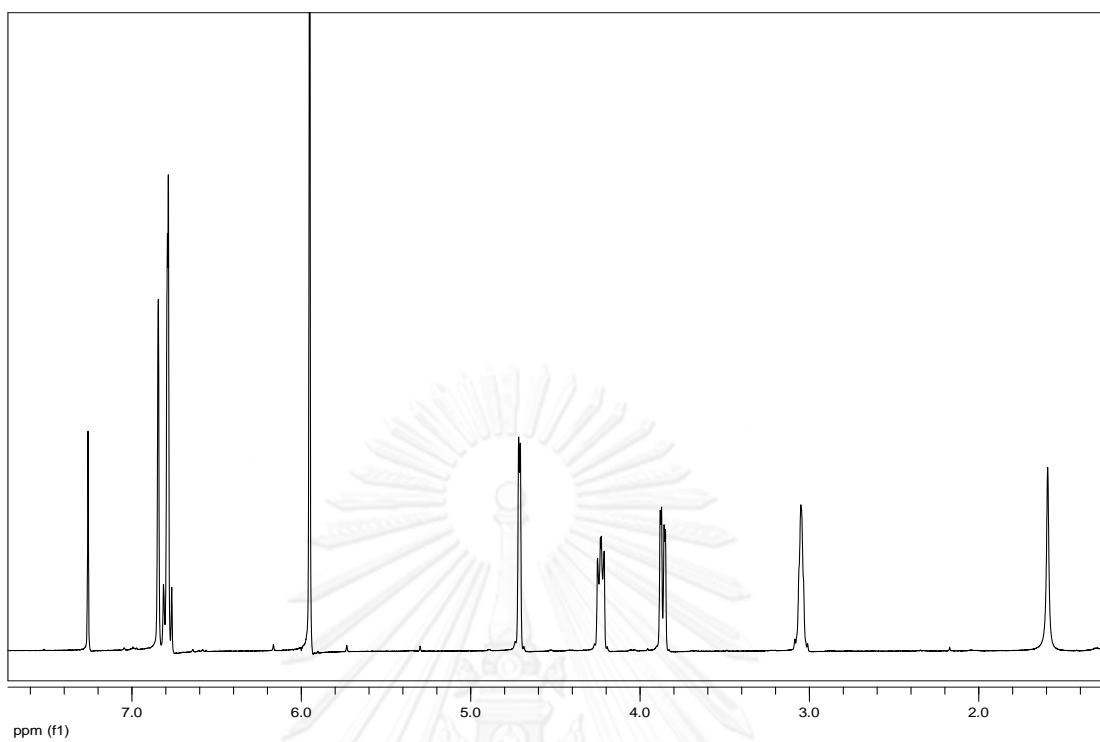
Figure 3.9 ^{1}H-NMR spectrum (400 MHz, in CDCl$_3$) of sesamin (**10**)
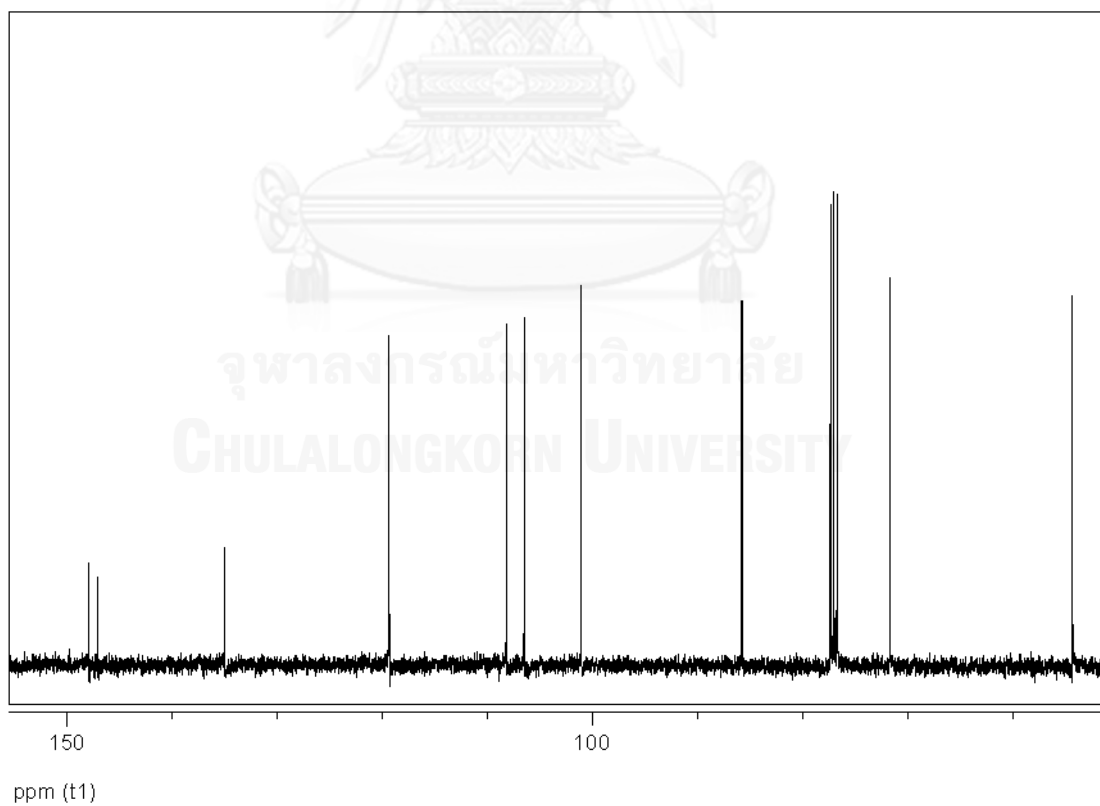
Figure 3.10 ^{13}C-NMR spectrum (100 MHz, in CDCl$_3$) of sesamin (**10**)
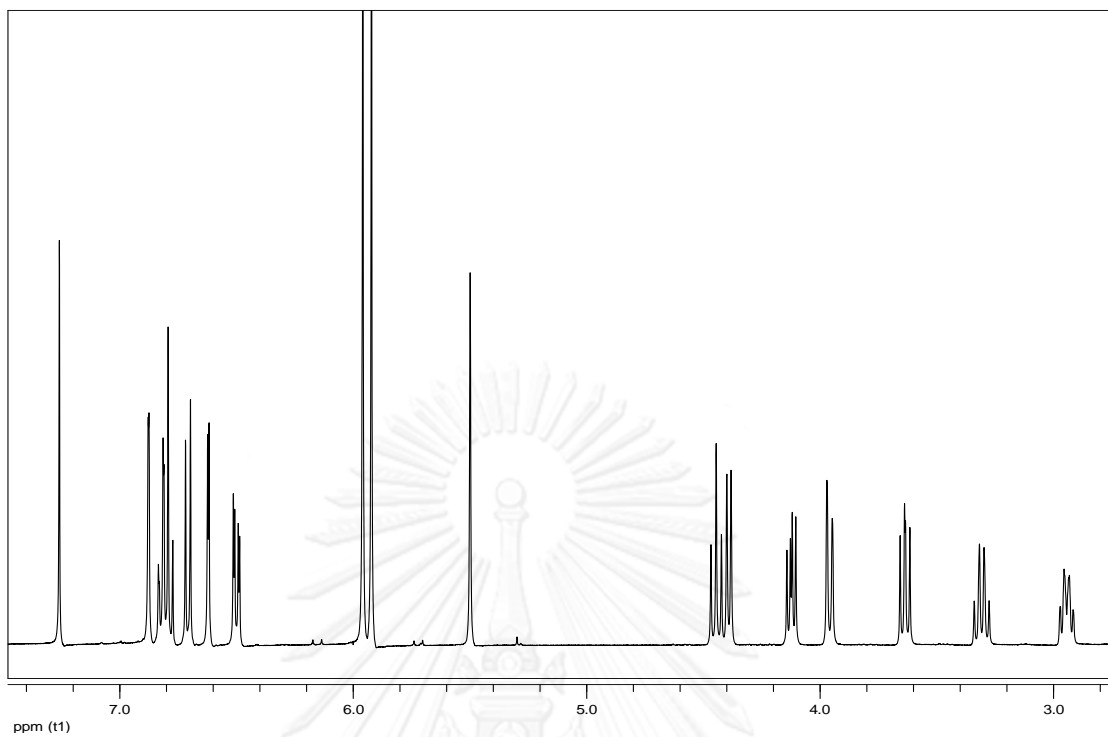
Figure 3.11 ^{1}H-NMR spectrum (400 MHz, in CDCl₃) of sesamolin (**11**)
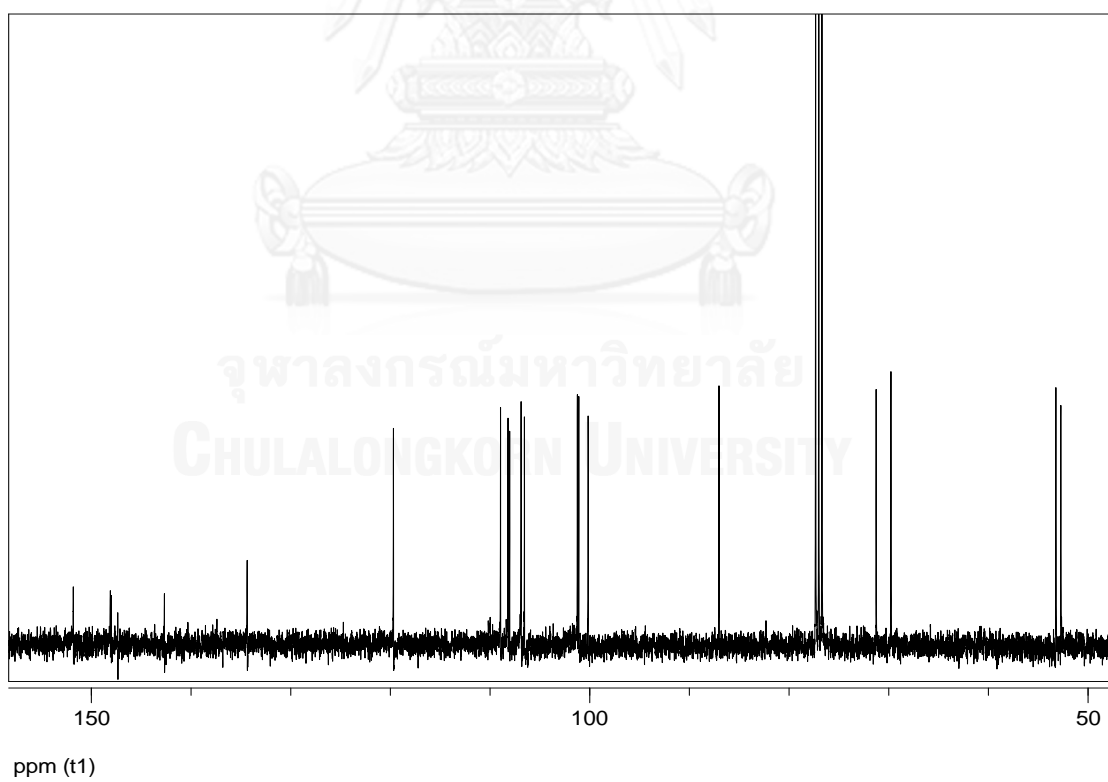
Figure 3.12 ^{13}C-NMR spectrum (100 MHz, in CDCl₃) of sesamolin (**11**)
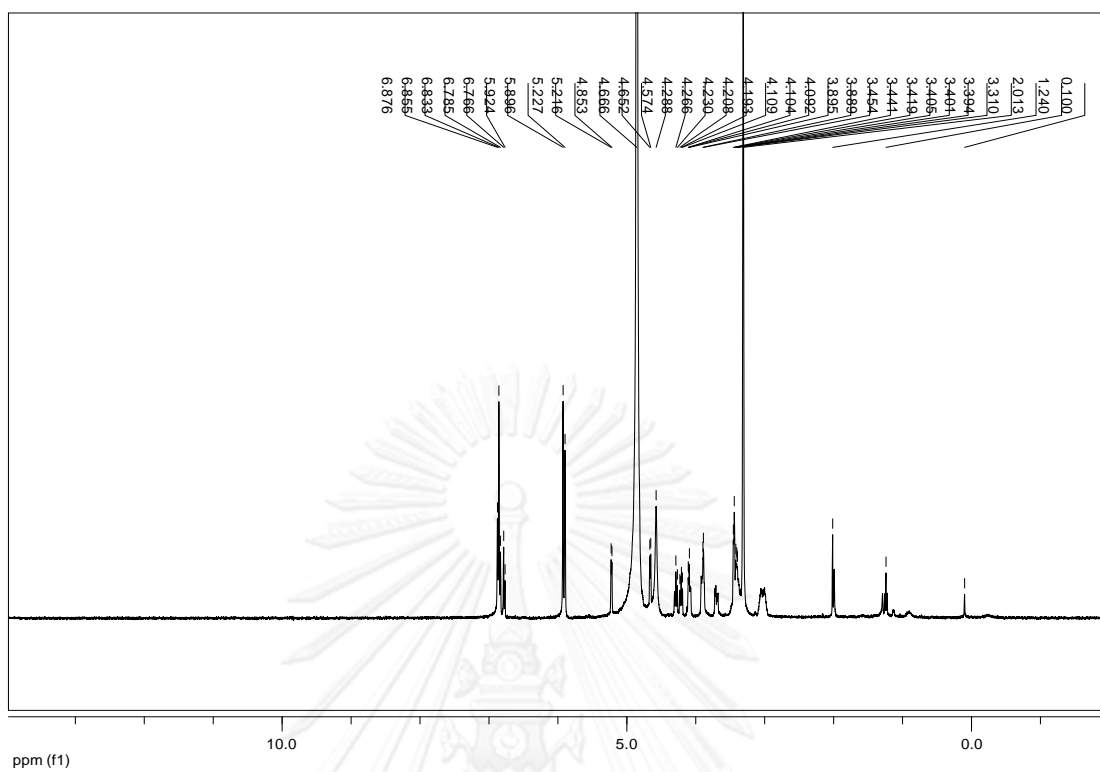
Figure 3.13 ^{1}H-NMR spectrum (400 MHz, in Methanol D₄) of sesaminol monoglucoside (**12**)
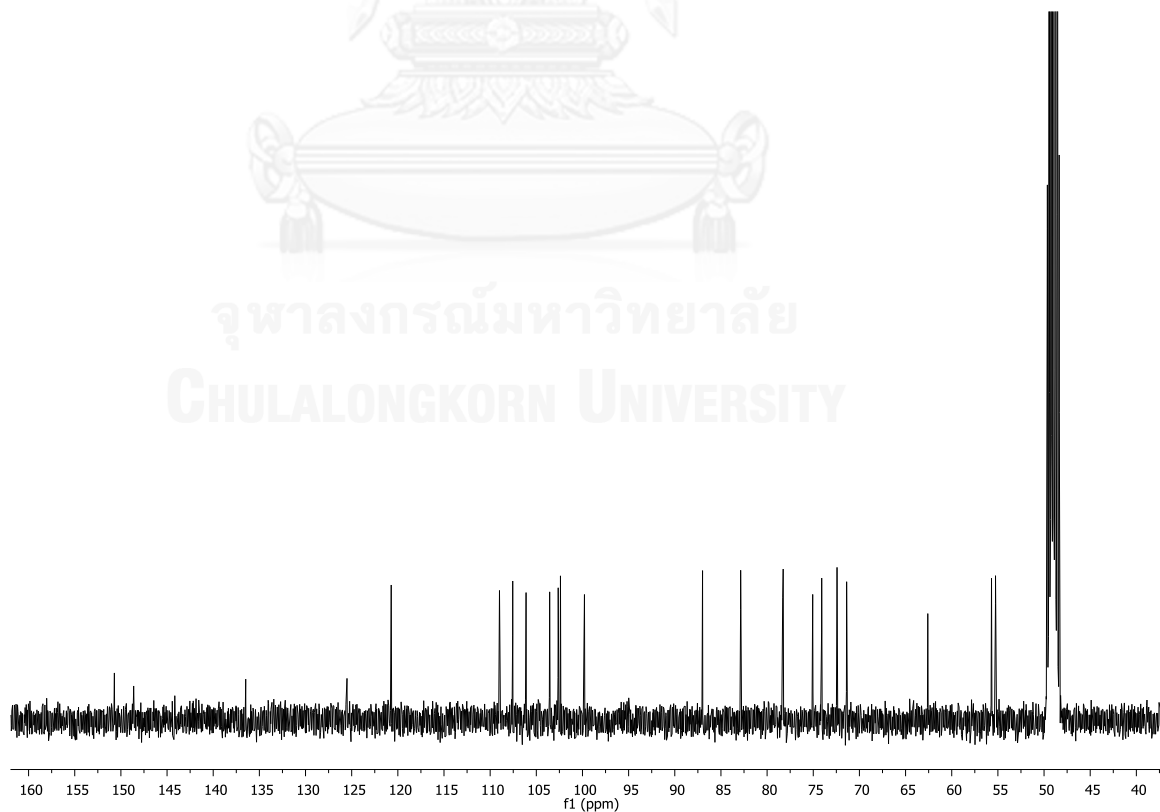
Figure 3.14 ^{13}C-NMR spectrum (100 MHz, in Methanol D₄) of sesaminol monoglucoside (**12**)

Mass Spectrum List Report

Analysis Info

Analysis Name	CUTD211253001.d	Acquisition Date	12/22/2010 1:47:19 AM
Method	tune_high_jaran_20100602.m	Operator	Administrator
Sample Name	WS24-2	Instrument	micrOTOF 72
	WS24-2		

Acquisition Parameter

Source Type	ESI			Set Corrector Fill	50 V
Scan Range	n/a	Ion Polarity	Positive	Set Pulsar Pull	400 V
Scan Begin	50 m/z	Capillary Exit	200.0 V	Set Pulsar Push	360 V
Scan End	4000 m/z	Hexapole RF	200.0 V	Set Reflector	1300 V
		Skimmer 1	50.0 V	Set Flight Tube	9000 V
		Hexapole 1	35.0 V	Set Detector TOF	2300 V
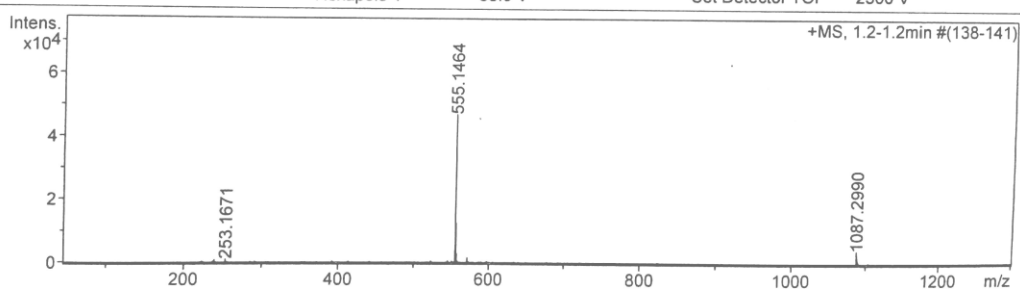
FWHM

Figure 3.15 HR-EIMS spectrum of sesaminol monoglucoside (**12**)

gCOSY_01
ww020
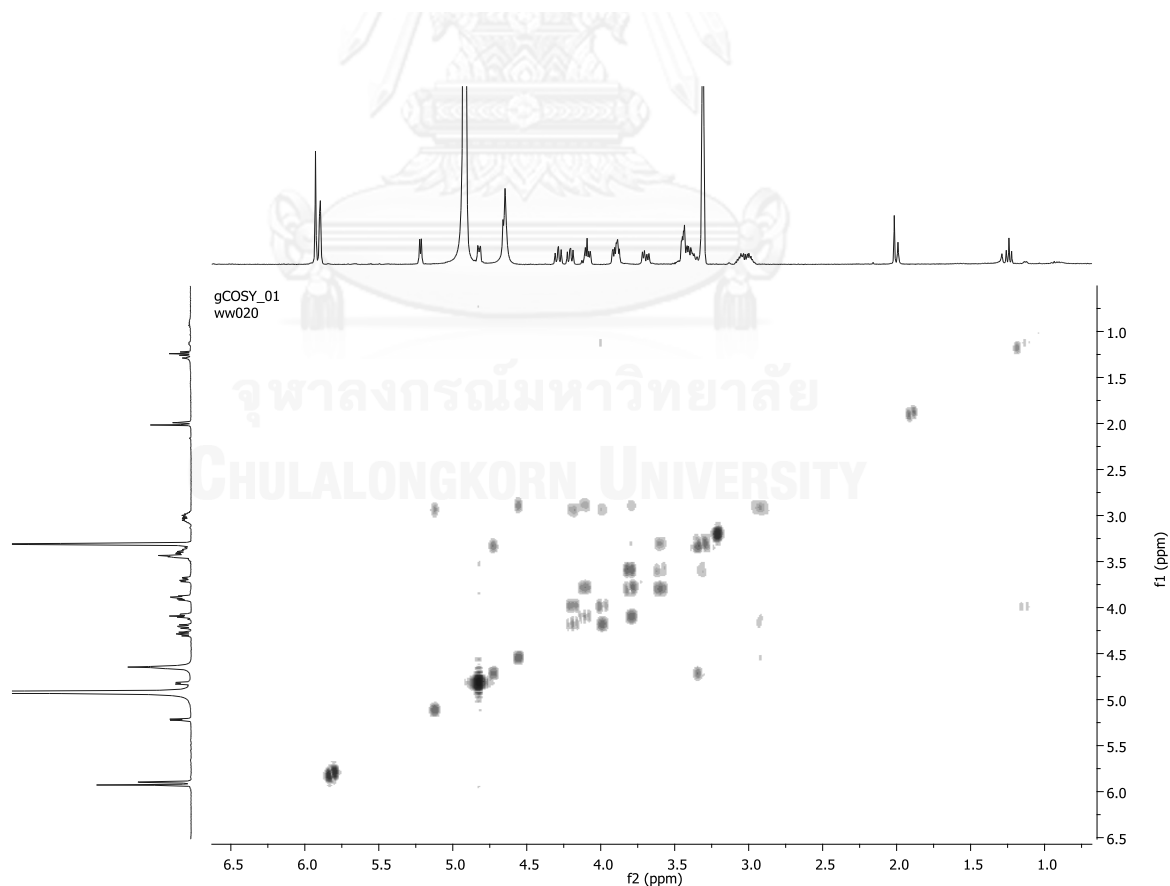
Figure 3.16 ^{1}H-^{1}H COSY spectrum (400 MHz, in Methanol D$_4$) of sesaminol monoglucoside (**12**)
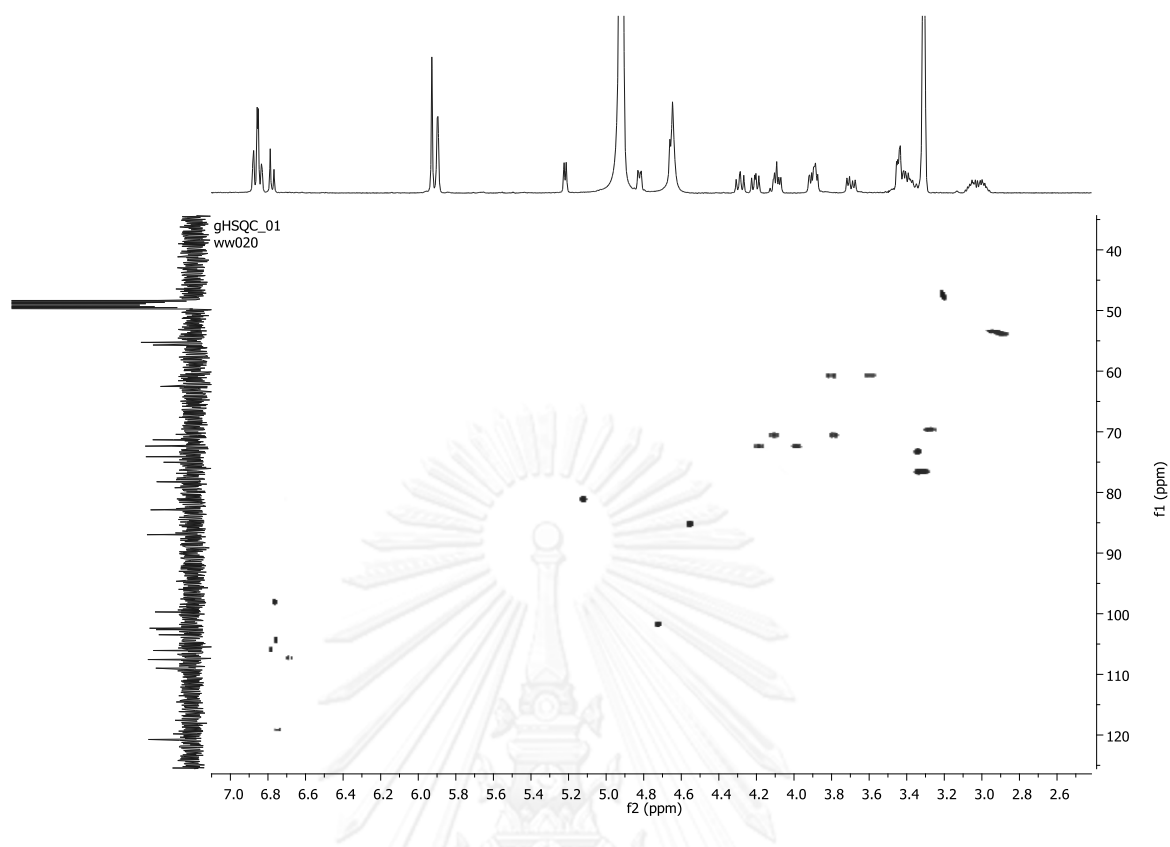
Figure 3.18 HSQC spectrum (400 MHz, in Methanol D$_4$) of sesaminol monoglucoside (**12**)
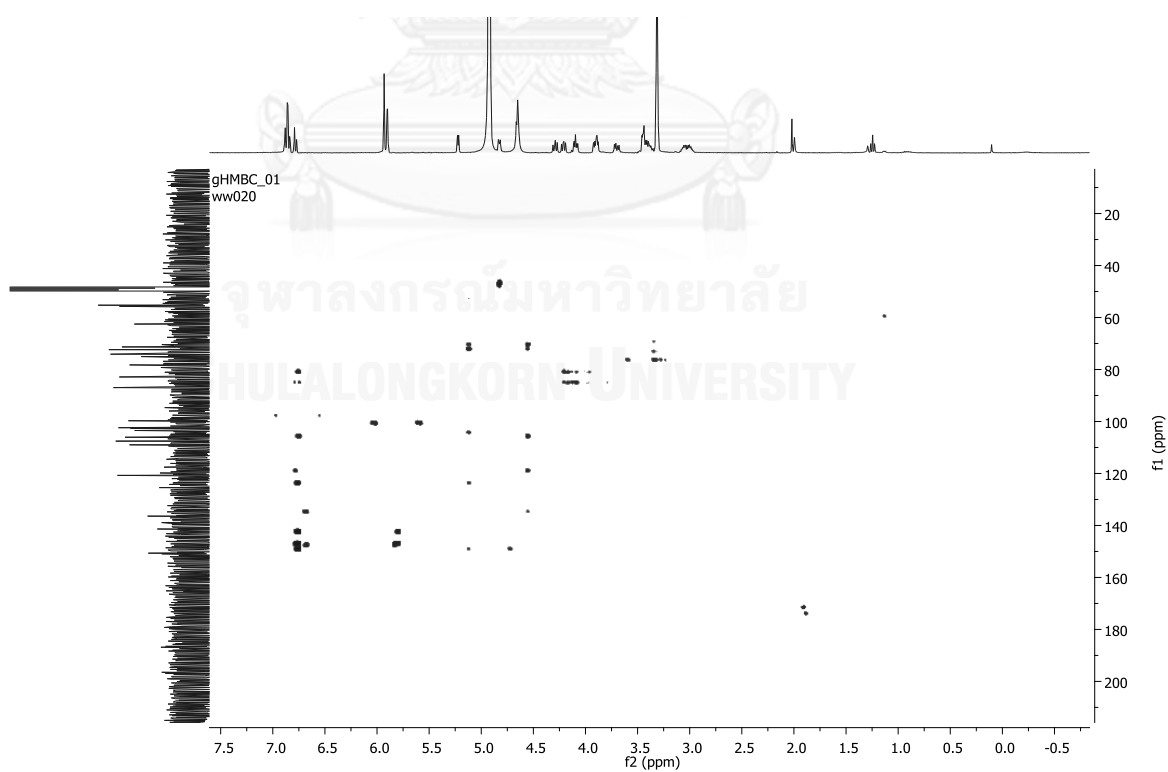
Figure 3. 17 HMBC spectrum (400 MHz, in Methanol D$_4$) of sesaminol monoglucoside (**12**)

CHAPTER IV

α-GLUCOSIDASE INHIBITORS FROM THE AERIAL PARTS OF *Orthosiphon aristatus* (Blume) Miq.

4.1 Introduction

4.1.1 Botanical aspect and distribution

Orthosiphon aristatus (syn. *O.grandiflorus*, *O.spicatus* and *O.stamineus*) is an herb of family Lamiaceae and known locally in Malaysia (Misai Kucing); Thailand (Yaa Nuat Maeo, Rau Meo or Cay Bac); Indonesia (Kumis Kucing or Remujung); France (Moustaches de Chat); or Europe (Java Tea) (Figure 4.1) (Ameer, Salman, Asmawi, Ibraheem, & Yam, 2012), which is a bush and high about to 1- 2 meter. This plant is the blue-white flower and short hair on the stems have hairs similarity cat's whisker. It is distributed throughout Southeast Asia and tropical Australia and planted as a garden tree.

4.1.2 Phytochemical and pharmacological investigation

In previous phytochemical studies of *O. aristatus*, three main groups of chemical constituents, flavonoids, organic acids and terpenoids, have been reported. The isolated flavonoids included eupatorin, sinensetin, ladanein, salvigenin, vomifoliol, scutellarein tetramethylether and tetramethyscutellarein (Lyckander & Malterud, 1996). Moreover, the organic acids including caffeic acid, rosmarinic acid (Tezuka et al., 2000) and 2,3-decaffeoyltartaric acid were reported in aqueous extract. Pimarane- and isopimarane-type ditepenoid are characteristic metabolites or chemical markers of plants in genes *Orthosiphon*. Over 20 ditepenoids such as orthosiphols A, B, D-N, orthosiphonones A-B, staminols A-B, stamina-lactones A-B, and neoorthosiphols A-B (Ohashi, Bohgaki, Matsubara, & Shibuya, 2000) were isolated.

Figure 4.1 *Orthosiphon aristatus* (Blume) Miq.

Orthosiphon aristatus (Laiaceae) is a popular traditional folk medicine of many diseases. It is used in Vietnam for edema urinary, lithiasis, eruptive fever, influenza and biliary lithiasis, in Indonesia for rheumatism, hypertension, diabetes, epilepsy, tonsillitis, renal calculus and gallstones (PT., 1995). The aforementioned traditional uses, especially antidiabetic activity, have been supported by *in vitro* and *in vivo* experiments. First investigation of antidiabetic effect was conducted in streptozotocin (STZ)-induced diabetic rats (MARIAM et al., 1996). Oral administration of the aqueous extract significantly reduced blood glucose level in both normal and diabetic rats. As its wide use in Southeast Asia for diabetes therapy, subsequent studies (Mohamed *et al.*, 2011) were carried out attempting to identify the active components responsible for this effect. Mohamed and coworkers demonstrated that fraction mainly containing eupatorin and sinensetin (**1**) possessed highest glucose lowering effect (Mohamed et al., 2012). In addition, the unchanged level of insulin throughout the experiment suggested that blood glucose was possibly suppressed by inhibiting intestinal glucosidases. Therefore, identifying active components putatively responsible for retarding α-glucosidase function is the aim of this investigation.
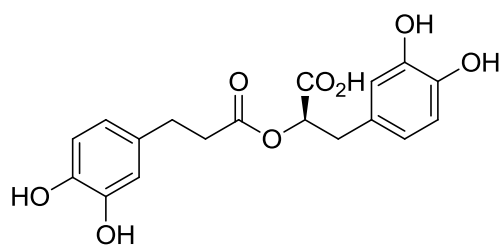
Rosmarinic acid
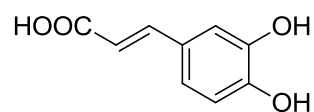
Caffeic acid
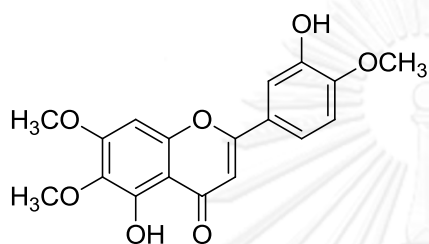
Eupatorin
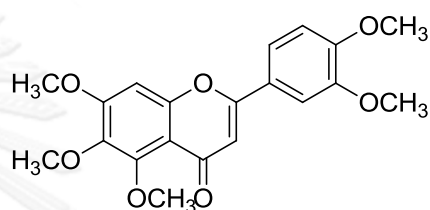
3,4',5,6,7-pentamethoxyflavone
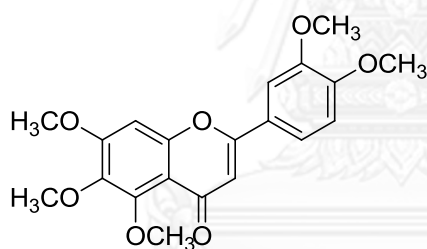
Sinensetin
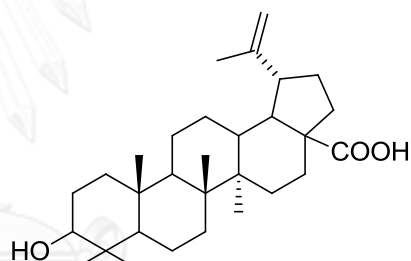
Betolinic acid
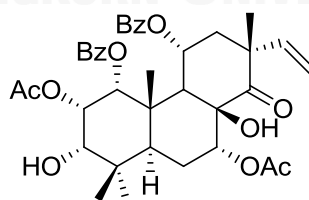
Orthosiphol A

Figure 4.2 Chemical compounds found in *Orthosiphon aristatus* (Blume) Miq.

4.2 Results and discussion

4.2.2 Isolation

Dried aerial parts of *O. aristatus* (200 g) were ground and extracted with methanol. The MeOH extract was suspended in water and partitioned with CH_2Cl_2. The CH_2Cl_2 extract was fractionated on silica gel vacuum column chromatography (VCC) using mixtures of EtOAc-hexane and EtOAc, yielding 7 major fractions. The combined fractions 6 eluted by EtOAc-hexane were purified by Sephadex LH-20 and silica gel EtOAc-hexane to afford sinensetin (**13**). Fraction 1 was further purified by Sephadex LH-20 (10:90 MeOH-CH_2Cl_2) and silica gel (1:99 MeOH- CH_2Cl_2) to yield salvigenin (**14**) and 3,7,4'-tri-*O*-methylkaempferol (**16**). Fraction 4 was subsequently purified by Sephadex LH-20 (10:90 MeOH-CH_2Cl_2) and silica gel (40:60 EtOAc-hexane) to furnish tetramethylscutellarein (**15**) and orthosiphol A (**17**). The isolation procedure is summarized in (Scheme 4.1)

.

Dried aerial parts of *Orthosiphon aristatus* (200 g)

1) Extract with MeOH

MeOH extract

2) Partition with CH$_2$Cl$_2$

CH$_2$Cl$_2$ crude extract

3) VLC, EtOAc:Hexane

F1   F2   F3   F4   F5   F6   F7

6) Sephadex LH-20
   MeOH:CH$_2$Cl$_2$
7) Siliga gel
   MeOH:CH$_2$Cl$_2$

8) Sephadex LH-20
   MeOH:CH$_2$Cl$_2$
9) Silica gel
   EtOAc:hexane

4) Sephadex LH-20
   MeOH:CH$_2$Cl$_2$
5) Siliga gel
   EtOAc-hexane

salvigenin (**14**,120 mg)

3,7,4'-tri-O-methylkaempferol (**16**, 87 mg).

sinensetin (**13**, 70 mg)

tetramethylscutellarein (**15**, 150 mg)

orthosiphol A (**17**, 120 mg)

Scheme 4.1 Isolation procedure of isolated compounds from aerial parts of *Orthosiphon aristatus* (Blume) Miq.

	R^1	R^2	R^3	R^4
13	CH$_3$	OCH$_3$	OCH$_3$	H
14	H	OCH$_3$	H	H
15	CH$_3$	OCH$_3$	H	H
16	H	H	H	OCH$_3$

17
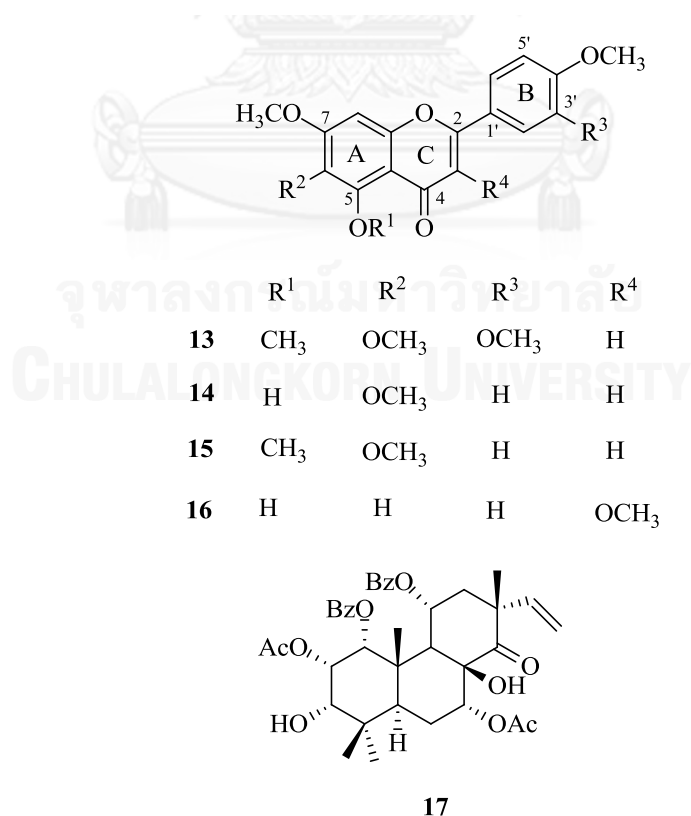
Figure 4.3 The chemical structures of isolated compounds from aerial parts of *Orthosiphon aristatus* (Blume) Miq.

4.2.3 Structure elucidation of sinensetin (13)

Flavone shows characteristic signals of H-3 (δ_H 6.53) as singlet and α,β unsaturated ketone (C-4) around δ_C 170-180 ppm. Sinensetin was obtained as colorless solid. The ^{1}H and ^{13}C showed a flavone pattern at 6.51 (H-3) and 182.7 (C-4). Five singlets at δ_H 4.02, 4.00, 3.98, 3.94 and 3.92 indicated the presence of 5 methoxy groups. The position of methoxy groups were inferred from splitting pattern of ^{1}H NMR. The signals at δ_H 7.50 (dd, J=12 Hz, 1H), 7.35 (d, J=2.1 Hz, 1H), 7.28 (d, 1H) indicated two methoxy groups at C-3' and C-4' of B ring. The signals at 6.82 suggested that C-5, C-6 and C-7 were occupied by three methoxy groups. In addition, the NMR data of seinesetin (13) were similar to those of previous report (J. Chen, Montanari, & Widmer, 1997)
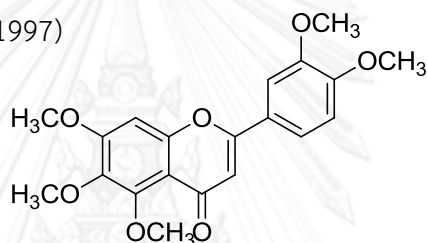
Figure 4.4 Sinesetin (13)

4.2.3 Structure elucidation of salvigenin (14)

Salvigenin was obtained as yellow solid. The ^{1}H and ^{13}C data of 2 were similar to those of 13 in that 14 showed H-3 (δ_H 6.51), H-8 (δ_H 6.54), and C-4 (δ_C 182.7). However, revealed a low-field signal of 5-OH (δ_H 12.75) and three methoxy groups (δ_H 3.94, 3.90 and 3.88). Two signals at δ_H 7.79 (d, J = 8.8 Hz, 2H) and 6.97 (d, J = 8.8 Hz, 2H) indicated p-substituted benzene of B ring, suggesting that C-6, C-7 and C-4' were occupied by methoxy groups. In addition, the NMR data of 14 were similar to those of previous report (SA Ayatollahi, 2009)
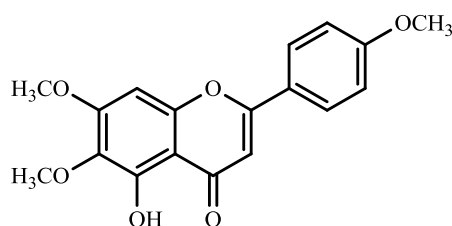
Figure 4.5 Salvigenin (14)

4.2.4 Structure elucidation of tetramethylscutellarein (15)

Tetramethylscutellarein was obtained as yellow needles. The ^{1}H NMR patterns [δ_H 7.77 (d, J = 8 Hz, 2H), 7.20 (d, 1H), 6.94 (d, J = 8 Hz, 1H), 6.73 (s, 1H)] in aromatic region of **15** were similar to those of **14,** except for the present of four methoxy groups (δ_H 4.05, 3.92, 3.85 and 3.82). Therefore, 5-OH of **14** was occupied by 5-OMe in **15**. Thus, the structure of tetramethylscutellarein was established for **15** (Ahmed, Rimpler, Rizk, Hammouda, & Ismail, 1970)
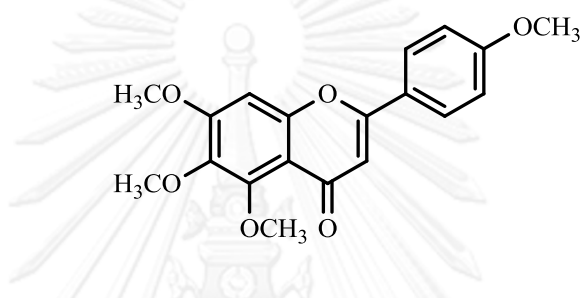
Figure 4.6 Tetramethylscutellarein (**15**)

4.2.4 Structure elucidation of 3,7,4'-Tri-*O*-methylkaempferol (16)

3,7,4'-Tri-*O*-methylkaempferol was obtained as yellow needles. The ^{1}H NMR spectrums showed signals of 5-OH (δ_H 12.60) and three methoxy groups (δ_H 3.84, 3.83, 3.80). The aromatic signals at 6.43 (d, J = 2.2, 1H) and 6.33 (d, J = 2.2, 1H) indicated that C-5 and C-7 were replaced by hydroxyl and methoxy, respectively. In addition, the signals at 8.07 (d, J = 9.0 Hz, 2H) and 7.00 (d, J = 9.0 Hz, 2H) suggested that C-4' was occupied by a methoxy group. However, the absence of H-3 signal typically resonated about 6.5 ppm indicated that C-3 was replaced by methoxy group. Therefore, the structure of 3,7,4'-Tri-*O*-methylkaempferoln was established for **16** (Rossi, Yoshida, & Soares Maia, 1997).
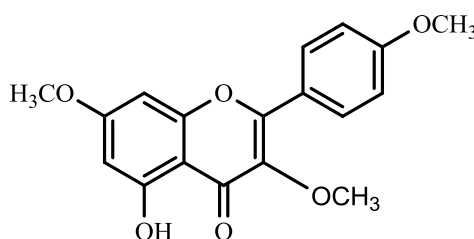
Figure 4.7 3,7,4'-Tri-*O*-methylkaempferol (**16**)

4.2.4 Structure elucidation of orthosiphol A (17)

As early mentioned, pimarane- and isopimarane-type diterpenoid have been reported as other major component of plants in genes *Orthosiphon*, which are distinct form diterpenoid of other genus by the present of one or more acetoxy (AcO) and benzoyl (BzO) groups. Orthosiphol A was obtained as white amorphous solid. The ^{1}H and ^{13}C NMR spectra showed signals of two acetoxyls (δ_H 1.90 and 2.21; δ_C 21.1, 21.1, 167.1 and 173) and two benzoyls [δ_H 7.21-7.78 (10 H), δ_C 170.1and 170.7)]. In addition the signals of four singlet methyls (δ_H 0.93, 1.06, 1.19 and 1.41), one ketone (δ_C 213.9) and one exomethylene [δ_H 4.64 (d, *J* = 12.0 Hz), 4.81(d, *J* = 16.0 Hz) and 5.71 (dd, *J* = 12.0, 16.0 Hz)] were also observed. Therefore, the structure of 5 was deduced to be orthosiphol A (**17**) (Masuda, Masuda, Shiragami, Jitoe, & Nakatani, 1992) base on their similar NMR data.
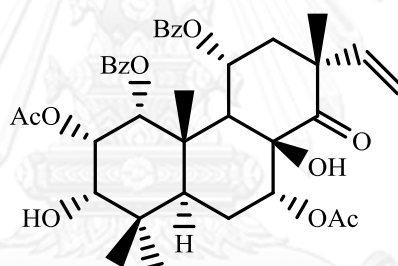
Figure 4.8 Orthosiphol A (**17**)

4.2.5 α-Glucosidase inhibitory activity of compounds 13-17

Compounds **13-17** were investigated for their α-glucosidase inhibition using the enzymes from barker's yeast and rat intestine.

Table 4.1 α-Glucosidase inhibitory effect of isolated compounds **13-1**

Compounds	α-glucosidase inhibitory IC_{50} (mM)		
	Baker's yeast	Rat intestinal	
		Maltase	Sucrase
13	NI	NI	NI
14	[a]NI	NI	NI
15	6.34±0.80	NI	NI
16	0.75±0.30	NI	NI
17	NI	6.54±0.40	NI
acarbose	0.40±0.4	0.005±0.14	0.002±0.02

[a]NI, no inhibition, inhibitory effect less than 30% at 10 mg/mL

The inhibitory effects against α-glucosidases from yeast and rat intestine of **13-17** were examined (Table 4.1). Flavonoids **15** and **16** revealed inhibition toward yeast α-glucosidase with IC_{50} values of 6.34 and 0.75 mM, respectively, whereas **13** and **14** showed no inhibition. Notably, flavonoids **14** and **16** are isomer that differ only in the position of one methoxy group, at 6-OMe in **14** and 3-OMe in **16**. A dramatic reduction in inhibitory effect from **16** to **14** suggested that the presence of 3-OMe on the C ring is critical in exerting inhibition. Of the isolated flavonoids, **16** is the only one having a methoxy group on the C ring. Although Tadera and coworkers (Tadera, Minami, Takamatsu, & Matsuoka, 2006) generalized that inhibitory activity increased considerably with an increase in the number of the hydroxyl group on the B ring, our observation did not meet this hypothesis. Moreover, our finding also enlightened that the presence of 3-OMe considerably enhances α-glucosidase inhibitory effect.

Interestingly, orthosiphol A (**17**) selectively inhibited maltase with an IC_{50} value of 6.54 mM. As rat intestinal maltase used in this experiment is closely similar to that of human intestine (Oki, Matsui, & Osajima, 1999) **17** is likely to be an active component responsible for blood glucose lowering through inhibiting glucosidase. To envision mechanism underlying this inhibition, a kinetic study of **17** toward maltase was performed. The Lineweaver-Burk plots (Figure 4.10 A) showed linearity at each concentration examined (1.75 and 3.54 mM); all of which intersected the x-axis at a single negative value. The kinetic analysis revealed that V_{max} decreased with increasing concentrations of **17** while K_m (2.16 mM) remained constant. This behavior indicated that **17** inhibit maltase in a noncompetitive manner.

The comparable values of K_i (4.03 mM) and K'_i (4.30 mM) obtained from secondary plots (Figures 4.10 B,C) suggested that **17** inhibits maltase by equally forming enzyme-inhibitor (EI) and enzyme-inhiitor-substrate (EIS) complexes (Figure 4.9).
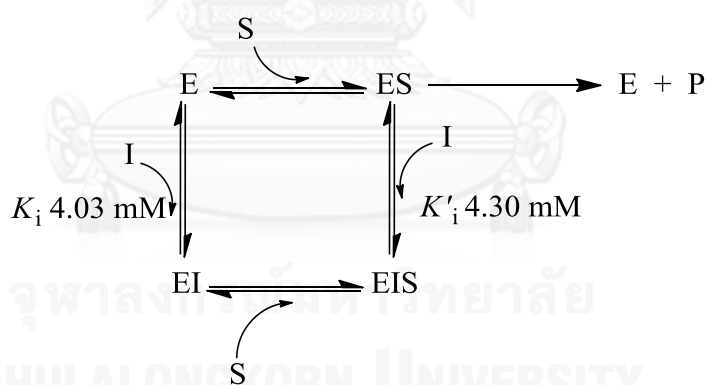
Figure 4.9 Proposed inhibitory mechanism of orthosiphol A (**17**) against maltase

In summary, we succeeded in identifying that orthosiphol A (**17**) in *O. aristatus* is putatively responsible for suppressing blood glucose through inhibiting maltase. Although various flavonoids (**13**-**16**) were isolated from this plant, none of them inhibit intestinal α-glucosidases (both maltase and sucrase). In addition, this finding also suggested that sinensetin (**13**), previously reported as a blood glucose lowering agent, is not likely to exert an antidiabetic property through inhibiting α-glucosidase. The combined effect of identified metabolites in this plant through different pathways in suppressing hyperglycemia is under investigation in our laboratory.
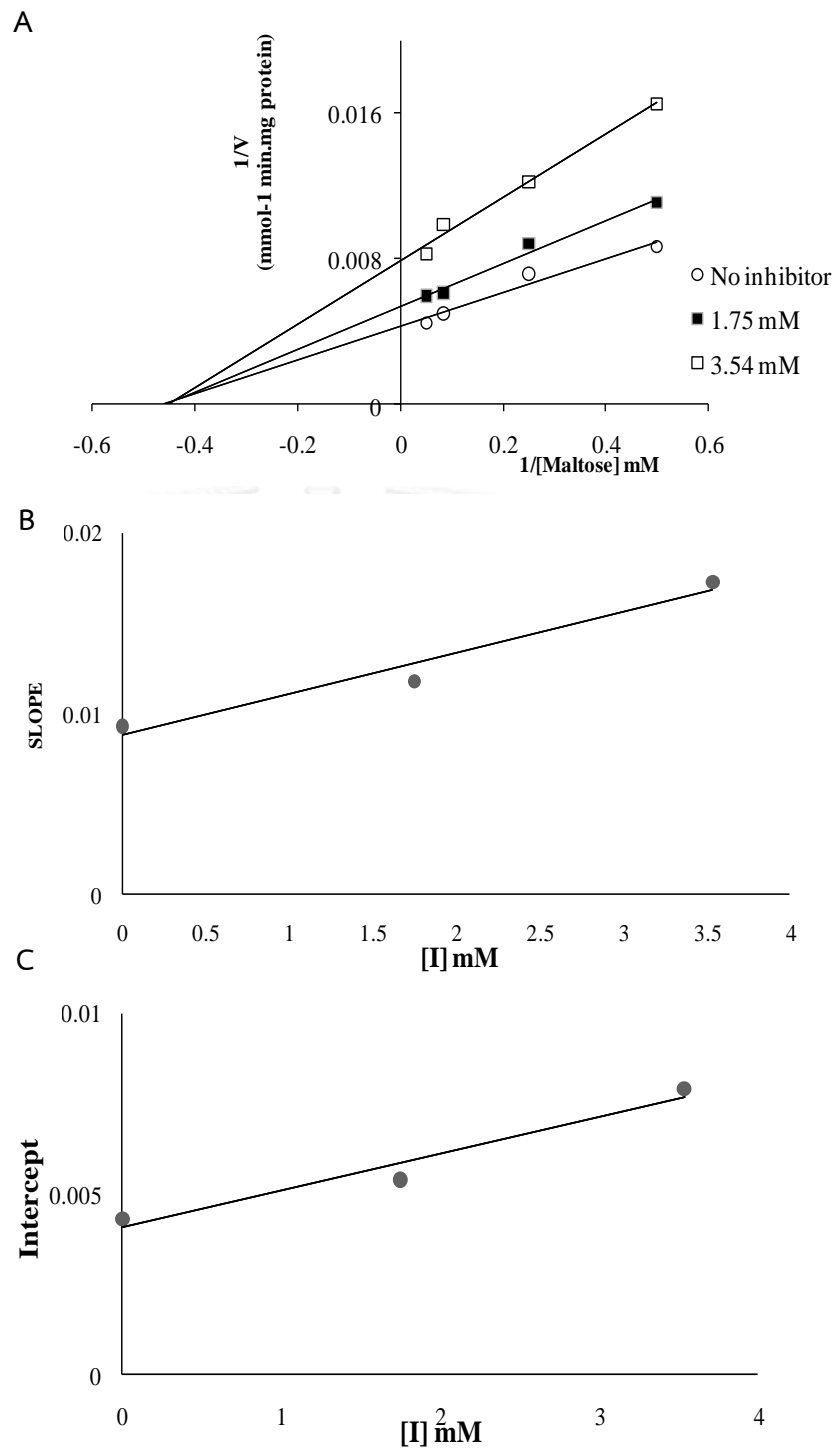
Figure 4.10 (A) Lineweaver-Burk plot of orthosiphol (17) A, 1/*V* aginst 1/[S]. (B) Secondary replot of slope *vs*. [*I*] from a primary Linewaaver-Burk plot for the determination of K_i. (C) Secondary replot of intercept *vs*. [I] from a primary Lineweaver-Burk plot for determination of $K_{i'}$

4.3 Experiment section

4.3.1 General experimental procedures

The general experimental procedures were evaluated by the same procedure previously described in Chapter 2.

4.3.2 Plant material

The aerial parts *Orthosiphon aristatus* were purchased from folk medicine drugstore (Bangkok, Thailand) in March 2012. Plant specimen was authenticated and deposited in the Herbarium of the Department of Botany, Faculty of Science, Chulalongkorn University.

4.3.3 Extraction and isolation

The dried aerial parts of *Orthosiphon aristatus* (200 g) were extracted with methanol The MeOH extract was suspended in water and partitioned with CH_2Cl_2. The CH_2Cl_2 extract was fractionated on silica gel vacuum column chromatography (VCC) using mixtures of EtOAc-hexane (5:95, 25:75, 50:50 and 60:40 v/v) and EtOAc, yielding 7 major fractions. The combined fractions 6 eluted by 60:40 EtOAc-hexane were purified by Sephadex LH-20 (10:90 MeOH-CH_2Cl_2) and silica gel (60:40 EtOAc-hexane) to afford sinensetin (**13**, 70mg). Fraction 1 was further purified by Sephadex LH-20 (10:90 MeOH-CH_2Cl_2) and silica gel (1:99 MeOH- CH_2Cl_2) to yield salvigenin (**14**, 120 mg) and 3,7,4'-tri-*O*-methylkaempferol (**16**, 87 mg). Fraction 4 was subsequently purified by Sephadex LH-20 (10:90 MeOH-CH_2Cl_2) and silica gel (40:60 EtOAc-hexane) to furnish tetramethylscutellarein (**15**, 150 mg) and orthosiphol A (**17**, 120 mg).

Sinensetin (13) Colorless solid; ^{1}H NMR (CDCl$_3$, 400 MHz) δ_H 7.5 (dd, *J* = 8,2 Hz, 1H), 7.35 (d, *J* = 2.1 Hz, 1H), 7.28 (d, *J* = 8 1H), 6.82 (s, H), 6.64 (s, 3H), 4.02 (s, 3H), 4.00 (s, 3H), 3.98 (s, 3H), 3.94 (s, 3H) and ^{13}C NMR (CDCl$_3$, 100 MHz) δ_C 177.16, 161.18, 157.71, 154.32, 152.63, 151.89, 149.35, 140.42, 124.17, 119.63, 111.22, 108.82, 107.39, 96.26, 62.18, 61.52, 56.30, 56.16, 56.08, 53.38

Salvigenin (14) Yellow solid; ^{1}H NMR (CDCl$_3$, 400 MHz) δ_H 12.74 (s, OH), 7.79 (d, J = 8.8 Hz, 2H), 6.97 (d, J = 8.8 Hz,2H), 6.54 (s, 1H), 6.51 (s, 1H), 3.94, 3.9, 3.88 (s,OMe) and ^{13}C NMR (CDCl$_3$, 100 MHz) δ_C 182.8, 164.0, 162.7, 158.8, 153.3, 153.1, 132.6, 128.0, 123.7, 114.6, 106.2, 104.2, 90.6, 60.9, 56.3, 55.6

Tetramethylscutellarein (15) Yellow needles; ^{1}H NMR (CDCl$_3$, 400 MHz) δ_H 7.77 (d, J = 8 Hz, 2H), 7.20 (d, 1H), 6.94 (d, J = 8 Hz, 1H), 6.73 (s, 1H), 6.53 (s, 1H), 4.05, 3.92, 3.85, 3.82 (4s, 12H×4) ^{13}C NMR (CDCl$_3$, 100 MHz) δ_C 177.2, 163.8, 159.5, 158.2, 154.2, 153.3, 138.1, 128.8, 122.5, 114.3, 112.7, 104.2, 91.5, 61.5, 60.8, 56.1, 55.6

3,7,4'-tri-*O*-methylkaempferol (16) Yellow needles; ^{1}H NMR (CDCl$_3$, 400 MHz) δ_H 12.6 (s, H), 8.07 (d, J = 9 Hz, H), 7.00 (d, J = 9 Hz, H), 6.43 (d, J = 2.2, H), 6.33 (d, J = 2.2, H), 3.84, 3.83, 3.80 (s,OMe) (s, H) ^{13}C NMR (CDCl$_3$, 100 MHz) δ_C 165.4, 161.7, 156.8, 148.0, 138.9, 130.0, 122.8, 114.0, 106.0, 97.8, 92.2, 60.1, 55.8, 55.4

Orthosiphol A (17) White amorphous solid; ^{1}H NMR (CDCl$_3$, 400 MHz) δ_H 7.21-7.78 (10H, t, 1&11-Bz), 5.82 (1H, m, H11), 5.63 (1H, dd, H15), 5.45 (1H, brt, J = 3.2 Hz, H7), 5.42 (1H,brt, J = 3.2 Hz, H2), 5.31 (1H,brd, J = 2.6 Hz, H1), 4.86 (1H, d, H16), 4.82 (1H, d, H16), 3.55 (1H, m, H3), 3.12 (1H, brd, J = 5.7 Hz, H9), 2.85 (1H, brs, 8-OH), 2.54 (1H, dd, H12), 2.45 (1H, dd, J = 10 and 4.5 Hz, H5), 2.1-2.22 (1H, m, H6), 2.21 (3H, s, 7-Ac), 2.20 (1H, d, 3-OH), 1.99 (1H, dd, H12), 1.90 (3H, s, 2-Ac), 1.43 (3H, s, H20), 1.01-1.15 (9H, s, H17,H18& H19). ^{13}C NMR (CDCl$_3$, 100 MHz) δ_C 209.1 (C14), 173 (2-Ac), 167.1 (7-Ac), 167 (11-Bz), 165 (1-Bz), 144.2 (C15), 136 (1-Bz), 135 (11-Bz), 128.3 (11-Bz), 127.2 (1-Bz), 112 (C16), 76.9 (C8), 75.1 (C1), 77.3 (C3), 71.2 (C7), 69.3 (C11), 65.8 (C2), 46.3 (C13), 44.1 (C10), 43.2 (C9), 39.0 (C12), 38.9 (C4), 34.6 (C5), 29.9 (C19), 26.9 (C17), 22.9 (C18), 21.2 (C6), 21.1 (2-Ac), 21.1 (7-Ac), 15.9 (C20).

4.3.4 α-Glucosidase inhibitory activity

The activity effects of isolated compounds were evaluated using the same procedure described in ChapterII.

Kinetic study of Orthosiphol A (17)

A kinetic analysis of maltase was carried out according to the above reaction except that the specific activity of maltase was maintained at 0.3 U/mL while the concentrations of **5** were varied at 0, 1.75 and 3.54 mM. The type of inhibition was determined from Lineweaver–Burk plots whereas the K_i and K_i' values were deduced from the secondary plots of slope *vs* [I] and the interception *vs* [I] of the Lineweaver–Burk plots, respectively.

Supporting information
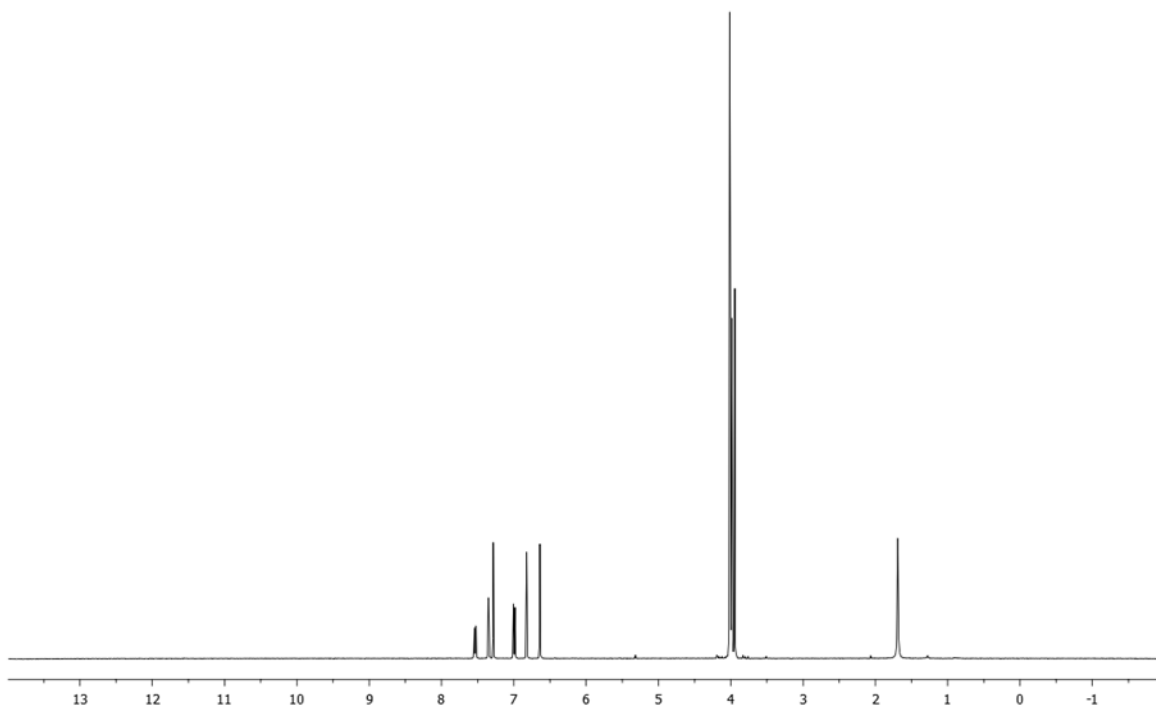
Figure 4.11 ^{1}H-NMR spectrum (400 MHz, in CDCl$_3$) of sinensetin (**13**)
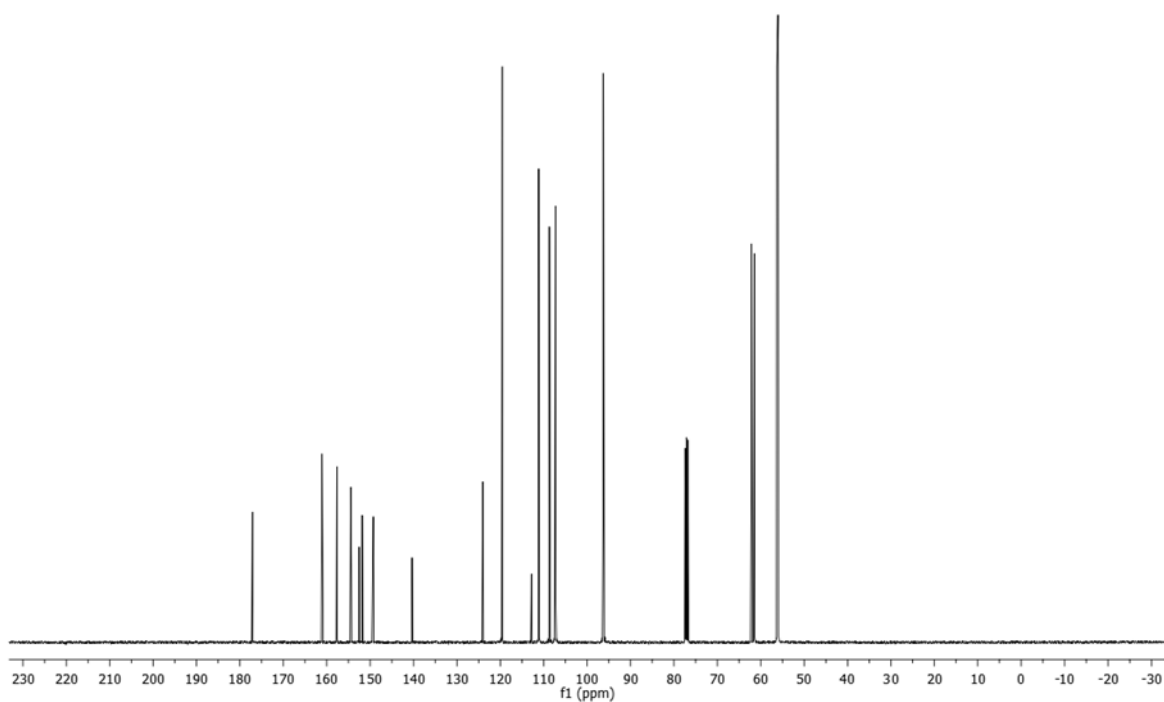
Figure 4.12 ^{13}C-NMR spectrum (100 MHz, in CDCl$_3$) of sinensetin (**13**)
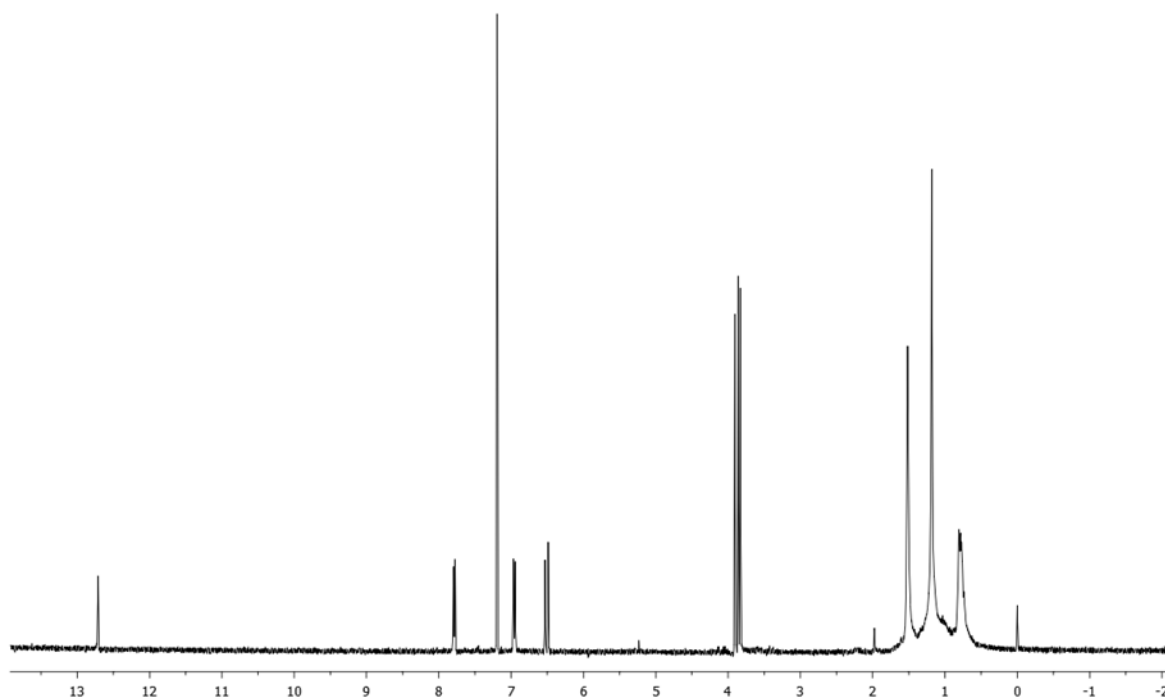
Figure 4.13 ^{1}H-NMR spectrum (400 MHz, in CDCl$_3$) of salvigenin (**14**)
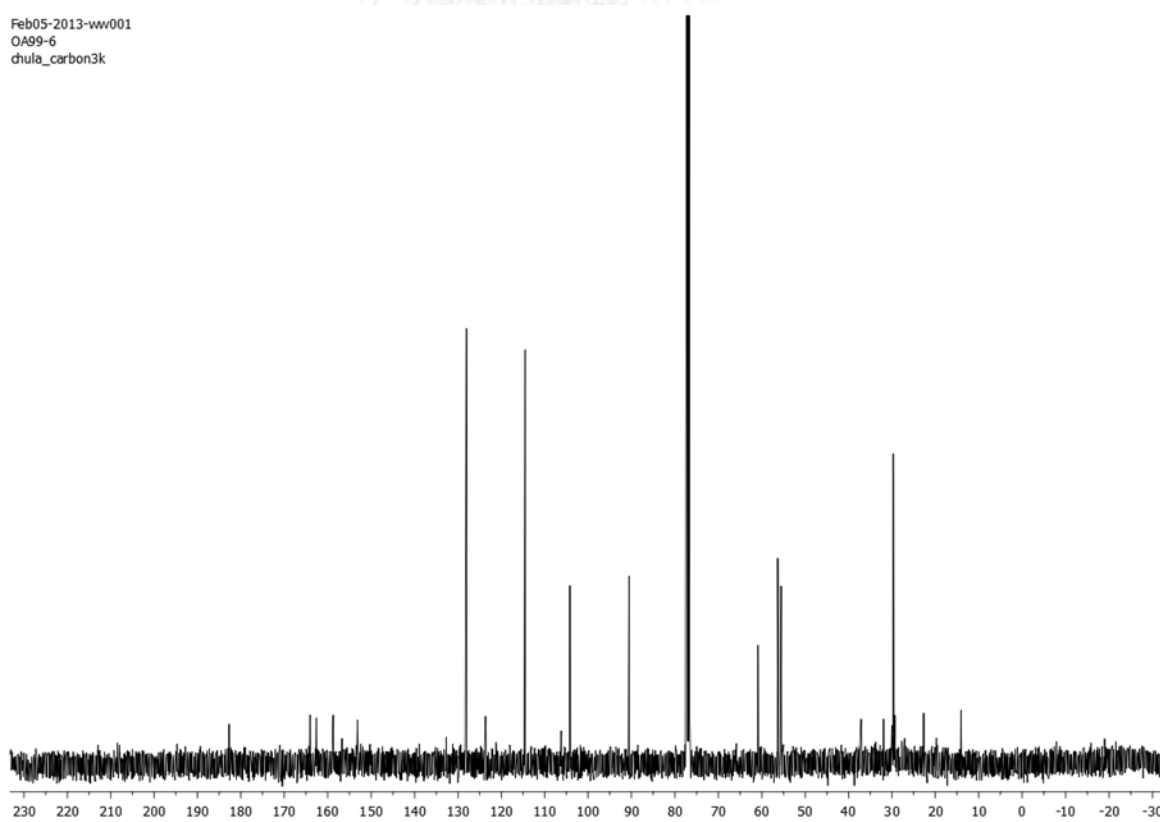
Figure 4.14 ^{13}C-NMR spectrum (100 MHz, in CDCl$_3$) of salvigenin (**14**)
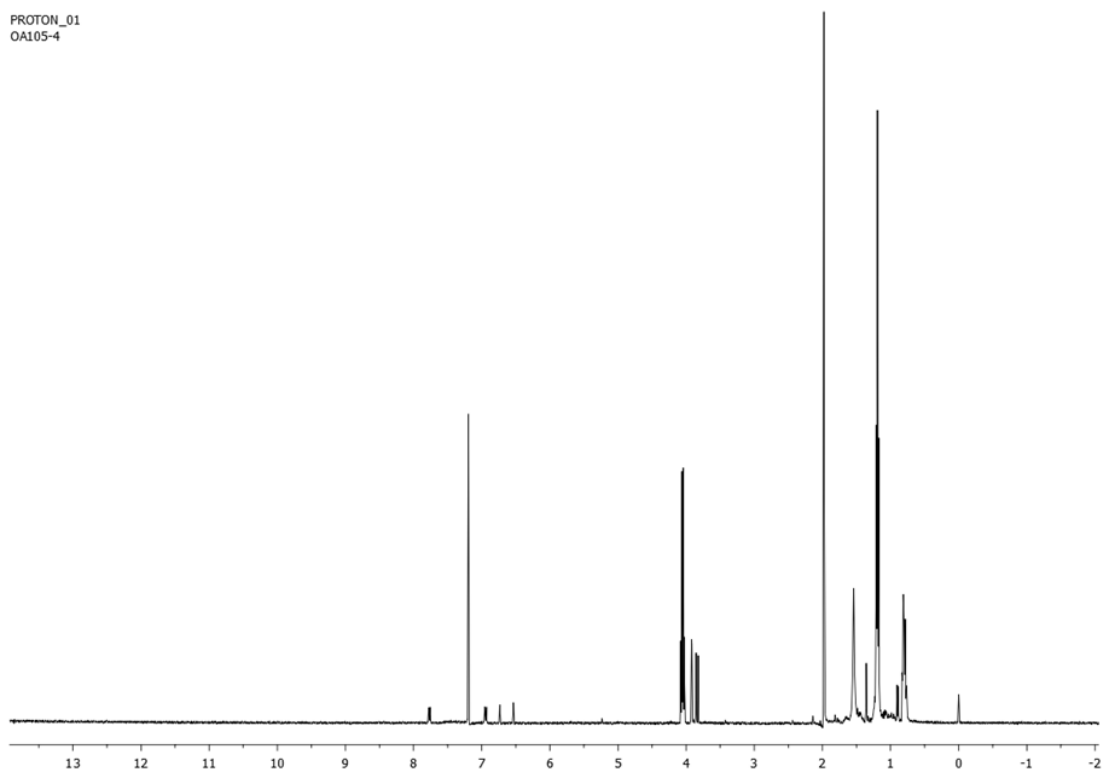
Figure 4.15 ^{1}H-NMR spectrum (400 MHz, in CDCl$_3$) of tetramethylscutellarein (**15**)
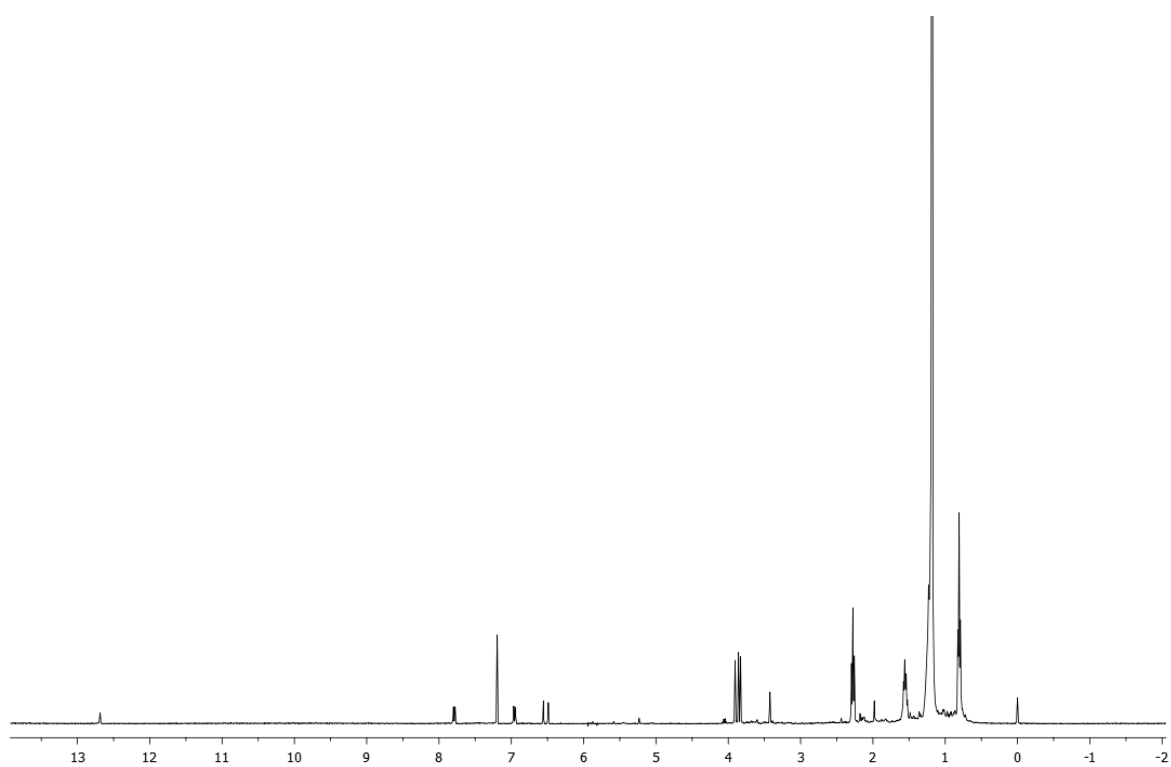
Figure 4.16 ^{1}H-NMR spectrum (400 MHz, in CDCl$_3$) of 3,7,4'-tri-*O*-methylkaempferol (**16**)
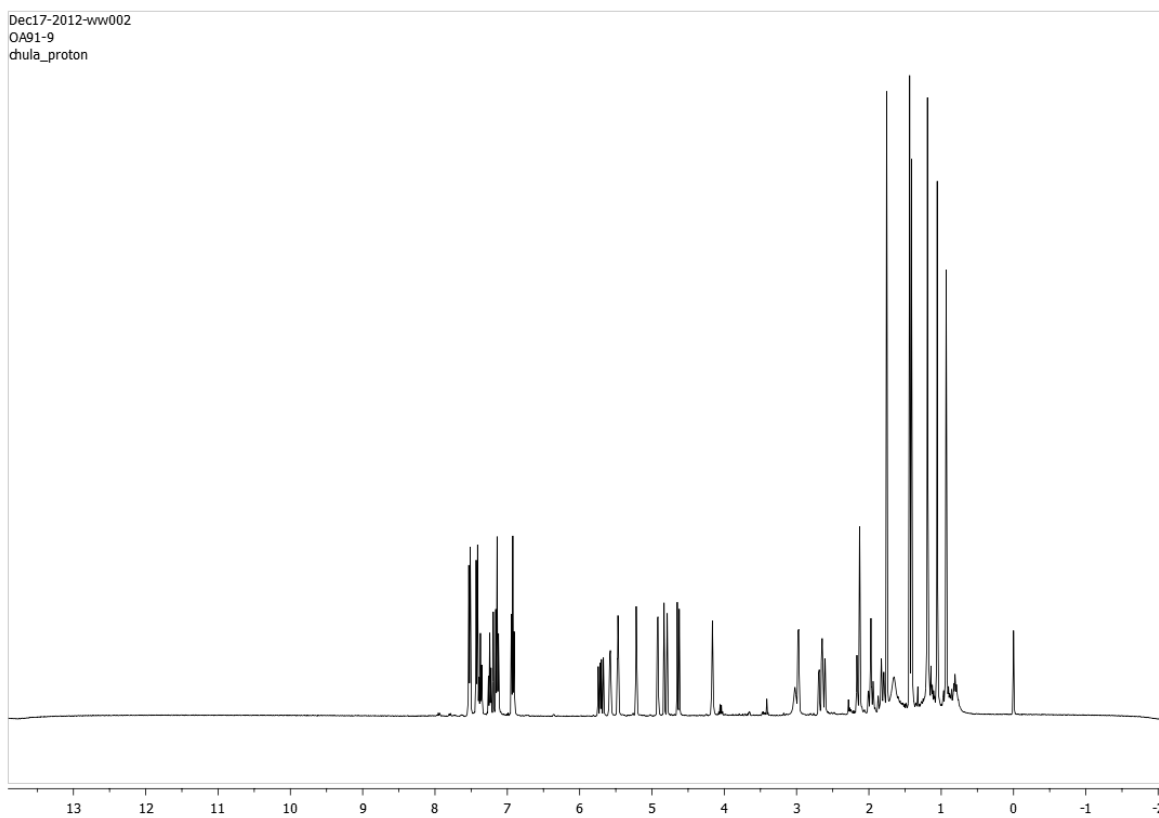
Figure 4.17 ^{1}H-NMR spectrum (400 MHz, in CDCl$_3$) of orthosiphol A (**17**)
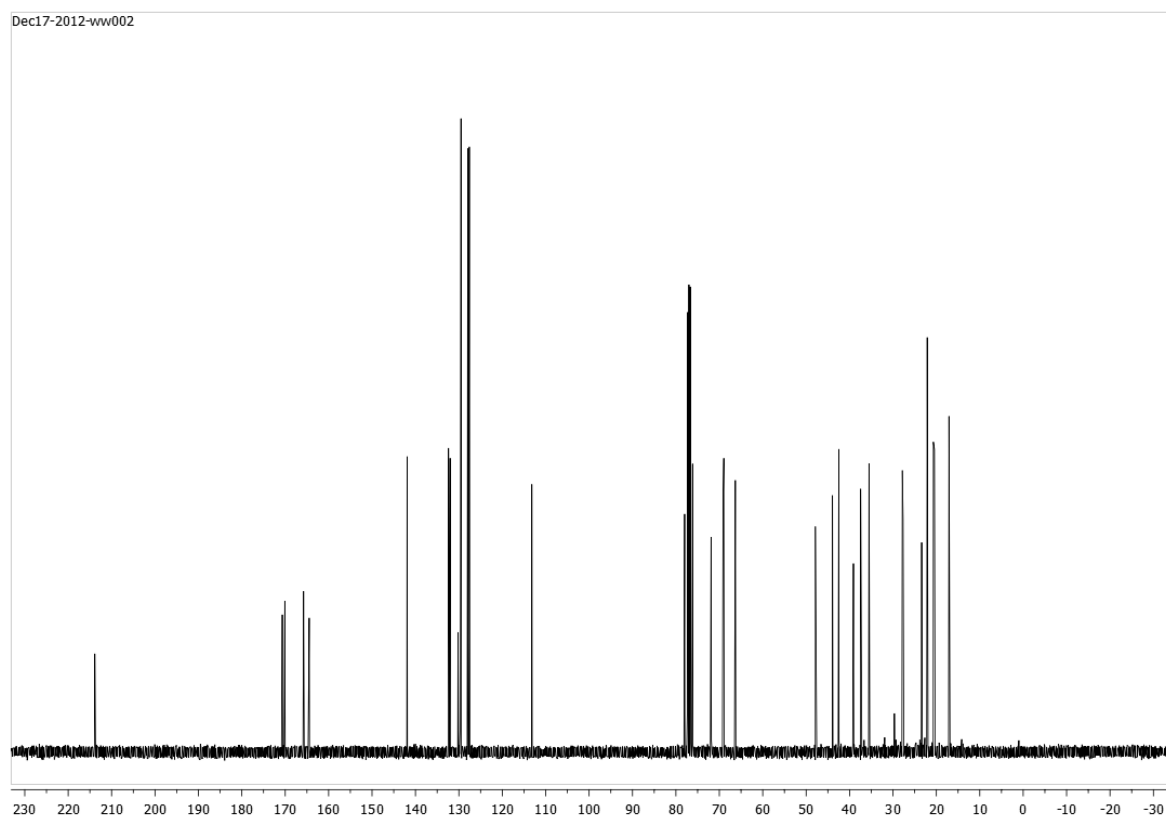
Figure 4.18 ^{13}C-NMR spectrum (100 MHz, in CDCl$_3$) of orthosiphol A (**17**)

CHAPTER V

DIFFERENTIAL EFFECT OF POLYPHENOL TO SOYBEAN FLOUR, NEW SOURCE OF α-GLUCOSIDASE INHIBITORS HAVING MULTIPLE HEALTH BENEFITS

5.1 Introduction

Daily consumption of berry has several beneficial effects to health especially lowering risk of hyperglycemia, cardiovascular disease (CVD), and lung cancer (Amin, Kucuk, Khuri, & Shin, 2009). Berries contain a variety of different phenolic compounds including anthocyanins (ANC), flavonols, proanthocyanidins (PAC) and stilbenes; they possess anti-inflammatory activity and reduction of oxidative stress, which are associated with aforementioned diseases.

In modern life, berry juice is popular for most consumers due to its palatability ready for drink. In fact, original berry juice is well-known for tart and astringent flavor. Therefore, berry juice was formulated by adding high level of sugar to make it more palatable. This result in the relatively high caloric count associated with berry juice consumption. To address this problem, Lila and coworkers at the Plants for Human Health Institute introduced approach that involved absorption of berry phenolics on to food-compatible materials, usually used protein, while high sugar content is removed. This lays on the fact that phenolics from exclusively tight affinity to proteins, through hydrogen bonding (Hagerman, Rice, & Ritchard, 1998), while affinity of protein-sugar complex is not observed. The schematic presentation of this approach is shown in Figure 5.1.
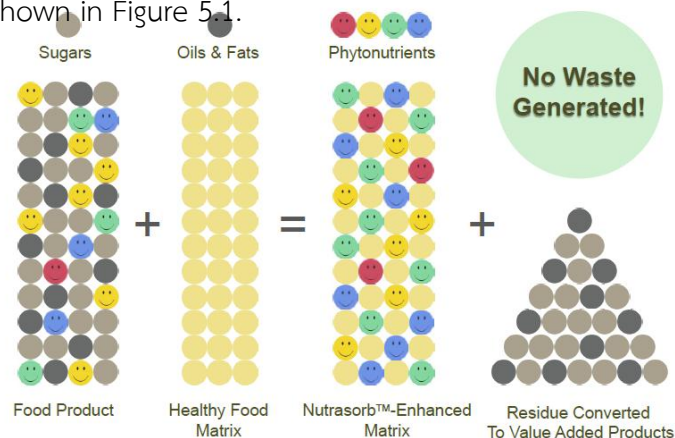
Figure 5.1 Schematic presentation of polyphenol-enriched protein

Of protein used to sorb phenolics—soy protein isolate (SPI), hemp protein isolate (HPI), medium-roast peanut flour (MPF), pea protein isolate (PPI) and defatted soybean four (DSF), the latter has been popularly used due mainly to relatively high protein content (50%). In addition the relatively large structure of protein (> 20 kDa) in DSF can sorb, concentrate, and stabilize phenolic compounds from berry juice (Roopchand et al., 2012). In this study the complexes between DSF and phenolic content from a variety of berry juice were prepared and evaluated for their α-glucosidase inhibitor, antioxidant and anti-inflammatory effect.

Commercially available juice from five berries—blueberry, cranberry, blackcurrant, muscadine grape and pomegranate were investigated. Blueberry (BB) (*Vaccinium angustifolium* Aition; *Vaccinium corymbosum* L.) (Figure 5.2 A) is rich in anthocyanin pigments and proanthocyanidins. Consequently, it was shown to have anti-diabetic properties effect in type 2 diabetic human volunteers by improved insulin sensitivity, after treatment with blueberries smoothie beverage (Martineau et al., 2006).

Cranberry (CB) (*Vaccinium macrocarpon* Ait) (Figure 5.2 B) fruits contain A-type proanthocyanidins (PAC),which are associated with antimicrobial activity, anti-inflammatory responses and preventing urinary tract infections (UTI) (Barbosa-Cesnik et al., 2011)

Blackcurrants (BLC) (*Riber nigrum*) (Figure 5.2 C) are high in anthocyanin mainly represented by delphinidin and cyanidin-3-glucoside or 3-rutino-side (Chandler & Harper, 1962). Previous studies indicated that delphinidin protected human HaCaT keratinocytes. Likewise, cyanidin-3-O-glucoside inhibited inflammation and induced apoptosis (Yun, Afaq, Khan, & Mukhtar, 2009).
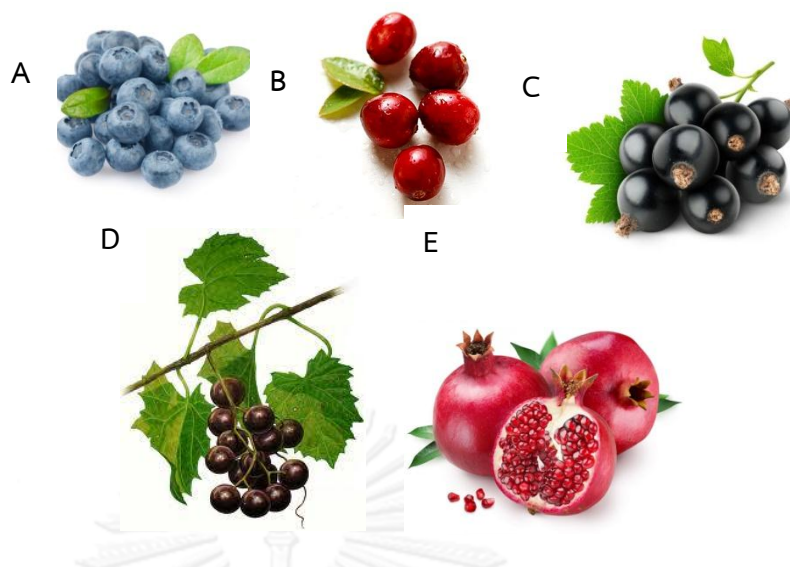
Figure 5.2 Phenolics fruits (A) Blue berry (B) Cranberry (C) Blackcurrants (D) Muscadine grape (E) Pomegranate

Muscadine grape (MG) (*Vitis rotundifolia*) (Figure 5.2 D) contains anthocyanin such as 3,5-diglucoside of delphinidin, cyanidin, petunidin and peonidin (Pastrana-Bonilla, Akoh, Sellappan, & Krewer, 2003). The extract of seed, skin combination of them showed anti-inflammatory properties on mouse ear (Bralley, Hargrove, Greenspan, & Hartle, 2007).

Pomegranate (PG) (*Punica granatum* L.) (Figure 5.2 E) is a rich source of polyphenols such as anthocyanins (Alighourchi, Barzegar, & Abbasi, 2008), which recently showed antioxidative, antihypertensive and anti-cancer properties. Antimicrobial activity of pomegranate peel extract against *Staphylococcus aureus*, *Escherichia coli* and *Yersinia enterocolitica* were observed (Al-Zoreky, 2009).

5.2 Results and discussion

5.2.1 Polyphenol captured in DSF

Prior to investigated biological activity of polyphenol-DSF complexes, the polyphenols, ANC, PAC and TP captured by DSF were examined.

Polyphenol-DSF complexes were prepared, using Roopchand (Roopchand et al., 2012) method, by mixing dilute juice (50 g/l) with DSF at room temperature. The flour pellet of polyphenol-DSF complexes were obtained by centrifuging and freeze-drying. ANC, PAC and TP contents (Figure 5.3) were quantified, using calorimetric method, after the removal of them from DSF.

The highest concentrations of ANC (9.52 mg/g) and PAC (4.83 mg/g) were found in blackcurrant-DSF complex (BLC-DSF). On the other hand, the highest TP (26.52 mg/g) was detected in blueberry-DSF complex (BB-DSF) followed by BLC-DSF (24.34 mg/g). However, muscadine grape-DSF complex (MG-DSF) and pomegranate-DSF complex (PG-DSF) were relatively low in ANC, PAC, and TP. Noticeably, BLC-DSF released ANC and PAC (9.52 and 4.83 mg/g) comparable to those found in fresh blackcurrant (14.80 and 6.64 mg/g). This result suggested that BLC-DSF would serve as alternative source of ANC and PAC without high caloric count of sugar.
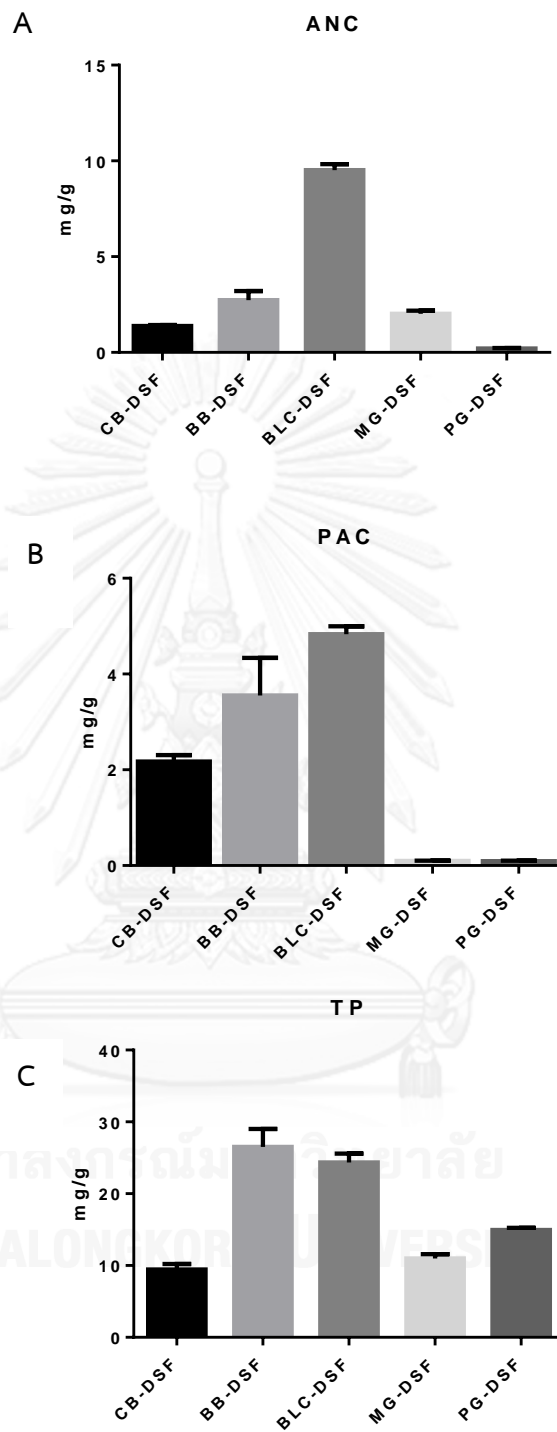
Figure 5.3 (A) Anthocyanins (ANC), (B) proanthocyanidins (PAC), and (C) total phenolics (TP) in polyphenol-enriched DSF calculated as mg/g

5.2.2 α-Glucosidase inhibitory activity of polyphenol-enriched DSF

Polyphenol-enriched DSF were investigated for α-glucosidase inhibitory activity by using baker's yeast and rat intestine as a source of enzymes.

Table 5. 1 α-Glucosidase inhibitory effect of polyphenol-enriched DSF

Polyphenol-enriched DSF	α-glucosidase inhibitory IC_{50} (mg/mL)		
	Baker's yeast	Rat intestinal	
		Maltase	Sucrase
CB-DSF	NI	14.99±0.62	8.27±0.47
BB-DSF	[a]NI	2.46±0.58	0.90±0.09
BLC-DSF	NI	10.54±0.41	5.09±0.94
MG-DSF	NI	7.15±0.24	15.19±0.32
PG-DSF	NI	6.29±0.60	4.46±0.30

[a]NI, no inhibition, inhibitory effect less than 30% at 10 mg/mL

This is the first research to investigate the inhibitory effect of polyphenol-enriched DSF. All polyphenol-enriched DSF showed no inhibition against α-glucosidase while their inhibitory activity toward maltase and sucrose were comparable.

The BB-DSF revealed slightly potent inhibition against maltase and sucrose over other polyphenol-enriched DSF with IC_{50} values of 2.46±0.58 and 0.90±0.09 mg/mL, respectively. The enhanced inhibition of BB-DSF was likely to be contributed by its highest TP (Figure 5.3 C).

The α-glucosidase inhibition and mechanism of individual pheonolic compounds have been reported; however, those of combined components of phenolic have rarely been published. To envision the mechanism underlying components in BB-DSF, kinetic study was carried out. The Lineweaver-Burk plots (Figure 5.4 A) of BB-DSF against maltase showed linearity at each concentration examined (0.75 and 0.5 mg/mL); all of which intersected at a single value in the

second quadrant. The kinetic analysis revealed that V_{max} decreased with increasing concentrations of BB-DSF while K_m (0.59 mg/mL) increased. This behavior indicated that BB-DSF inhibited maltase by two different pathways; competitive by forming enzyme-inhibitor (EI) and noncompetitive by forming enzyme-substrate-inhibitor (ESI) complexes (Figure 5.6 A). To determine the affinity of inhibitor in EI and ESI complexes, the secondary plots were constructed. The secondary plot of slope vs inhibitor concentration revealed K_i value of 1.04 mg/mL, while of Y-intercept vs inhibitor concentration showed K'_i value of 0.068 mg/mL.

The affinity of BB-DSF was rationalized that inhibitor can bind to one inhibitor can bind either to ESI. The 16-time lower value of K'_i suggested that the inhibitor preferably bind to ES intermediate to from ESI complex.

The mechanism underlying inhibition against sucrase was also determined using the above method. The lines in Lineweaver-Burk plots (Figure 5.5 A) of BB-DSF against sucrase intersected at a single value in the second quadrant. The kinetic analysis revealed that V_{max} decreased with increasing concentrations of BB-DSF while K_m (333.3 mg/mL) increased. The secondary plots (Figures 5.5 B and C) showed K_i and K'_i values of 0.82 and 1.09 mg/mL, respectively. The comparable (~ 1.3 time) affinity constants suggested that BB-DSF inhibited sucrase by noncompetitive manner (Figure 5.6 B).
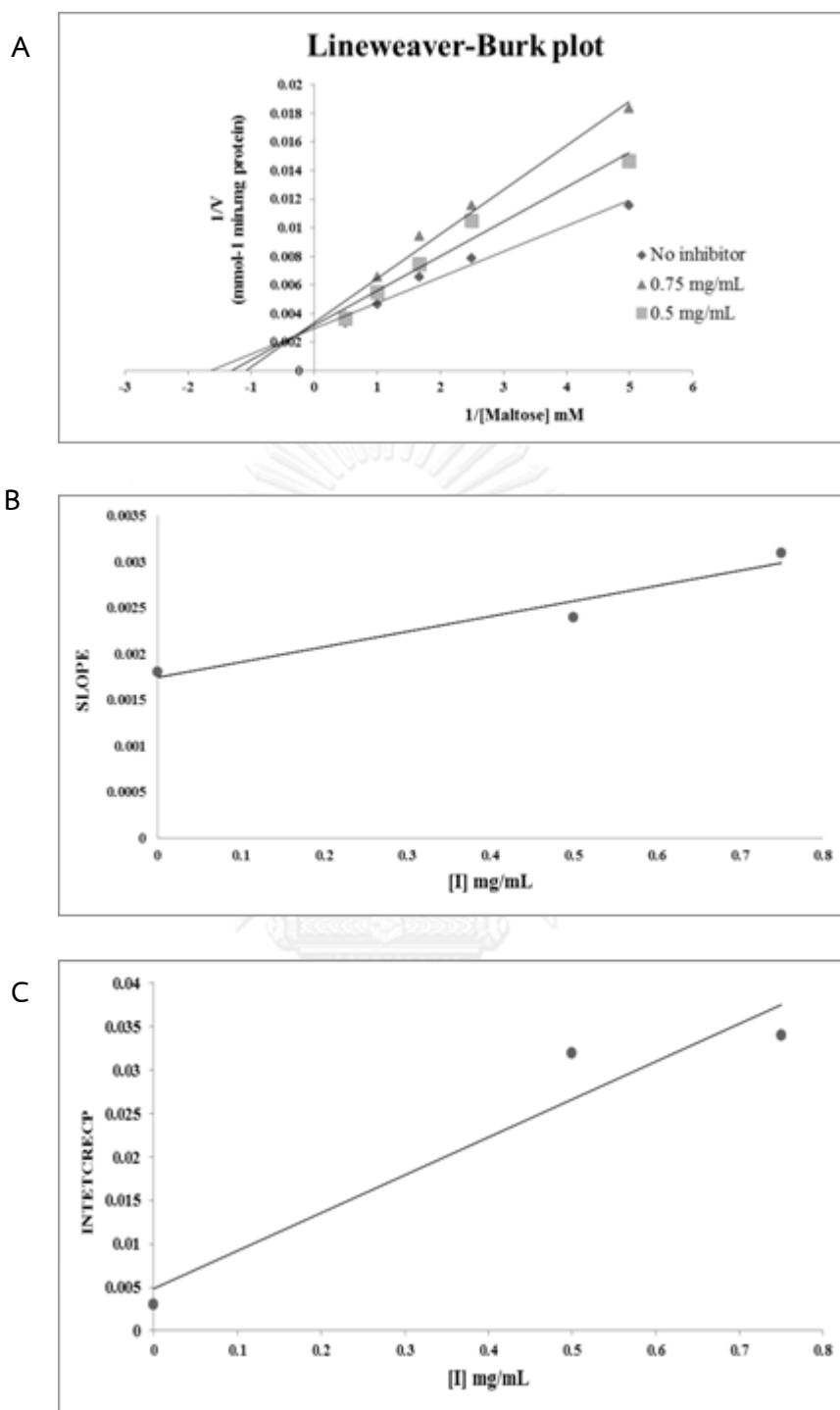
Figure 5.4 (A) Lineweaver-Burk plot of BB-DSF in maltase, $1/V$ aginst $1/[S]$. (B) Secondary replot of slope *vs*. $[I]$ from a primary Linewaaver-Burk plot for the determination of K_i. (C) Secondary replot of intercept *vs*. $[I]$ from a primary Lineweaver-Burk plot for determination of $K_{i'}$.
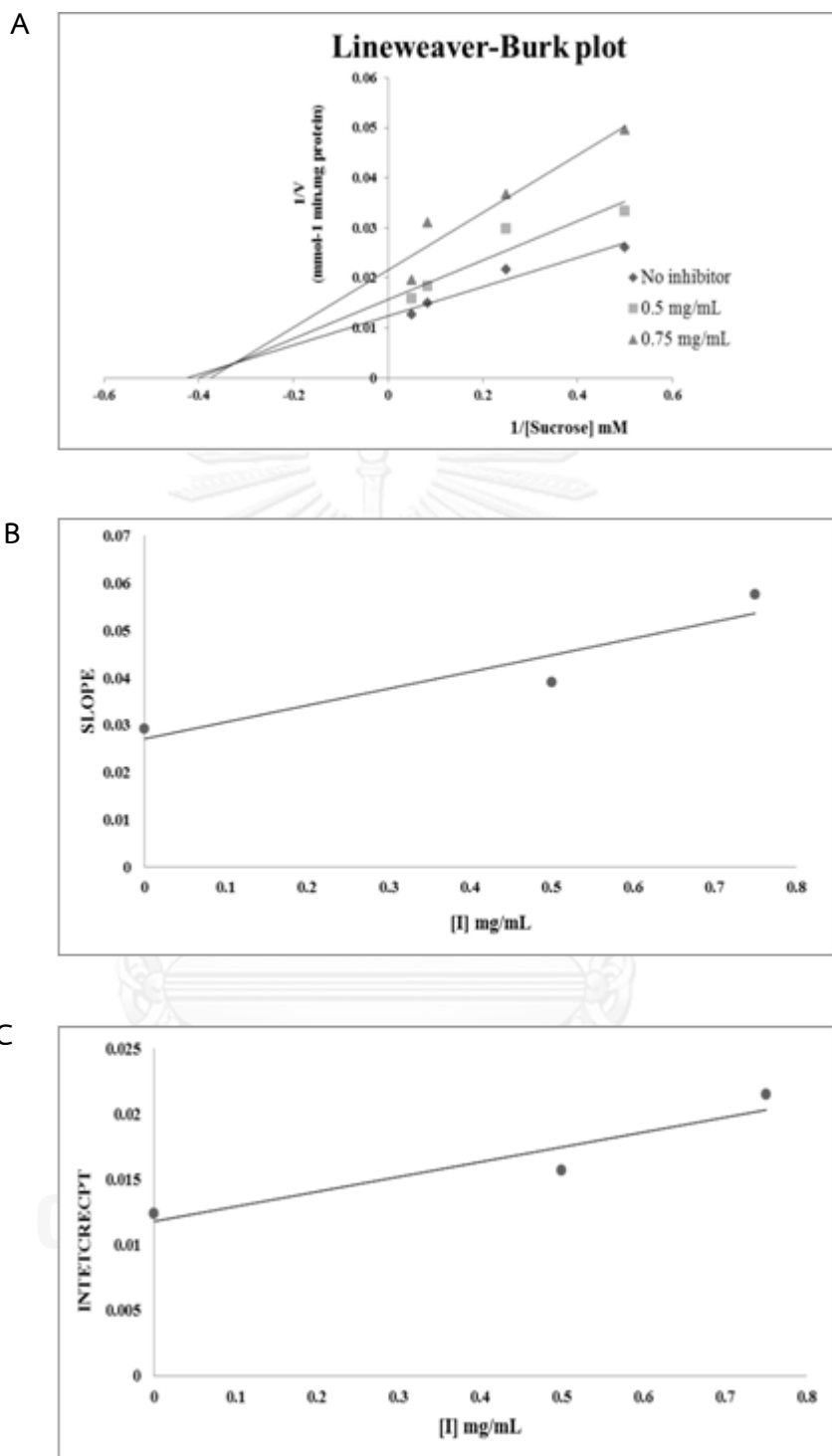
Figure 5.5 (A) Lineweaver-Burk plot of BB-DSF in sucrase, $1/V$ aginst $1/[S]$. (B) Secondary replot of slope *vs*. [*I*] from a primary Linewaaver-Burk plot for the determination of K_i. (C) Secondary replot of intercept *vs*. [I] from a primary Lineweaver-Burk plot for determination of $K_{i'}$.

A

$$S$$

$$E \rightleftharpoons ES \longrightarrow E + P$$

I

I

K_i 1.04 mg/mL

K'_i 0.068 mg/mL

$$EI \rightleftharpoons EIS$$

$$S$$

B

$$S$$

$$E \rightleftharpoons ES \longrightarrow E + P$$

I

I

K_i 0.82 mg/mL

K'_i 1.09 mg/mL

$$EI \rightleftharpoons EIS$$

$$S$$
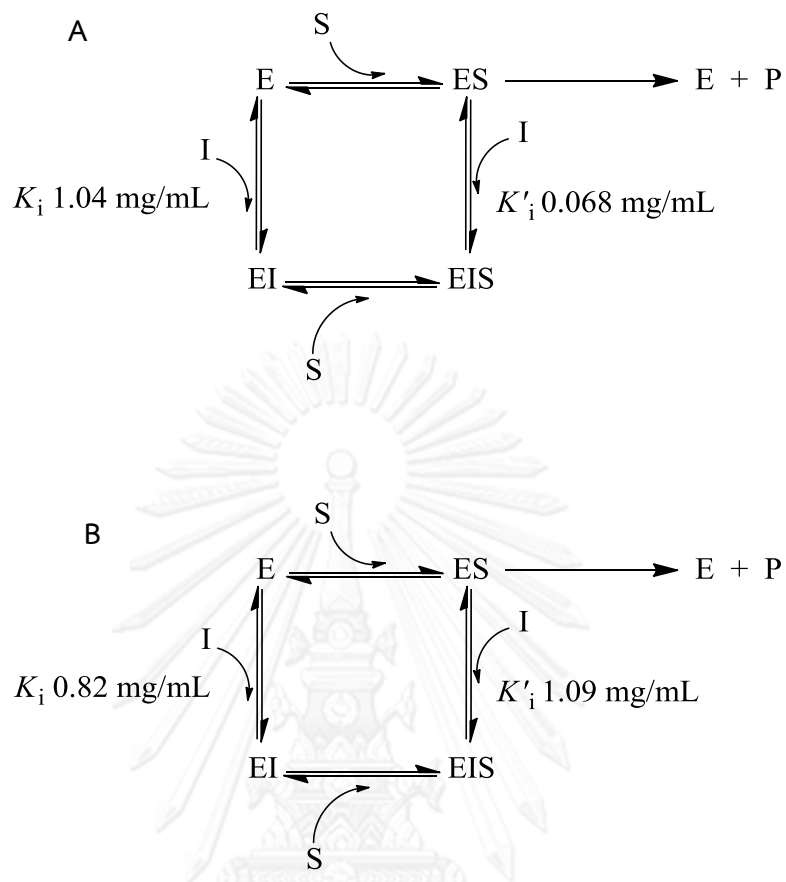
Figure 5.6 Proposed inhibitory mechanism of BB-DSF against (A) maltase, (B) sucrase

5.2.3 Antioxidant activity

The antioxidant activity of polyphenol-enriched DSF was evaluated using DPPH assay as a stable radical. Since the polyphenol-enriched DSFs would be developed as functional food, their antioxidant potency was described in term of concentration of commercial available Trolox$^{®}$ per dried weight. In Table 5.2, BLC-DSF showed and BB-DSF had the highest DPPH scavenging capacity value of 64.95±4.86, 62.01±10.39 µM TE/dw. Noticeably, antioxidation potency of fresh BB (Grace, Esposito, Dunlap, & Lila, 2013) and BB-DSF is comparable (46.5±4.5 vs 62.01±10.39). This result also suggested that polyphenol-enriched DSF process does not other or reduced bioactivity of phenolic contents in this functional food.

Table 5.2 DPPH activity of polyphenol-enriched DSF

Polyphenol-enriched DSF	DPPH scavenging capacity (µM TE/dw)
CB-DSF	19.27±7.60
BB-DSF	62.01±10.39
BLC-DSF	64.95±4.86
MG-DSF	23.70±1.20
PG-DSF	50.10±2.56

5.2.4 Anti-inflammatory Assay

The lipopolysaccharide (LPS) is the distinct cell wall component found only in Gram-negative bacteria. It has been used as an inducer of inflammatory pathway by triggering while blood cell to release pro-inflammatory cytokines and enzymes such as interleukin-1β, cyclooxgenase-2 (COX-2), inducible nitric oxide synthase (iNOS), and interleukin-6 (IL-6) (Figure 5.7).
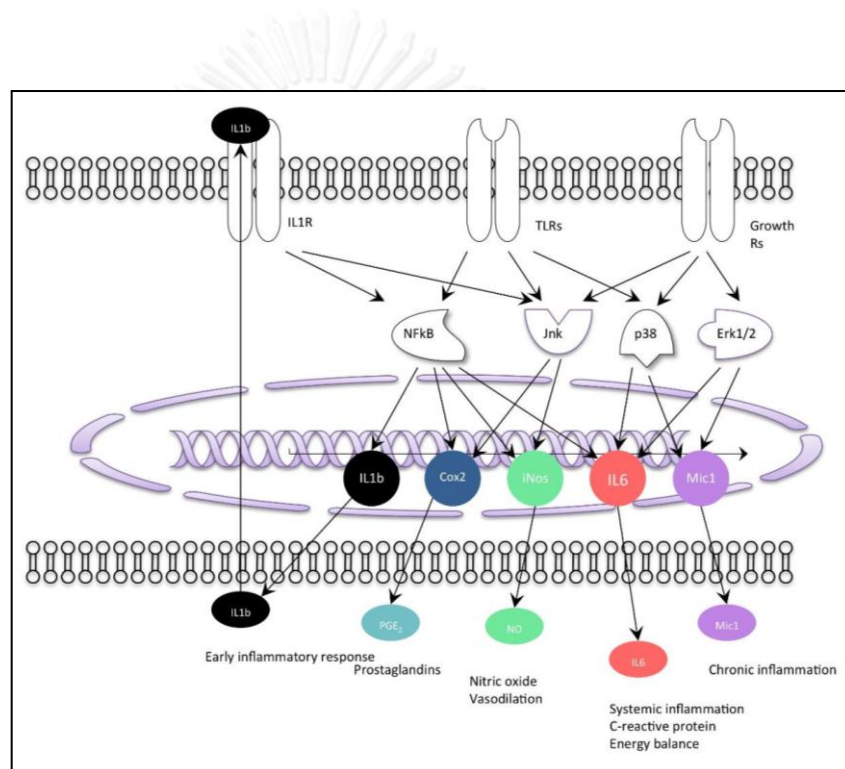
Figure 5.7 Genes involved in inflammatory response in macrophages. Five genes involved in acute and chronic inflammation were used as indicators of the inflammatory response.

This investigation used four genetic four genetic biomarkers in the acute-phase response, inflammatory response, and humoral immune response were determined in the LPS-stimulated murine RAW 264.7 macrophage. In the experiments were used to quantify the relative amount of transcripts for target genes with the total RNA under polyphenol-enriched DSF (50, 150 µg/mL). The negative control (no LPS-treatment) maintained for all expressed genes; the induction control (treated with LPS) revealed the maximum of marker genes; and the positive control (treated with LPS and DEX). Dexamethasone (Dex) is an anti-inflammatory glucocorticoid acting as a positive control to suppress inflammation at 1 uM.

The polyphenol-enriched DSF extracts appeared to reduce expression of all inflammatory response genes to varying degrees. Treatment with polyphenol-enriched DSF showed inhibited LPS-elicited induction of pro-inflammatory inducible cytokine IL-1β, IL6 and one enzyme coding genes nitric oxide synthase (iNOS) (Figure 5.8 A,B, and C). All polyphenol-enriched DSF were highly enriched with ANC, PAC, and TP (Figure 5.3 A, B, and C) and exhibited does-dependent inhibition of LPS-elicited induction of iNOS in RAW 264.7 cell. Therefore, the data suggested that polyphenol-enriched DSF strong anti-inflammatory activity. Noticeably, the result also indicated that CB-DSF and BC-DSF exhibited inhibition of iNOS and IL6 agree with polyphenol-rich fraction and crude extract of fresh cranberry and blueberry(Grace et al., 2013). The anti-inflammatory bioactivity of berries is likely condition by combination of flavonoid contained in the extracts, has been noted in previous research (Cuevas-Rodríguez et al., 2010).
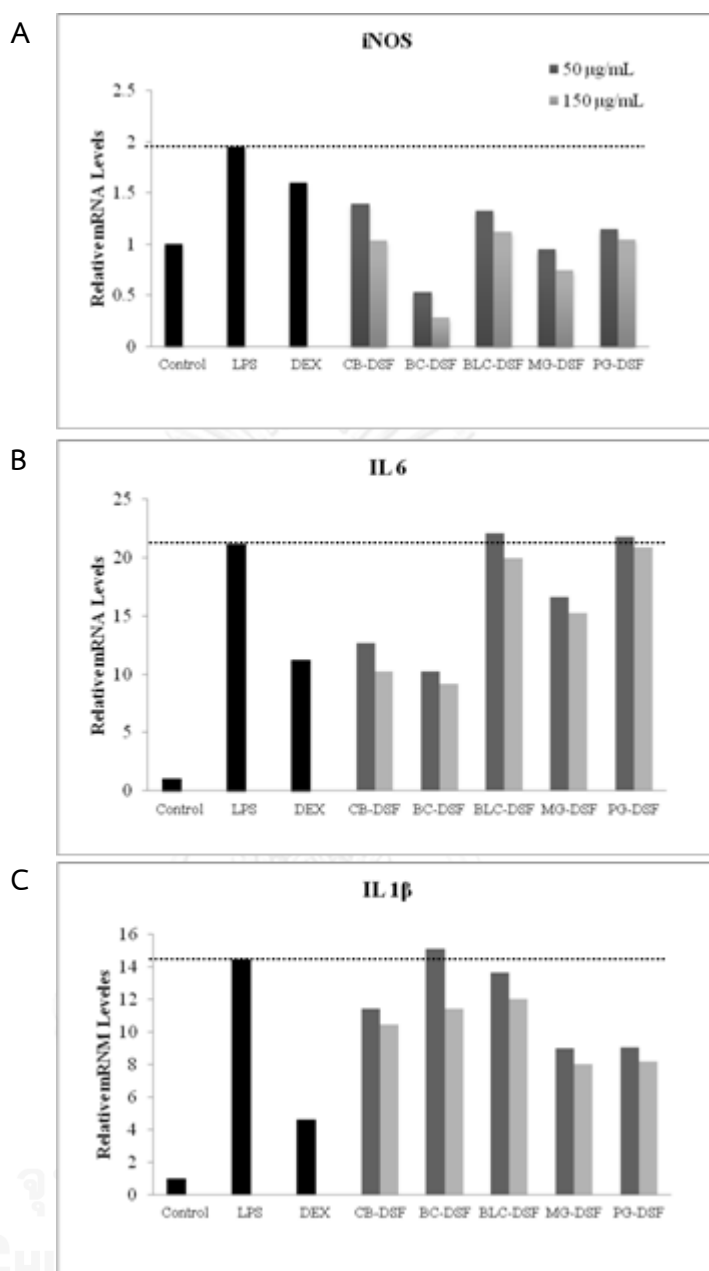
Figure 5.8 Anti-inflammatory activity of polyphenol-enriched DSF; effect on the mRNA expression of the inflammatory biomarker genes in the LPS-stimulated RAW264.7 macrophages at 50, 150 μl/mL, (A) iNOS assay, (B) IL6 assay, and (C) IL1β assay

5.3 Experiment section

5.3.1 Sorption of berry polyphenols to protein

Defatted soybean flour (DSF) (Hodgson Mill Inc., IL), and cranberry juice (Ocean Spray Cranberries Inc., Lakeville-Middleboro, MA, USA), blueberry (Fruit fast Brownwood Acres Foods Inc. USA), blackcurrants (Nelson, New Zealand). muscadine grape (Wray, GA, USA) and pomegranate (Fruit fast Brownwood Acres Foods Inc. USA) were purchased form grocery store. All fruit juice concentrates were diluted each juice 4X in water. The experiment were performed using defatted soybean four (100g/l) mixed with 4X diluted of juice on magnetic stir plate. In all triplicate samples were prepared for each condition tested. Juice flour mixtures were centrifuged for 10 min at 12,000 rpm (Beck-man, JA17 rotor and the supernatants were filtered prior to quantification of anthocyanins, proanthocyanidins or total polyphenols. Polyphenol-enriched DSF was freeze-dried and powdered for further analysis.

Figure 5.9 Sorption of blueberry polyphenols to defatted soybean flour (DSF) A: Blueberry-DSF, B: Cranberry-DSF (Roopchand et al., 2012)

5.3.2 Quantification of total anthocyanins, total proanthocyanidins and total phenolics

The total monometic anthocyanins (mg/L) was calculated as cyanidin 3-O-glucoside according to the formula: A (MW) (DF) 100/ (ε x 1), which molecular weight (MW, 449 g/mol) of cyanidin 3-O-glucoside. The pH differential method was used total anthocyanins in CB-DSF, BB-DSF, BLC-DSF, MG-DSF and PG-DSF were measured at 520 nm and 700 nm with UV/VIS (SpectraMax M3, Sunnyvale, CA, USA) spectrophotometer. The absorbance (A) was then calculated as $(A_{520}-A_{700})_{pH1.0}-(A_{520}-A_{700})_{pH4.5}$. The total phenolics were diluted concentration and detected with Folin-Ciocalteu reagent. The sample were read at 726 nm based on a created gallic acid standard curve. Total of proanthocyanidins were detected using the 4-dimethylaminoiannamaldehyde (DMAC) method in a 96-well plate and read at 640 nm of each well in the plate every minute for 30 min (SpectraMax M3, Sunnyvale, CA, USA) and the concentration of proanthocyanidins in the solution based on procyanidin A2 equivalents.

5.3.3 Glucosidase inhibition assay

The inhibitory activity of polyphenol-enriched DSF against α-glucosidase form rat intestine (maltase and sucrose). Maltase and sucrase were received from rat intestinal acetone powder (Sigma, St. Louis); therefore, the powder (1 g) was homogenized with 0.9% NaCl (30 ml) and centrifugation (12,000 g) for 30 min. Polyphenol-enriched DSF (100μl) were incubated with crude enzyme solution (maltase, 100μl; sucrase, 100μl, respectively). The substrate solution (maltose: 10mM, 100μl; sucrose: 100mM, 100μl, respectively) in 0.1 M phosphate buffer (pH 6.9);therefore, incubate reaction 37°C for maltose (20 min) and sucrose (60 min). The mixtures were suspended in boiling water for 10 min to stop reaction were determined by the glucose assay kit and measured at 500 nm. The percentage inhibition was calculated by $[(A_0-A_1)/A_0] \times 100$, where A_1 and A_0 are the absorbance with and without the sample, respectively. The IC_{50} value was deduced from a plot of percentage inhibition

Kinetic study of α-glucosidase inhibition

The kinetic study was was performed according to the above reaction except that the quantity of α-glucosidase from rat intestinal. The activity (maltase and sucrase) were maintained at 0.45 and 0.09 U/mg protein, respectively, while the concentration of each tested inhibitor was varied at 0, 0.5 and 0.75 mg/mL. The type of inhibition was investigated from Lineweaver–Burk plots, where the K_i and K_i' values were determined from the secondary plots of slope vs. [I] and the interception vs. [I] of the Lineweaver–Burk plot.

5.3.4 Free radical scavenging (DPPH assay)

The DPPH activity was measured using stable DPPH and Trolox as reference substance. The polyphenol-enriched DSF was extracted and diluted with 80% methanol. Add 100 μl of each samples was pipette into 3.9 ml of DPPH solution (0.08M in 95% ethanol). The reaction was incubated 3 hr at room temperature, read at 515 nm against ethanol as blank using a Shimadazu UV-2450 spectrophotometer. Trolox (0, 25, 50, 100, and 250 μg/mL) was determined standard antioxidant. The DPPH activity was reported in micromoles of Trolox equivalents per gram dry weigh (μmol TE/g dw).

5.3.5 Cell culture

The Raw 264.7 cell line (murine macrophage ATCC#TIB71) donated from KLB). The LPS-activated RAW264.7 macrophage cells were maintained in DMEM supplemented with 10% fetal bovine serum and antibiotics, at 37°C in 5% CO_2 incubator. Cells were seeded into 24-well culture plates, and treated for 5h with LPS alone or combined with respective concentrations of polyphenol-enrich DSF extracts at 50 ug/mL and 150 ug/mL.

5.3.6 Quantitative PCR Analysis

Total RNA was extracted from RAW264.7 murine macrophage cell culture using Trizol reagent. RNA was quantified spectrophotometrically by the 260/280 index and it was in all the samples between 1.8 and 2.1 using NanoDrop. The cDNAs were synthesized with 2μg of RNA for each sample, using the high capacity cDNA reverse transcription kit. The synthesized cDNAs were diluted 20-fold. Five microliters of diluted samples was used for PCR reactions of 20μl final volume, containing 1μl of each gene-specific primer, 3μl of PCR-grade water, and 10μl SYBR Green 2x Supermix. Quantitative PCR amplifications were performed on an ABI 7300 Real-Time Detection System using 1 cycle at 50℃ for 2 min and 1 cycle of 95℃ for 10 min, followed by 40 cycles of 15s at 95℃ and 1 min at 60℃. Quantification was based on Ct difference performed according to the ''delta–delta Ct method using the following equation: expression ratio = $2^{-\Delta\Delta Ct}$, where $\Delta\Delta Ct = (Ct_{target} - Ct_{reference})_{Time\ x} = (Ct_{target} - Ct_{reference})_{Time\ control}$, which produces a ratio of the target gene expression relative to uniformly expressed housekeeping genes.

CHAPTER VI

CONCLUSION

Base on the results of α-glucosidase form edible plants, The active compounds from leaves of *Piper sarmentosum* Roxb , white *Sesamum indicum* L.seed pulp and from aerial part of *Orthosiphon aristatus* (Blume) Miq were identified. The isolation of the CH_2Cl_2 extract from the leave of *Piper sarmentosum* Roxb afforded seven compounds, consisting of three new phenylpropanoyl amides name chaplupyrrolidones A (**1**) and B (**2**) and deacetylsarmentamide B (**7**), in addition to four known phenylropanoids named *N*-(3-(4'methoxyphenyl)propanoyl)pyrrole (**3**), *N*-(3-phenylpropa- noyl)pyrrole (**4**), asaricin (**5**) and cinnamic acid (**6**), Furthermore, two known flavonoids glycoside isolated form MeOH extracts names kaemforol-3-*O*-rhamnoside (**8**) and dihydrokaempferol-3-*O*-glucoside (**9**) were also isolated (Figure 6.1). The isolation of MeOH extract form white *Sesamum indicum* L.seed pulp resulted in three lignans named sesamin (**10**), sesamolin (**11**) and sesaminol monoglucoside (**12**) (Figure 6.2). The flavonoids named sinensetin (**13**), salvigenin (**14**), tetramethylscutellarein (**15**) and 3,7,4'-tri-*O*-methylkaempferol (**16**) together with a diterpenoid named orthosiphol A (**17**) were isolated from CH_2Cl_2 extract of aerial part of *Orthosiphon aristatus* (Blume) Miq (Figure 6.3).
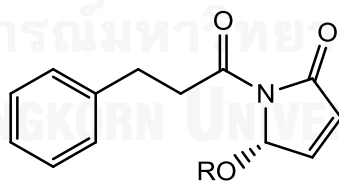
chaplupyrrolidone A; R = H (**1**, new compound)
chaplupyrrolidone B; R = CH_3 (**2**, new compound)
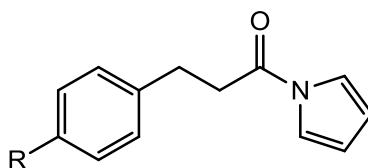
N-(3-(4'-Methoxyphenyl)propanoyl)pyrrole; R = OCH_3(**3**)
N-(3-phenylpropanoyl)pyrrole; R = H (**4**)

asaricin (**5**)

cinnamic acid (**6**)

deacetylsamentamide B (**7,** new compound)

kamforal-3-*O*-rhamnoside (**8**)

dihydrokamferol-3-*O*-glucoside (**9**)
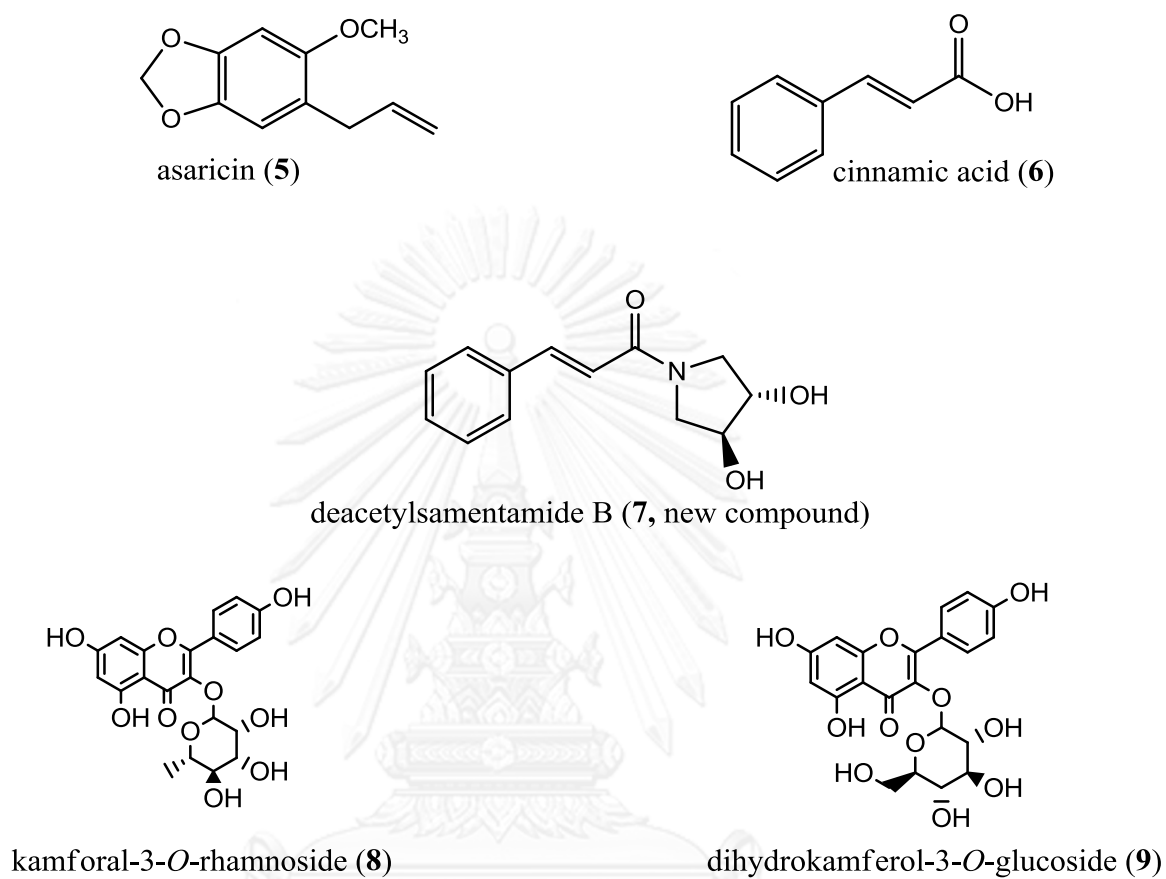
Figure 6.1 The chemical structures of isolated compounds from *Piper sarmentosum* Roxb Leave

sesamin (**10**)

sesamolin (**11**)

sesaminol monoglucoside (**12**)
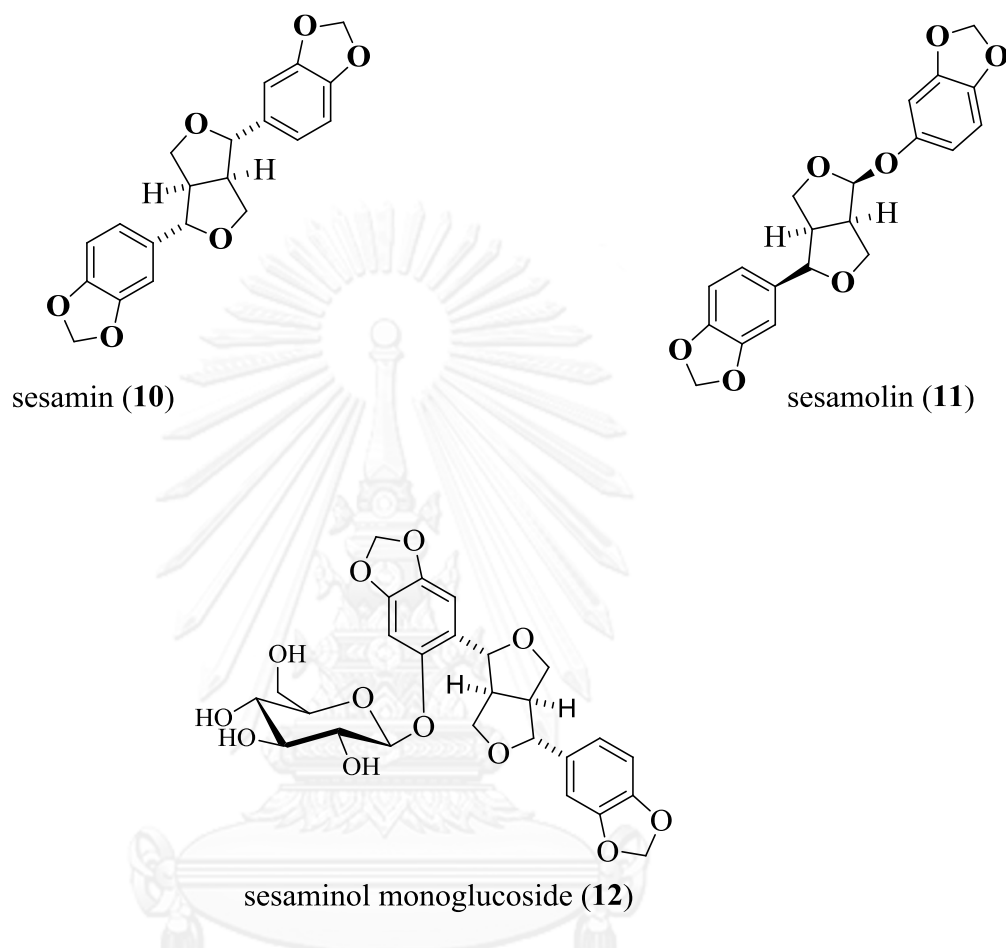
Figure 6.2 The chemical structures of isolated compounds from white *Sesamum indicum* L. seed pulp.

sinensetin (**13**)

salvigenin (**14**)

tetramethylscutellarein (**15**)

3,7,4'-tri-O-methylkaempferol (**16**)
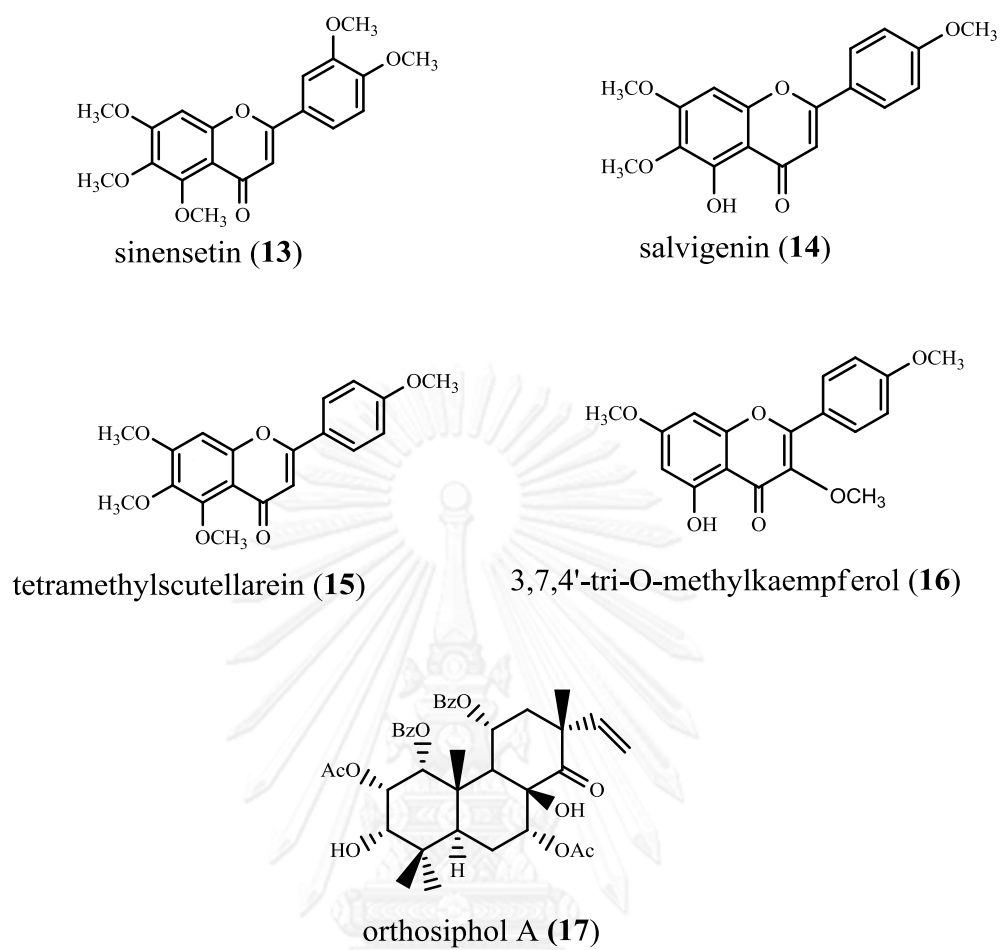
orthosiphol A (**17**)

Figure 6.3 The chemical structure of isolated compounds from aerial part of *Orthosiphon aristatus* (Blume) Miq.

Present study of the inhibitory activity against α-glucosidase from barker's yeast and rat intestinal (maltase and sucrase) isolated from *Piper sarmentosum* Roxb leaves was detected using colorimetric method. Chaplupyrrolidones A (**1**) and B (**2**) act yeast α-glucosidase inhibitors with IC_{50} values of 7842.0 and 430.0 µM, respectively. The kinetic of chaplupyrrolidones A (**1**) revealed on indicated that acts as a noncompetitive manner. White defatted sesame attempted to isolate of various lignans. Of all isolated compounds, sesamin (**10**) and sesamolin (**11**) were against yeast α-glucosidase inhibitors with IC_{50} values of 450, 200 µM, respectively. The kinetic study inhibited by sesamin through competitive inhibitor type. The isolated compounds from aerial part of *Orthosiphon aristatus* (Blume) Miq showed inhibitory against α-glucosidase from barker's yeast and rat intestinal (maltase and sucrase). Tetramethylscutellarein (**15**) and 3,7,4'-tri-*O*-methylkaempferol (**4**) were against yeast α-glucosidase inhibitors with IC_{50} values of 6.34, 0.75 mM, respectively, while orthosiphol A (**15**) showed against rat α-glucosidase inhibitors (maltase) with IC_{50} value of 6.54 mM. The kinetic determined of orthosiphol A (**17**) in noncompetitive manner.

In addition, we demonstrated that can effectively sorb, concentrate and stabilize bioactive polyphenols from fruits juice and while high sugar content can be completely removed. BB-DSF and BLC-DSF were rich in AN, PAC and PAC. All polyphenol-enriched DSF were showed potent inhibition against rat α-glucosidase (maltase and sucrase). BB-DSF was the most potent rat α-glucosidase inhibitors with IC_{50} values of 2.46 (maltase) and 0.90 mg/mL (sucrase), respectively. The mechanism underling inhibition against maltase was proved to be mixed-type manner while sucrase inhibited by noncompetitive manner. All polyphenol-enrich DSF demonstrated higher level of phenolic components, antioxidant capacity (DPPH) and exhibited LPS-elicited induction in RAW 264.7 cells. The data suggested that polyphenol-enriched DSF can provide a high-protein, low-sugar ingredient for novel food and dietary supplements.

REFERENCES

Acharjee, S., Ghosh, B., Al-Dhubiab, B. E., & Nair, A. B. (2013). Understanding Type 1 Diabetes: Etiology and Models. *Canadian Journal of Diabetes, 37*(4), 269-276.

Ahmed, Z. F., Rimpler, H., Rizk, A. M., Hammouda, F. M., & Ismail, S. I. (1970). The flavonoid constituents of certain Centaurea species grown in Egypt. *Phytochemistry, 9*(7), 1595-1601.

Al-Zoreky, N. S. (2009). Antimicrobial activity of pomegranate (*Punica granatum* L.) fruit peels. *International Journal of Food Microbiology, 134*(3), 244-248.

Alighourchi, H., Barzegar, M., & Abbasi, S. (2008). Anthocyanins characterization of 15 Iranian pomegranate (*Punica granatum* L.) varieties and their variation after cold storage and pasteurization. *European Food Research and Technology, 227*(3), 881-887. doi: 10.1007/s00217-007-0799-1

Ameer, O. Z., Salman, I. M., Asmawi, M. Z., Ibraheem, Z. O., & Yam, M. F. (2012). Orthosiphon stamineus: traditional uses, phytochemistry, pharmacology, and toxicology. *J Med Food, 15*(8), 678-690. doi: 10.1089/jmf.2011.1973

Amin, A. R., Kucuk, O., Khuri, F. R., & Shin, D. M. (2009). Perspectives for cancer prevention with natural compounds. *J Clin Oncol, 27*(16), 2712-2725. doi: 10.1200/jco.2008.20.6235

Barbosa-Cesnik, C., Brown, M. B., Buxton, M., Zhang, L., DeBusscher, J., & Foxman, B. (2011). Cranberry Juice Fails to Prevent Recurrent Urinary Tract Infection: Results From a Randomized Placebo-Controlled Trial. *Clinical Infectious Diseases, 52*(1), 23-30. doi: 10.1093/cid/ciq073

Bigoniya, P., Nishad, R., & Singh, C. S. (2012). Preventive effect of sesame seed cake on hyperglycemia and obesity against high fructose-diet induced Type 2 diabetes in rats. *Food Chemistry, 133*(4), 1355-1361.

Borges de Melo, E., da Silveira Gomes, A., & Carvalho, I. (2006). α- and β-Glucosidase inhibitors: chemical structure and biological activity. *Tetrahedron, 62*(44), 10277-10302.

Bralley, E. E., Hargrove, J. L., Greenspan, P., & Hartle, D. K. (2007). Topical anti-inflammatory activities of *Vitis rotundifolia* (muscadine grape) extracts in the tetradecanoylphorbol acetate model of ear inflammation. *J Med Food, 10*(4), 636-642.

Bridges, C. G., Brennan, T. M., Taylor, D. L., McPherson, M., & Tyms, A. S. (1994). The prevention of cell adhesion and the cell-to-cell spread of HIV-1 in vitro by the α-glucosidase 1 inhibitor, 6-O-butanoyl castanospermine (MDL 28574). *Antiviral Research, 25*(2), 169-175.

Chandler, B., & Harper, K. (1962). A procedure for the absolute identification of anthocyanins: the pigments of blackcurrant fruit. *Australian Journal of Chemistry, 15*(1), 114-120.

Chanwitheesuk, A., Teerawutgulrag, A., & Rakariyatham, N. (2005). Screening of antioxidant activity and antioxidant compounds of some edible plants of Thailand. *Food Chemistry, 92*(3), 491-497.

Chen, H., Feng, R., Guo, Y., Sun, L., & Jiang, J. (2001). Hypoglycemic effects of aqueous extract of Rhizoma Polygonati Odorati in mice and rats. *Journal of Ethnopharmacology, 74*(3), 225-229.

Chen, J., Montanari, A. M., & Widmer, W. W. (1997). Two New Polymethoxylated Flavones, a Class of Compounds with Potential Anticancer Activity, Isolated from Cold Pressed Dancy Tangerine Peel Oil Solids. *Journal of Agricultural and Food Chemistry, 45*(2), 364-368. doi: 10.1021/jf960110i

Chen, L., Magliano, D. J., & Zimmet, P. Z. (2012). The worldwide epidemiology of type 2 diabetes mellitus[mdash]present and future perspectives. *Nat Rev Endocrinol, 8*(4), 228-236.

Chiasson, J. L., & Rabasa-Lhoret, R. (2004). Prevention of type 2 diabetes: insulin resistance and beta-cell function. *Diabetes, 53 Suppl 3*, S34-38.

Clerc, P., Simon, S.,. (1989). *Tables of Spectral Data for Structure Determination of Organic Compounds*: Springer Berlin Heidelberg.

Cuevas-Rodríguez, E. O., Dia, V. P., Yousef, G. G., García-Saucedo, P. A., López-Medina, J., Paredes-López, O., . . . Lila, M. A. (2010). Inhibition of Pro-inflammatory Responses and Antioxidant Capacity of Mexican Blackberry (Rubus spp.) Extracts. *Journal of Agricultural and Food Chemistry, 58*(17), 9542-9548.

Escandón-Rivera, S., González-Andrade, M., Bye, R., Linares, E., Navarrete, A., & Mata, R. (2012). α-Glucosidase Inhibitors from *Brickellia cavanillesii*. *Journal of Natural Products, 75*(5), 968-974.

Fukuda, Y., Nagata, M., Osawa, T., & Namiki, M. (1986). Contribution of lignan analogues to antioxidative activity of refined unroasted sesame seed oil. *Journal of the American Oil Chemists' Society, 63*(8), 1027-1031.

Grace, M. H., Esposito, D., Dunlap, K. L., & Lila, M. A. (2013). Comparative Analysis of Phenolic Content and Profile, Antioxidant Capacity, and Anti-inflammatory Bioactivity in Wild Alaskan and Commercial Vaccinium Berries. *Journal of Agricultural and Food Chemistry*.

Hagerman, A. E., Rice, M. E., & Ritchard, N. T. (1998). Mechanisms of Protein Precipitation for Two Tannins, Pentagalloyl Glucose and Epicatechin16 (4→8) Catechin (Procyanidin). *Journal of Agricultural and Food Chemistry, 46*(7), 2590-2595.

Kakuda, T., Sakane, I., Takihara, T., Ozaki, Y., Takeuchi, H., & Kuroyanagi, M. (1996). Hypoglycemic effect of extracts from *Lagerstroemia speciosa* L. leaves in genetically diabetic KK-AY mice. *Bioscience, biotechnology, and biochemistry, 60*(2), 204-208.

Kang, M. H., Kawai, Y., Naito, M., & Osawa, T. (1999). Dietary defatted sesame flour decreases susceptibility to oxidative stress in hypercholesterolemic rabbits. *J Nutr, 129*(10), 1885-1890.

Khaleel, A.-S. G., M. H.; El-bagry, R. I.; Sleem, A. A. and Shabana, M. . (2007). Chemical and biological study of the residual aerial parts of *Sesamum indicum* L. . *Journal of Food and Drug Analysis, 15*, 249-257.

Krentz, A., & Bailey, C. (2005). Oral Antidiabetic Agents. *Drugs, 65*(3), 385-411.

Krentz, A. J., & Sinclair, A. J. (2012). Chapter 36 - The Evolution of Glucose-Lowering Drugs for Type 2 Diabetes. In D. Bagchi & N. Sreejayan (Eds.), *Nutritional and Therapeutic Interventions for Diabetes and Metabolic Syndrome* (pp. 459-474). San Diego: Academic Press.

Likhitwitayawuid, K., Ruangrungsi, N., Lange, G. L., & Decicco, C. P. (1987). Structural elucidation and synthesis of new components isolated from *Piper sarmentosum* (piperaceae). *Tetrahedron, 43*(16), 3689-3694.

Lyckander, I. M., & Malterud, K. E. (1996). Lipophilic flavonoids from Orthosiphon spicatus prevent oxidative inactivation of 15-lipoxygenase. *Prostaglandins, Leukotrienes and Essential Fatty Acids, 54*(4), 239-246.

MARIAM, #160, A., ASMAWI, #160, Z., M., . . . A. (1996). *Hypoglycaemic activity of the aqueous extract of Orthosiphon stamineus* (Vol. 67). Amsterdam, PAYS-BAS: Elsevier.

Martineau, L. C., Couture, A., Spoor, D., Benhaddou-Andaloussi, A., Harris, C., Meddah, B., . . . Haddad, P. S. (2006). Anti-diabetic properties of the Canadian lowbush blueberry *Vaccinium angustifolium* Ait. *Phytomedicine, 13*(9–10), 612-623.

Masuda, T., Masuda, K., Shiragami, S., Jitoe, A., & Nakatani, N. (1992). Orthosiphol A and B, novel diterpenoid inhibitors of TPA (12-O-tetradecanoylphorbol-13-acetate)-induced inflammation, from *Orthosiphon stamineus*. *Tetrahedron, 48*(33), 6787-6792.

Matsui, T., Ueda, T., Oki, T., Sugita, K., Terahara, N., & Matsumoto, K. (2001). **α**-Glucosidase Inhibitory Action of Natural Acylated Anthocyanins. 2. **α**-Glucosidase Inhibition by Isolated Acylated Anthocyanins. *Journal of Agricultural and Food Chemistry, 49*(4), 1952-1956.

Moazzami, A., & Kamal-Eldin, A. (2006). Sesame seed is a rich source of dietary lignans. *Journal of the American Oil Chemists' Society, 83*(8), 719-723.

Moazzami, A. A., Andersson, R. E., & Kamal-Eldin, A. (2006). HPLC Analysis of Sesaminol Glucosides in Sesame Seeds. *Journal of Agricultural and Food Chemistry, 54*(3), 633-638.

Moazzami, A. A., Haese, S. L., & Kamal-Eldin, A. (2007). Lignan contents in sesame seeds and products. *European Journal of Lipid Science and Technology, 109*(10), 1022-1027.

Mohamed, E. A., Siddiqui, M. J., Ang, L. F., Sadikun, A., Chan, S. H., Tan, S. C., . . . Yam, M. F. (2012). Potent alpha-glucosidase and alpha-amylase inhibitory activities of standardized 50% ethanolic extracts and sinensetin from *Orthosiphon stamineu*s Benth as anti-diabetic mechanism. *BMC Complement Altern Med, 12*, 176.

Nakabayashi, A., Kitagawa, Y., Suwa, Y., Akimoto, K., Asami, S., Shimizu, S., . . . Yamada, H. (1995). alpha-Tocopherol enhances the hypocholesterolemic action of sesamin in rats. *International journal for vitamin and nutrition research. Internationale Zeitschrift fur Vitamin- und Ernahrungsforschung. Journal international de vitaminologie et de nutrition, 65*(3), 162-168.

Nakano, D., Ogura, K., Miyakoshi, M., Ishii, F., Kawanishi, H., Kurumazuka, D., . . . Matsumura, Y. (2006). Antihypertensive effect of angiotensin I-converting enzyme inhibitory peptides from a sesame protein hydrolysate in spontaneously hypertensive rats. *Bioscience, biotechnology, and biochemistry, 70*(5), 1118-1126.

Nath, R., Chakraborty, P. K., & Chakraborty, A. (2001). Effect of Climatic Variation on Yield of Sesame (*Sesamum indicum* L.) at Different Dates of Sowing. *Journal of Agronomy and Crop Science, 186*(2), 97-102.

Ohashi, K., Bohgaki, T., Matsubara, T., & Shibuya, H. (2000). Indonesian medicinal plants. XXIII. Chemical structures of two new migrated pimarane-type diterpenes, neoorthosiphols A and B, and suppressive effects on rat thoracic aorta of chemical constituents isolated from the leaves of *Orthosiphon aristatus* (Lamiaceae). *Chem Pharm Bull (Tokyo), 48*(3), 433-435.

Oki, T., Matsui, T., & Osajima, Y. (1999). Inhibitory Effect of **α**-Glucosidase Inhibitors Varies According to Its Origin. *Journal of Agricultural and Food Chemistry, 47*(2), 550-553.

Pastrana-Bonilla, E., Akoh, C. C., Sellappan, S., & Krewer, G. (2003). Phenolic Content and Antioxidant Capacity of Muscadine Grapes. *Journal of Agricultural and Food Chemistry, 51*(18), 5497-5503.

Peungvicha, P., S. Thirawarapan, S., Temsiririrkkul, R., Watanabe, H., Kumar Prasain, J., & Kadota, S. (1998). Hypoglycemic effect of the water extract of *Piper sarmentosum* in rats. *Journal of Ethnopharmacology, 60*(1), 27-32.

PT., E. (1995). *Medicinal Herb index in indonesia*. Indonesia: PT Eisai.

Ridtitid, W. R., Peerati; Reanmongkol, Wantana; Wongnawa, Malinee. (2007). Studies of the anti-inflammatory and antipyretic activities of the methanolic extract of *Piper sarmentosum* Roxb. leaves in rats. *Songklanakarin Journal of Science & Technology, 29*(6), 1519-1526.

Roopchand, D. E., Grace, M. H., Kuhn, P., Cheng, D. M., Plundrich, N., Poulev, A., . . . Raskin, I. (2012). Efficient sorption of polyphenols to soybean flour enables natural fortification of foods. *Food Chemistry, 131*(4), 1193-1200.

Rossi, M. H., Yoshida, M., & Soares Maia, J. G. (1997). Neolignans, styrylpyrones and flavonoids from an Aniba species. *Phytochemistry, 45*(6), 1263-1269.

Rukachaisirikul, T., Siriwattanakit, P., Sukcharoenphol, K., Wongvein, C., Ruttanaweang, P., Wongwattanavuch, P., & Suksamrarn, A. (2004). Chemical constituents and bioactivity of *Piper sarmentosum*. *J Ethnopharmacol, 93*(2-3), 173-176.

Rukachaisirikul, T., Siriwattanakit, P., Sukcharoenphol, K., Wongvein, C., Ruttanaweang, P., Wongwattanavuch, P., & Suksamrarn, A. (2004). Chemical constituents and bioactivity of *Piper sarmentosum*. *Journal of Ethnopharmacology, 93*(2–3), 173-176.

SA Ayatollahi, A. S., F Kobarfard. (2009). Two Flavones from Salvia leriaefolia. *Iranian Journal of Pharmaceutical Research, 8*, 179-184.

Saralamp P, C. W., Temsiririrkkul R. (1996). *Medical Platns in Thailand* (Vol. 1): Amarin Printing and Puslishing.

Sengupta, S., Mukherjee, A., Goswami, R., & Basu, S. (2009). Hypoglycemic activity of the antioxidant saponarin, characterized as **α**-glucosidase inhibitor present in Tinospora cordifolia. *Journal of Enzyme Inhibition and Medicinal Chemistry, 24*(3), 684-690.

Stöhr, J. R., Xiao, P.-G., & Bauer, R. (2001). Constituents of Chinese Piper species and their inhibitory activity on prostaglandin and leukotriene biosynthesis in vitro. *Journal of Ethnopharmacology, 75*(2–3), 133-139.

Tadera, K., Minami, Y., Takamatsu, K., & Matsuoka, T. (2006). Inhibition of alpha-glucosidase and alpha-amylase by flavonoids. *Journal of nutritional science and vitaminology, 52*(2), 149-153.

Tezuka, Y., Stampoulis, P., Banskota, A. H., Awale, S., Tran, K. Q., Saiki, I., & Kadota, S. (2000). Constituents of the Vietnamese medicinal plant *Orthosiphon stamineus*. *Chem Pharm Bull (Tokyo), 48*(11), 1711-1719.

Tuntiwachwuttikul, P., Phansa, P., Pootaeng-On, Y., & Taylor, W. C. (2006). Chemical constituents of the roots of *Piper sarmentosum*. *Chemical & pharmaceutical bulletin, 54*(2), 149-151.

Wagman, A. S., & Nuss, J. M. (2001). Current therapies and emerging targets for the treatment of diabetes. *Curr Pharm Des, 7*(6), 417-450.

Yao, Y., Cheng, X., Wang, L., Wang, S., & Ren, G. (2011). A Determination of Potential **α**-Glucosidase Inhibitors from Azuki Beans (*Vigna angularis*). *International Journal of Molecular Sciences, 12*(10), 6445-6451.

Yilmazer-Musa, M., Griffith, A. M., Michels, A. J., Schneider, E., & Frei, B. (2012). Grape Seed and Tea Extracts and Catechin 3-Gallates Are Potent Inhibitors of **α**-Amylase and **α**-Glucosidase Activity. *Journal of Agricultural and Food Chemistry, 60*(36), 8924-8929.

Yoshikawa, M., Murakami, T., Yashiro, K., & Matsuda, H. (1998). Kotalanol, a potent alpha-glucosidase inhibitor with thiosugar sulfonium sulfate structure, from antidiabetic ayurvedic medicine *Salacia reticulata*. *Chemical & pharmaceutical bulletin, 46*(8), 1339-1340.

Yun, J.-M., Afaq, F., Khan, N., & Mukhtar, H. (2009). Delphinidin, an anthocyanidin in pigmented fruits and vegetables, induces apoptosis and cell cycle arrest in human colon cancer HCT116 cells. *Molecular Carcinogenesis, 48*(3), 260-270.
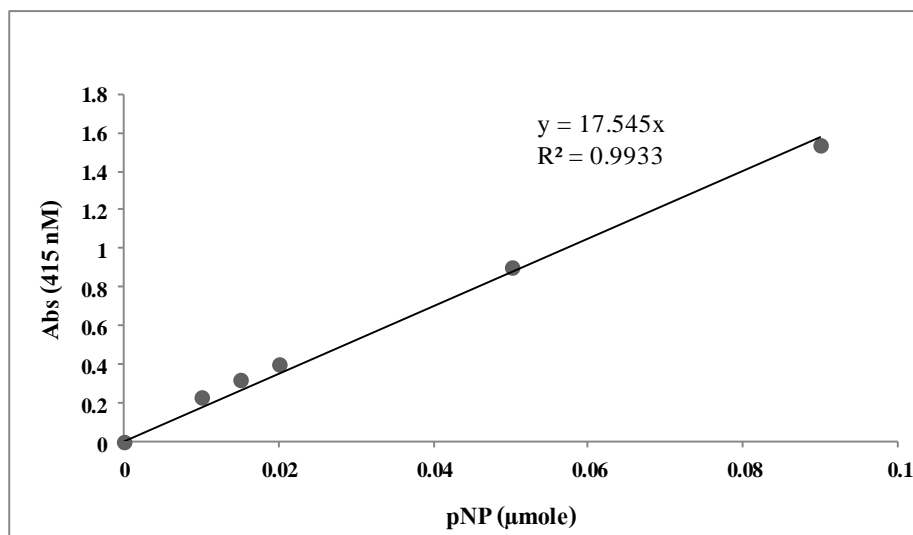
APPENDIX

APPENDIX A

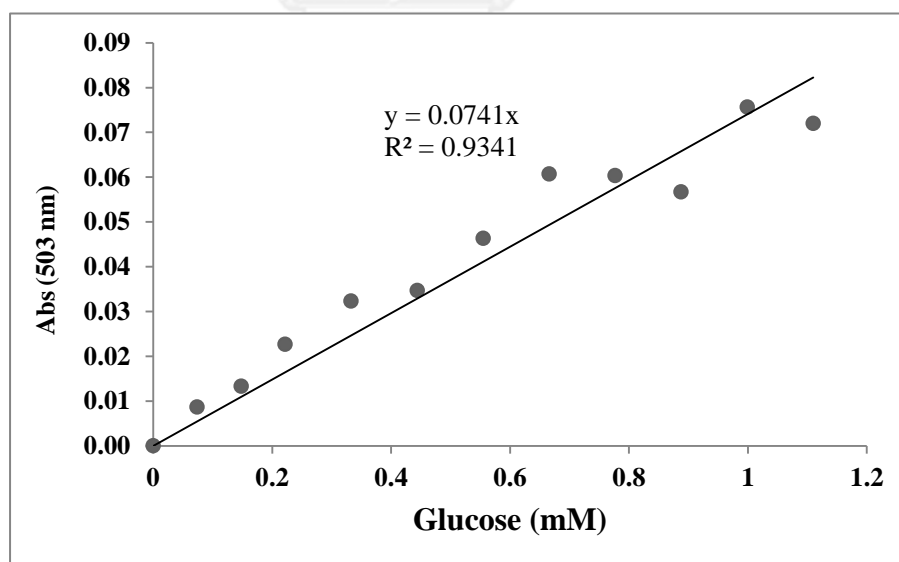**Figure A.**1 Standard curve of pNP

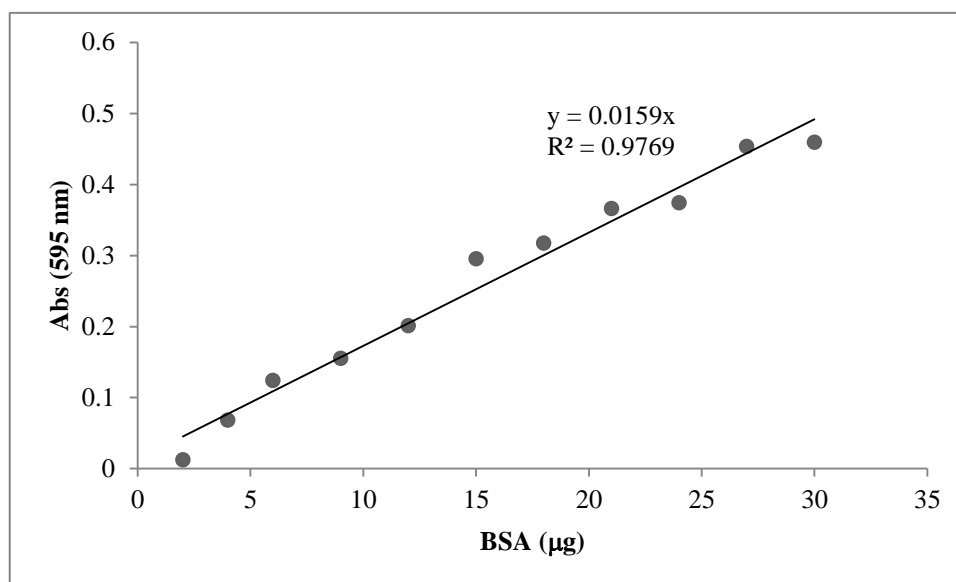**Figure A.2** Standard curve of glucose

APPENDIX A

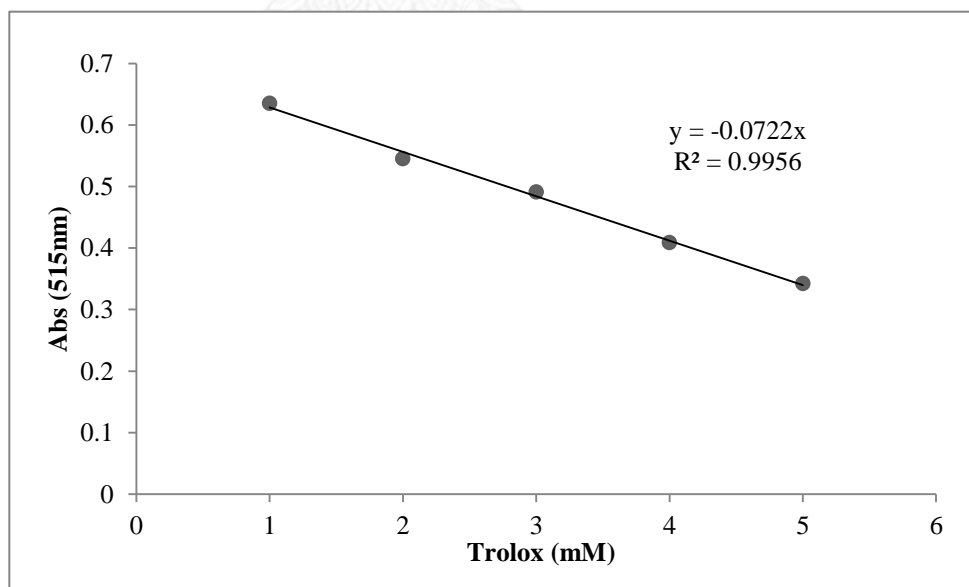
Figure A.3 Standard curve of BSA
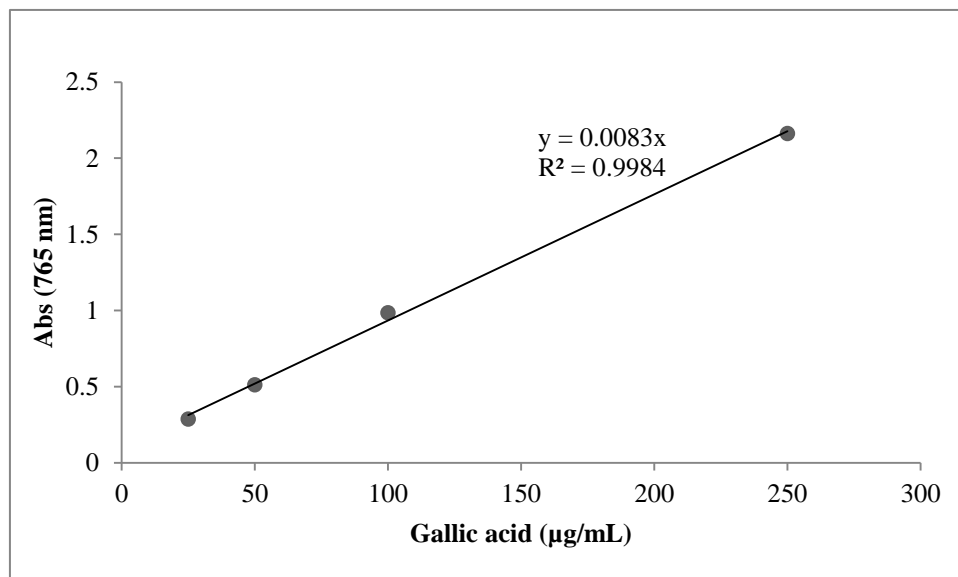

Figure A.4 Standard curve of Trolox

APPENDIX A

Figure A.5 Standard curve of gallic acid
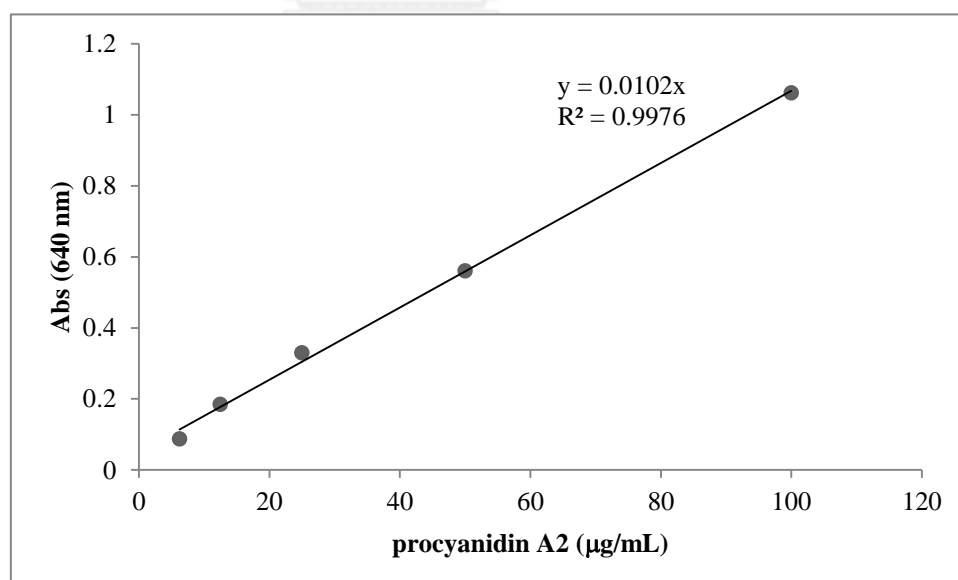

Figure A.6 Standard curve of procyanidin A2

APPENDIX B

PERSONAL INFORMATION

SCHOLARSHIPS

June 2009 – May 2013

Academic scholarship from Office of the Higher Education Commission through the Strategic Scholarships Fellowships Frontier Research Networks (Specific for Southern region) for the Join PhD Program Thai Doctoral degree program; a CHE-SSR-Ph.D. SW Scholarship

PUBLICATIONS

Damsud, T., Adisakwattana, S., & Phuwapraisirisan, P. (2013). Three new phenylpropanoyl amides from the leaves of *Piper sarmentosum* and their α-glucosidase inhibitory activities. *Phytochemistry Letters, 6*(3), 350-354.

Damsud, T., Grace, H., Adisakwattana, S., & Phuwapraisirisan, P. (2014). Orthosiphol A from the Aerial Parts of *Orthosiphon aristatus* is Putatively Responsible for Hypoglycemic Effect via α-Glucosidase Inhibition. *Natural Product Communications, 9*, xxx.

Rattanangkool, E., Kittikhunnatham, P., **Damsud, T.**, Wacharasindhu, S., & Phuwapraisirisan, P. (2013). Quercitylcinnamates, a new series of antidiabetic bioconjugates possessing α-glucosidase inhibition and antioxidant. *European Journal of Medicinal Chemistry, 66*(0), 296-304.

Wikul, A., **Damsud, T.**, Kataoka, K., & Phuwapraisirisan, P. (2012). (+)-Pinoresinol is a putative hypoglycemic agent in defatted sesame (*Sesamum indicum*) seeds though inhibiting α-glucosidase. *Bioorganic & Medicinal Chemistry Letters, 22*(16), 5215-5217.

VITA

Mr.Thanakorn Damsud was born on May 29, 1983 in Trang province, Thailand. He graduated with a Bachelor of Science degree in Food and Nutrition, Faculty of Public Health, Mahidol University in 2007 and a Master of Science degree in Biochemistry, Faculty of Science, Chulalongkorn University in 2009. He has further studied for the Doctor of Philosophy (Ph.D.) degree in Biotechnology, Faculty of Science, Chulalongkorn University since 2009.